**UNIVERSITY OF CALGARY**

# Latest Pleistocene and Holocene Paleo-Environments, Rose Basin, Glacier National Park, MT

by

David Matthew MacLeod

**A THESIS**

**SUBMITTED TO THE FACULTY OF GRADUATE STUDIES**

**IN PARTIAL FULFILMENT OF THE REQUIREMENTS FOR THE**

**DEGREE OF MASTER OF SCIENCE**

**DEPARTMENT OF GEOLOGY AND GEOPHYSICS**

**CALGARY, ALBERTA**

**MAY, 2003**

*Your file Votre référence*
*ISBN: 0-612-87347-1*
*Our file Notre référence*
*ISBN: 0-612-87347-1*

**UNIVERSITY OF CALGARY**

**FACULTY OF GRADUATE STUDIES**

The undersigned certify that they have read, and recommend to the Faculty of Graduate Studies for acceptance, a thesis entitled "Latest Pleistocene and Holocene Paleo-Environments, Rose Basin, Glacier National Park, MT" submitted by David Matthew MacLeod in partial fulfillment of the requirements for the degree of Master of Science.

Supervisor, Dr. Gerald Osborn, Geology and Geophysics

Dr. Len Hills, Geology and Geophysics

External Examiner, Dr. Derald Smith, Geography

May 30/03.

Date

**Abstract**

The sedimentary record of Otokomi Lake, Glacier National Park, Montana was studied in order to indirectly determine the emplacement date of an adjacent Crowfoot moraine. The presence of Saint Helens Jy ash at the bottom of the longest percussion core limited drainage basin deglaciation to pre 11,400 B.P., although 14,100 B.P. was the estimated basal date of the core. Correlative shifts in pollen, loss on ignition, coarse (> 1mm) grain size, magnetic susceptibility and X-ray grayscale data, at depth of 185 cm, were interpreted to be related to a sedimentary change in Otokomi Lake brought about by the emplacement of the adjacent Crowfoot moraine. The estimated emplacement date for the moraine is 10,590 B.P., which is within the Younger Dryas interval. This information supports the hypothesis that the Crowfoot moraine family represents a regional western North American response to Younger Dryas cooling.

**Acknowledgements**

Funding for this research was provided by Dr. Osborn's NSERC operating grant, an NSERC PGSA scholarship, and an iCORE graduate scholarship.

My sincere thanks goes out to Dr. Osborn, whose mentoring style enabled me to approach this project as I saw fit. As such, I have truly been able to appreciate the successes of the project and the challenges of self-directed research.

Many people aided me with the collection of field data for this project and to them I am also grateful. Elissa Lynn, Domi Diaz, and Miranda Hupman made up my able bodied team of field assistants during the summer of 2001. Dr. Ian Spooner, Dr. Osborn, David Mazzucchi, Elissa Lynn, and Tim Mang all helped with the collection of the percussion cores in April, 2000.

I would also like to thank those who intellectually contributed to this work during many stimulating discussions: Dr. Osborn for his critical assessment of all my latest theories and ideas, Dr. Len Hills for sharing his expertise on pollen identification, Dr. Robert Marr for his tireless assistance with microprobe data interpretation and Dr. Ian Spooner for helping me decipher the complicated stratigraphy of my percussion cores. Thanks also to all the technical staff who expertly guided me through various experimental procedures: Lorraine Bloom, Brenda Mottle, Murray Smith and Deb Glatiotis.

Special thanks goes to Jana Hanova for patiently listening to my frequent accounts of the project's progress over the past year and a half, and for her insightful contributions to the data interpretation.

Thanks to the staff of Glacier National Park for allowing this project to be conducted within their borders, including the accommodating staff at the West Glacier Science Center, Joe Fowler, Leo Marnell, Dan Jacobs and the helpful trail crew.

Thank you to my family for encouraging me at every step along my sinuous path of post-secondary education, I appreciate your continued support.

Lastly, thanks to the staff at The Source Skateboard Park. For a student too busy writing a thesis to spend entire days snowboarding, the indoor four-foot mini-ramp was just the ticket.

**Table of Contents**

**List of Tables**

**List of Figures**

## 1. Introduction

The Younger Dryas has been widely recognized as a cool period, dated between 11,000 and 10,000 $^{14}C$ years before present (hereafter "B.P."), which interrupted the warm Bølling/Alleröd period that followed the Wisconsinan Glaciation (Wright, 1989). Its uniqueness as a Quaternary climatic event is related to both the extremely abrupt nature with which it ended and the relatively short duration of the entire event (Dansgaard et al., 1989; Taylor et al., 1993; Alley at al., 1993). Although the cooling related to the event was first recognized in coastal areas that border the North Atlantic (Wright, 1989), more recent studies have demonstrated Younger Dryas-aged cooling over a much wider geographic area (Kudras et al., 1991; Scott et al., 1995; Osborn et al., 1996; Mikolajewicz et al., 1997; Rutter et al., 2000; Zhou et al., 2001; Briner et al., 2002; Kovanen, 2002). In spite of the mounting evidence for global cooling during the Younger Dryas, some studies have shown no evidence for climate change during that interval, or even evidence of climatic warming (Heine, 1994, Heine and Heine, 1996; Singer et al., 1998; Bennett et al., 2000). In addition, data correlation between studies that claim Younger Dryas cooling is often difficult. Due to the complexity of the earth's climate system, local climatic variability may be responsible for the cooling experienced at many sites (Rodbell, 2000).

This study was conducted to further explore the geographic extent of cooling during the Younger Dryas through the investigation of a regionally identifiable feature associated with such cooling. Luckman and Osborn (1979) identified a family of glacial moraines in the Rocky Mountains of North America they named Crowfoot moraines. These moraines have a geographic range extending from Jasper, B.C. to Wyoming

(Reasoner et al., 1994; Gosse et al., 1995). All moraines in this family are overlain by Mazama ash, which constrains their emplacement to pre 6730 B.P. (Hallett et al., 1997). Using the sedimentary record of a nearby lake, the emplacement date of the type Crowfoot moraine in Banff National Park was estimated to be between 11,330 B.P. and 10,100 B.P. (Reasoner et al., 1994), which is during the Younger Dryas interval. The aim of the present study was to determine the emplacement date of another moraine in the Crowfoot family in order to test the hypothesis that this moraine family represents a widespread glacial response to climatic cooling during the Younger Dryas. Rose Basin in Glacier National Park, Montana was chosen as the study site for this project. The basin contains a putative Crowfoot moraine immediately adjacent to Otokomi Lake. The sedimentary record of this lake was studied in detail, in hopes of indirectly determining the emplacement date of the adjacent moraine.

## 2. Previous Research

### 2.1 Latest Pleistocene and Early Holocene Glacial Activity in the North American Cordillera

Several researchers have noted pre-Younger Dryas glacial activity in the post-Wisconsinan geologic record of the North American Cordillera. This activity ranges in age from 11,200 B.P to11,800 B.P. and represents both cirque glacier activity and the advancement of the Cordilleran ice sheet (Davis and Osborn, 1987; Zielinski and Davis, 1987; Heine, 1996; Osborn and Gerloff, 1997; Kovanen, 2002). Although both the cause of these advances and their relation to one another are unknown, the possibility exists that they represent a period of widespread glacial re-advance in the North American Cordillera.

Many paleoclimatic reconstructions in areas of the North American Cordillera that lack Crowfoot moraines have provided evidence for glacial activity or cool conditions during the Younger Dryas interval; Engstrom et al. (1990) demonstrated cooling in southeastern Alaska with lacustrine pollen and geochemical data; Matthews et al. (1993) identified cool and wet conditions on the B.C. coast using benthic foraminifera and fossil pollen data; Gosse et al. (1995) found evidence for glacial advance in the mountains of Wyoming using cosmogenic $^{10}$Be; Menounos and Reasoner (1997) provided lacustrine sedimentary evidence for glacial advance in the Colorado Rockies; Briner et al. (2002) used cosmogenic $^{10}$Be and $^{26}$Al data, in conjunction with radiocarbon dates from lacustrine sediment, to provide evidence for glacial advance in southwestern Alaska; Friele and Clague (2002) used geomorphologic evidence in conjunction with carbon dating to demonstrate the readvance of a valley glacier in the southern Coast Mountains of B.C. These studies, along with that of Reasoner et al. (1994), are all part of the growing body of evidence for cool conditions during the Younger Dryas interval in western North America.

Although there have been some claims of early Holocene glacial re-advance in the Canadian Rockies (Harris and Howell, 1977; Beget, 1983), this work has recently been criticized (Osborn and Gerloff, 1997). The majority of the evidence related to early-Holocene climate in the Rockies would suggest warm conditions characterized by forest expansion and glacial retreat (Luckman and Osborn, 1979; Luckman and Kearney, 1986; Luckman, 1988; Tomkins, 2000). The remainder of the Holocene glacial advances recognized in the North American Cordillera appear to postdate the deposition of

Mazama ash (Fulton, 1971; Osborn, 1986; Ryder and Thomson, 1986; Osborn and Gerloff, 1997), and as such, do not bear on this discussion.

**2.2 Late-Wisconsinan Deglaciation of Northwestern MT and Glacier National Park**

During the height of the late Wisconsinan glaciation, Glacier National Park was covered by glacial ice. It was an area of ice fields and valley glaciers bordered on the west by the Cordilleran Ice Sheet and on the east by a narrow expanse of open plains (Alden, 1953; Waitt and Thorson, 1983). Based on a study of late-Pleistocene sediment exposures and bog sediments, Carrara (1989) concluded that Glacier National Park was extensively deglaciated prior to 11,400 B.P. This included Marias Pass on the continental divide immediately to the south of the park (elevation 5232 feet asl). Southwest of Glacier National Park, in the Mission Mountains, Gerloff et al. (1995) concluded that deglaciation predated 11,200 B.P. due to the presence of Glacier Peak G tephra in a lacustrine sedimentary record from 6192 feet asl. East of the Mission Mountains in the Sun River Canyon, Lemke et al. (1975) concluded that valley ice had retreated 11 km upvalley by 11,200 B.P., based on the presence of Glacier Peak tephra in an ancient alluvial fan deposit. In the Bitterroot Mountains of west central Montana, the sedimentary record from a bog at 7059 feet asl indicates deglaciation by 12,000 B.P. (Mehringer et al., 1977). Based on a lake-sediment study on the Great Plains of Montana, east of Glacier National Park, it was concluded that the glacial ice of the Two Medicine Glacier, which was fed by ice from Two Medicine Valley and Marias Pass, had retreated from the Great Plains by 12,200 B.P. (Barnosky, 1989)

Besides the Crowfoot moraines identified by Carrara (1987) and Osborn (1985), there is little evidence for late Pleistocene / early Holocene glacial activity following the

broad period of deglaciation described above; Gerloff (1994) identified a moraine near Piper Lake, which is overlain by Glacier Peak ash, giving it a minimum age of 11,200 B.P.; Osborn (1985) suspected that a moraine near Iceberg Lake in Glacier National Park was a product of a pre-Crowfoot glacial advance, however sufficient dating control was lacking.

**2.3 Alpine Paleolimnology**

Due to the sensitivity of alpine environments to climate change, the alpine setting is often used for paleoclimatic work (Gerloff et al., 1995). Much of the work in these environments has involved the study of lake sediments. For example, Niessen and Kelts (1989) studied the Holocene sedimentary evolution of an alpine lake in Switzerland. Both Reasoner et al. (1994) and Menounos and Reasoner (1997) used paleolimnology to postulate the timing of glacial advances in the North American Rockies. Andrews et al. (1982) studied several alpine lake cores from the Colorado Rockies in order to characterize past variations in both sediment and organic influx in the basins. Mazzucchi et al. (in press) used the lacustrine record of Pyramid Lake in British Columbia, Canada to reconstruct regional changes in Holocene Climate. Dirszowsky and Desloges (1997) examined the temporal relationship between glacier activity, sediment production and the lacustrine sedimentary record of proglacial Chephren Lake, Alberta, Canada

Last and Smol (2001) provided a detailed review of the diverse array of analytical techniques used in paleolimnology. Although the majority of these techniques can be applied in a variety of settings, those commonly employed in the alpine environment include palynology, combustion analysis, magnetic susceptibility, tephrochronology, textural analysis, isotopic characterization, macrofossil analysis (including carbon

dating), and charcoal analysis. In order for the data that is generated by applying these techniques to be properly interpreted, an understanding of lake sedimentation has to be attained (Håkanson, 1977; Bradley et al., 1996; Gilbert et al., 1997). Although many investigators have studied sedimentation processes in alpine lakes, for example: Luckman (1975), Mankiewicz et al. (1975), Shaw (1977), Lambert and Hsü (1979), Gilbert and Shaw (1981), Weirich (1984), Brown and Walsh (1992) and Eden and Page (1998), the conclusions made are usually not valid for all lakes. This is because alpine lake environments are very diverse and, as a consequence, have a diverse array of sedimentary regimes. Therefore each lake must be individually assessed if the processes of sedimentation within it are to be fully understood (Larsen and Macdonald, 1993).

Despite the heterogeneity of alpine lake environments, there are processes unique to the alpine that affect lake sedimentation; glacial activity in the catchment of a lake can have large effects on both sediment and water input (Reasoner et al., 1994; Dirszowsky and Desloges, 1997; Menounos and Reasoner, 1997; Lewis et al., 2002); lake basin slumping and associated turbidity currents are relatively common in alpine lakes due to steep basin morphologies and high sediment inputs (Gilbert and Shaw, 1980; Weirich, 1984; Dirszowski and Desloges, 1997); the steeply sloping drainage basins of many alpine lakes facilitate both mass movement and high-energy fluvial erosion, which can introduce large amounts of coarse sediment into the lacustrine environment (Luckman, 1975; Gardner, 1983; Dirszowski and Desloges, 1997; Eden and Page, 1998).

# 3. Methods

## 3.1 Field Methods

### 3.1.1 Site Selection

Because of the objective of this study, there were several criteria that had to be met when selecting a suitable lake for sediment coring. These included: proximity of a Crowfoot moraine, lake size, catchment geometry, and site accessibility.

Glacier National Park, Montana was chosen as the general study area for this project based on the number of Crowfoot moraines previously identified there (Osborn, 1985; Carrara and McGimsey, 1988). Air photos of the park were obtained from the Glacier National Park Air Photo Archive in West Glacier, Montana. They were taken in 1968 at a scale of 1:15,840. The primary use of the photos was to identify Crowfoot moraines in the park. These were easily distinguished from younger moraines because of their high degree of weathering, abundant vegetation cover and location relative to the younger moraines. Only Crowfoot moraines with lakes immediately downstream of them were of interest to this study. This is because the sedimentary record of lakes in glacial environments is well suited for recording upstream variations in glacial activity (Dirszowsky and Desloges, 1997; Menounos and Reasoner, 1997; Lewis et al., 2002).

The candidate lakes in Glacier National Park were assessed for their suitability in paleoclimatic study. Lakes that appeared small enough to have dried up during arid times, would have an incomplete sedimentary record following Wisconsinan de-glaciation, and therefore were of little use to this study. This determination was somewhat arbitrary, and depended only on observations of lake surface area and of lake depth. Lake depth was estimated from a lake's photographic tone, whereby deeper water was associated with

darker tones and shallower water with lighter tones. Only lakes with dark tones that had a surface area larger than four hectares were considered for this study.

The catchment geometry of potential study lakes was also studied, in order to estimate the possible sources and rates of sediment influx into the basin. Lakes that appeared to have the adjacent moraine as the dominant source of coarse sediment influx were considered the most appropriate for use in this study. Lakes subject to high volumes of coarse sediment input from talus slopes or alluvial fans were given a lower priority.

Site access was also an important factor in choosing a study lake, because of the need to transport a large amount of equipment to and from the site. Sites requiring more than 15 km of hiking from the nearest roadway were labeled as remote sites and not considered.

Using the above procedure, Otokomi Lake, in Rose Basin was chosen as the study site. A detailed description of the site can be found in chapter 4.

### 3.1.2 Coring Methods

Two coring methods were used in this study: 1) Percussion coring and 2) Gravity Coring. Each method allows for efficient sediment recovery at different stratigraphic levels. The sediment recovered in percussion cores often includes a portion of the underlying glacial till, demonstrating the ability of this system to sample nearly the entire post-glacial sedimentary record (Spooner et al., 1997; Reasoner et al., 1994; Beierle, 1997). In contrast, the gravity core is able to collect an undisturbed sample of the recently deposited water-rich sediment on the surface of the lakebed (Glew, 1991). When used in conjunction, these coring methods provide a means to collect a sedimentary record that can cover the entire depositional history of a lake.

### 3.1.2.1 Percussion Coring System

Reasoner (1986) first described the percussion coring system used in this study. The system consists of a core head, a driver, and a 3 m length of PVC sewer pipe outfitted with a metal core catcher (Fig. 1). A second section of 3 m sewer pipe may be attached below the first in order to achieve a maximum coring depth of 6 m.

The collection procedure was a modified version of the methods described by Reasoner (1986). The Reasoner methodology was employed up to the point of core retrieval through the lake ice. As the core head and PVC pipe assembly were emerging from the lake, holes were drilled at 5 cm intervals into the pipe, which allowed lake water to drain from inside. The draining of the overlying water reduced the downward pressure on the collected sediment, therefore minimizing sediment loss from the bottom of the pipe. The first drill hole that drained brown in color was considered to be just below the water / sediment interface and signaled the end of drilling. The core head and PVC pipe assembly were then brought the rest of the way to the ice surface. The length of pipe containing the collected sediment was then cut into 50 cm sections with a hacksaw. Each section was capped, cleaned, labeled and stored in the snow until they were transported from the site. The core sections were immediately frozen upon arriving at the University of Calgary. A notable drawback of this extraction method is that the drilling process disturbs a portion of the sediment at the top of the core barrel.

Two locations were cored in Otokomi Lake using the above procedure. Each site fell approximately along the long axis of the lake. C1 was collected opposite an inlet stream that bisects the Crowfoot moraine, and C2 was located about 100 m east of C1.

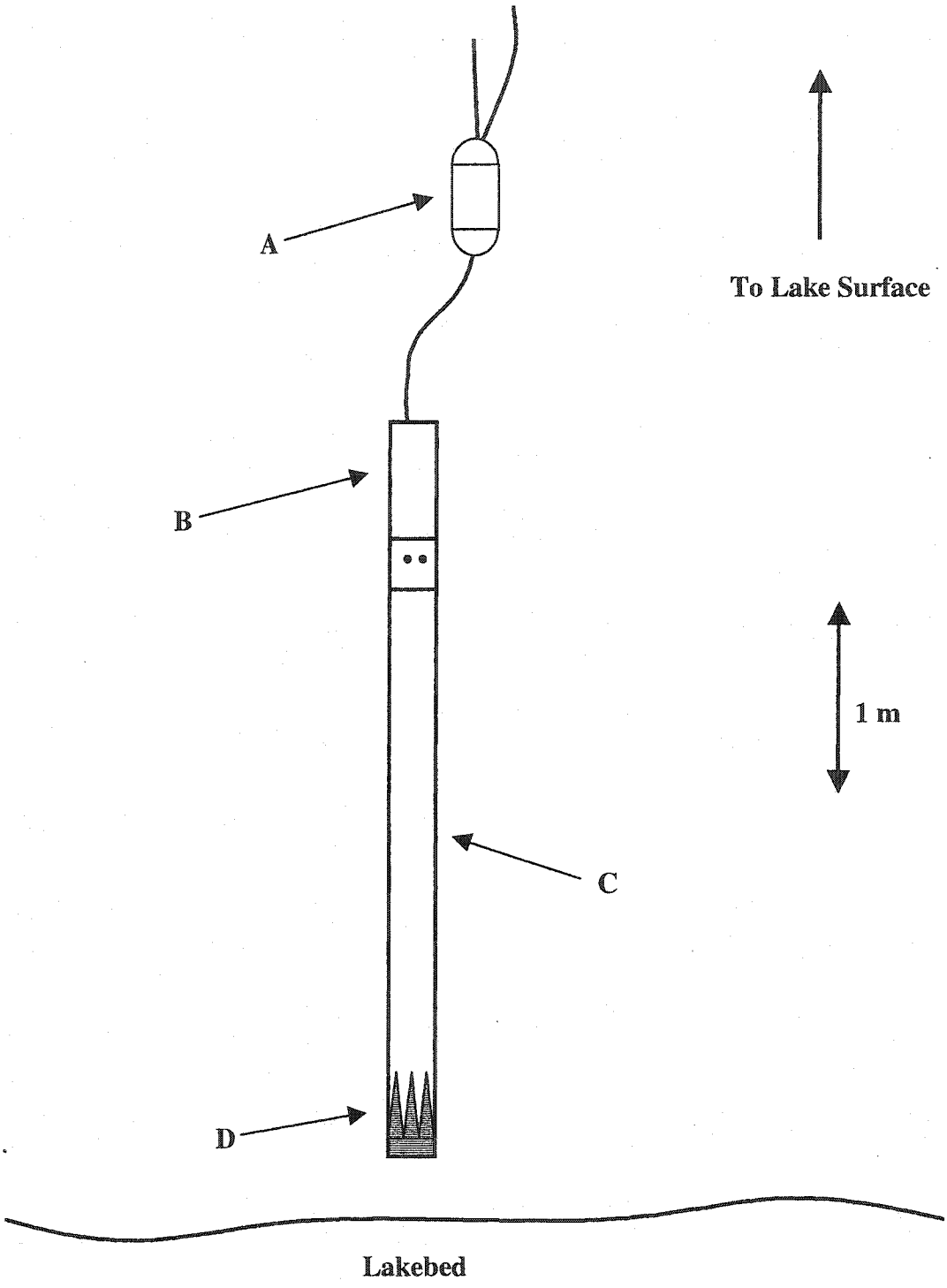


**Figure 1.** Schematic representation of the percussion coring apparatus: **A**: Driver, **B**: Core Head, **C**: Core Barrel, **D**: Core Catcher

### 3.1.2.2 Gravity Coring System

The gravity coring system used was first described by Glew (1991), and provides a means with which to collect up to 1 m of the most recently deposited lakebed sediment. Because of the lightweight nature of the gravity coring system, it was employed in the summer, off of the side of an anchored dinghy. The coring system consists of a hollow Plexiglas tube, approximately 3 inches in diameter, connected on its upper end to a solid brass housing (Fig. 2). The brass housing contains a spring-loaded plunger with a rubber stopper. Following core penetration into the lakebed this plunger is released via a brass messenger weight that travels down the main line. Sealing of the upper end of the Plexiglas tube with the rubber stopper in this manner ensures that the collected sediment remains in the core barrel during retrieval.

One core was collected from Otokomi Lake using this method. An attempt was made to collect this core from the same location as percussion core C1, however the drift of the anchored dinghy made this task difficult. The core was transported from the site, and also stored, in a vertical position in order to preserve the stratigraphic relationships of the sediment layers inside. The location of all three cores collected from Otokomi Lake can be seen in Figure 3.

### 3.1.3 Sonar Profiling

Basin morphology plays a controlling role in the sedimentation dynamics of lacustrine environments (Mankiewicz et al., 1975; Hilton at al., 1986; Larsen and MacDonald, 1993). Therefore, an understanding of basin morphology is an important part of interpreting lacustrine deposits. Although a rigorous battery of depth sounding measurements can provide a general picture of lakebed morphology and water depth,

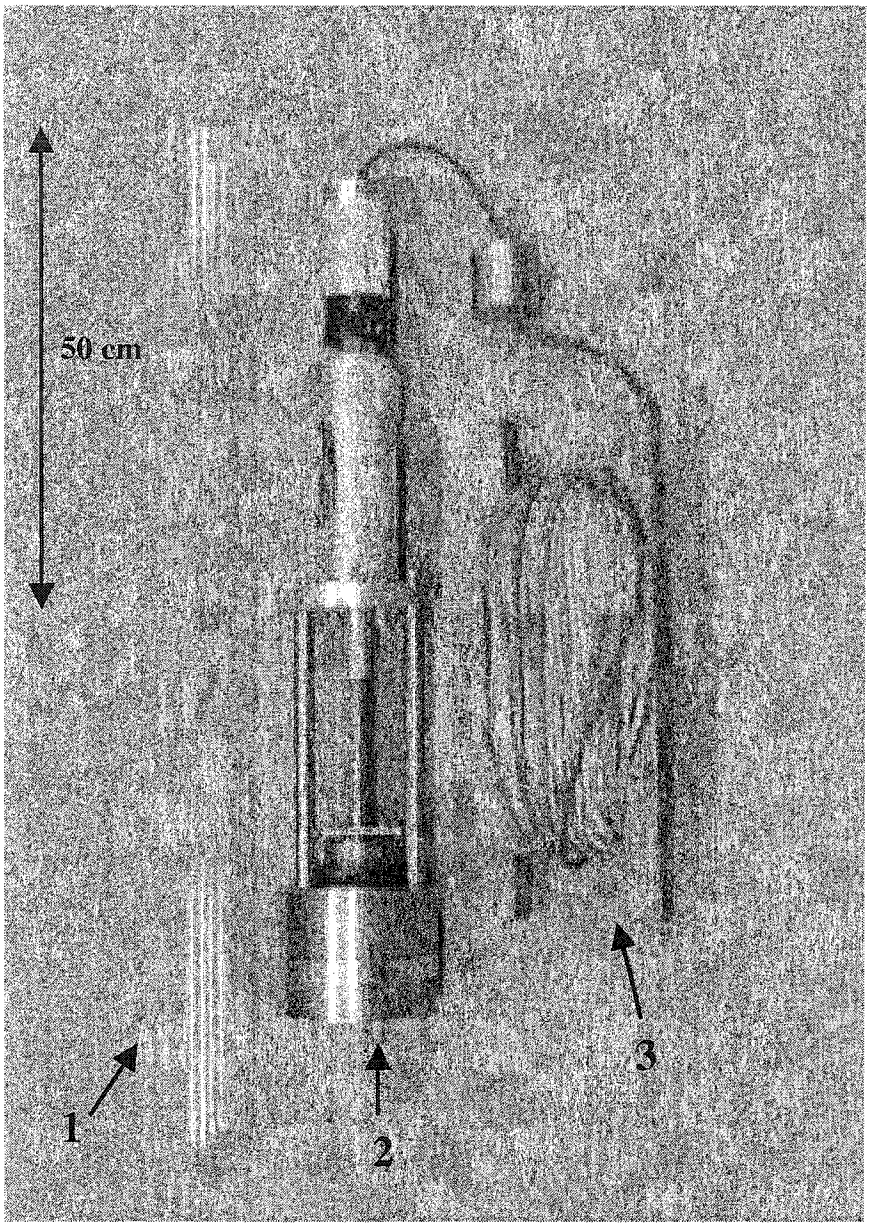


**Figure 2.** Photograph of the gravity coring apparatus. **1:** Plexiglas Core Tube, **2:** Housing with Spring-loaded Plunger, **3:** Main Line

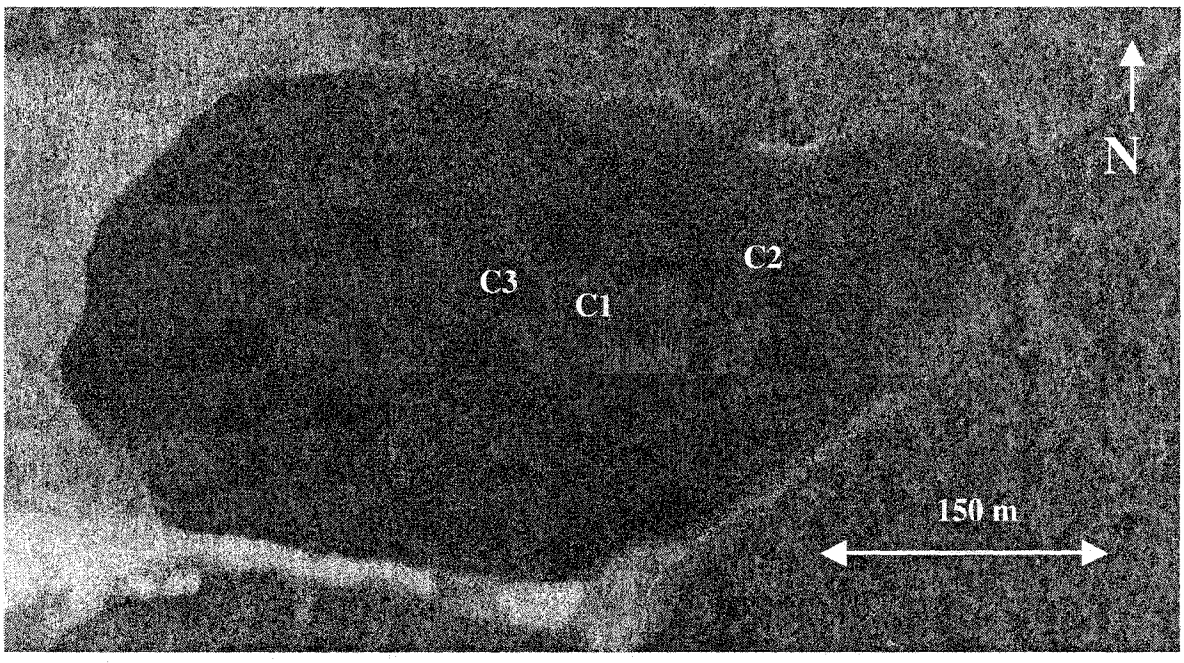


**Figure 3.** Photograph of Otokomi Lake showing the locations of core collection. C1 and C2 represent the percussion cores and C3 represents the gravity core.

there are distinct advantages to obtaining information through sonar profiling. Depth sounding measurements provide single points of information, whereas sonar profiling provides a continuous measure of lakebed depth across a given transect. Therefore, the quantity of data obtainable by sonar profiling greatly exceeds that of depth sounding, over a given collection period. As well as providing data on water depth, sonar profiling can also provide data on substrate type and thickness. This is because the signal sent by the sonar unit is able to penetrate the lakebed and reflect off of underlying structures.

Otokomi Lake was profiled using a King 1570 sonar unit. The unit consists of a metal transceiver that sends and receives the sonar signal, the main body, and a 12 V car battery (Fig. 4). The main body serves to display the sonar data while it is being collected, both through a paper printout and a digital display. The main body also has several control knobs, which modify both the mode of data collection and how the data is displayed.

Because of the remote nature of the site, and restrictions placed on users of U.S. National Parks, the sonar data were not collected from a motorized vessel. The sonar profiling was performed off the side of a small inflatable two-person dinghy propelled with a modified kayak paddle. The transceiver was mounted to the side of the dinghy, so that it sat approximately 6 inches below the water surface when the dinghy was manned (Fig. 5). Seven transects were performed, with five of them being transverse to the long axis of the lake, one along the long axis, and one oblique to the long axis of the lake (Fig. 6).

Because the sonar data were collected after the percussion coring was completed, they were merely used to help interpret the sedimentary record of the cores. In order to do

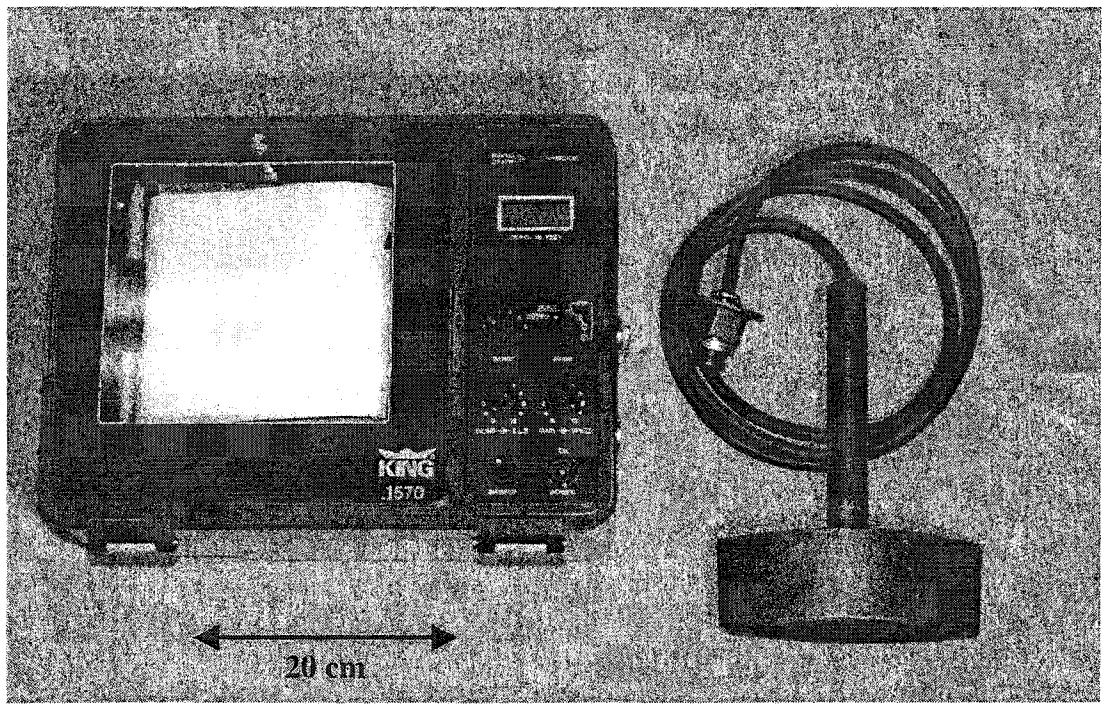


**Figure 4.** Photograph of King 1570 sonar unit. The transceiver, electronic cable and main body are shown. A 12 V car battery powers the unit.

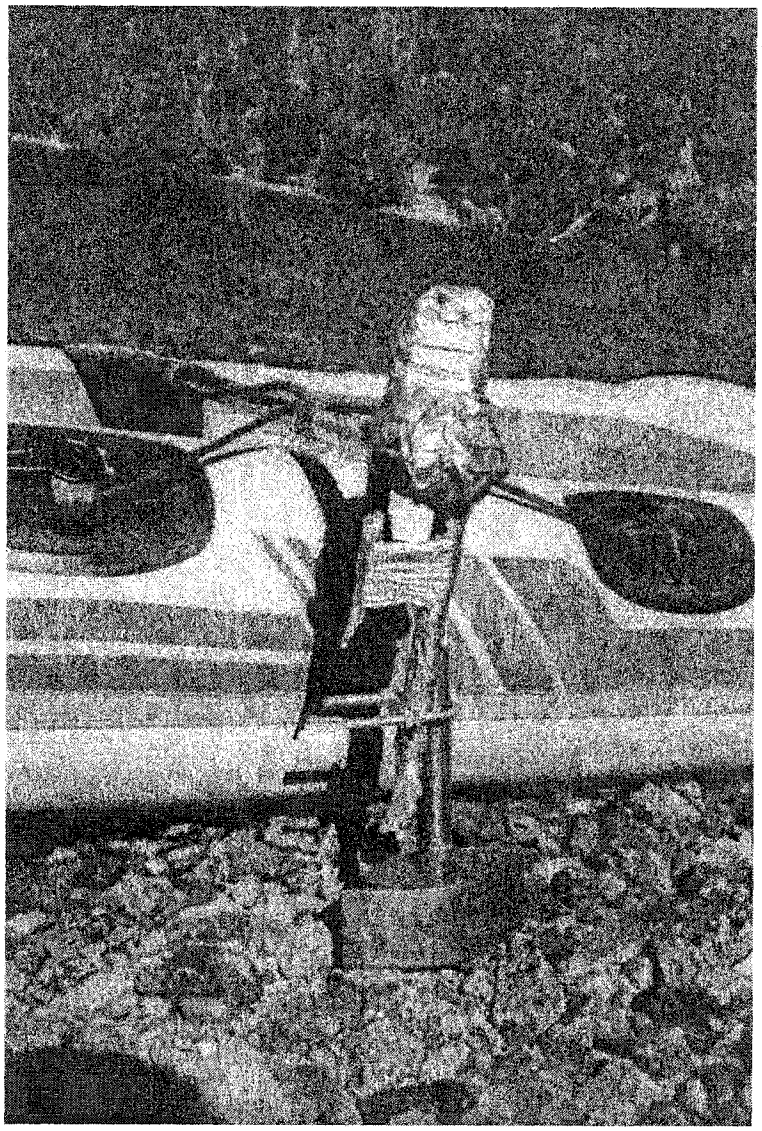

**Figure 5.** Photograph of sonar transceiver attached to the side of the dinghy. This arrangement allowed the transceiver to sit approximately 6 inches below the water's surface when the dinghy was manned.

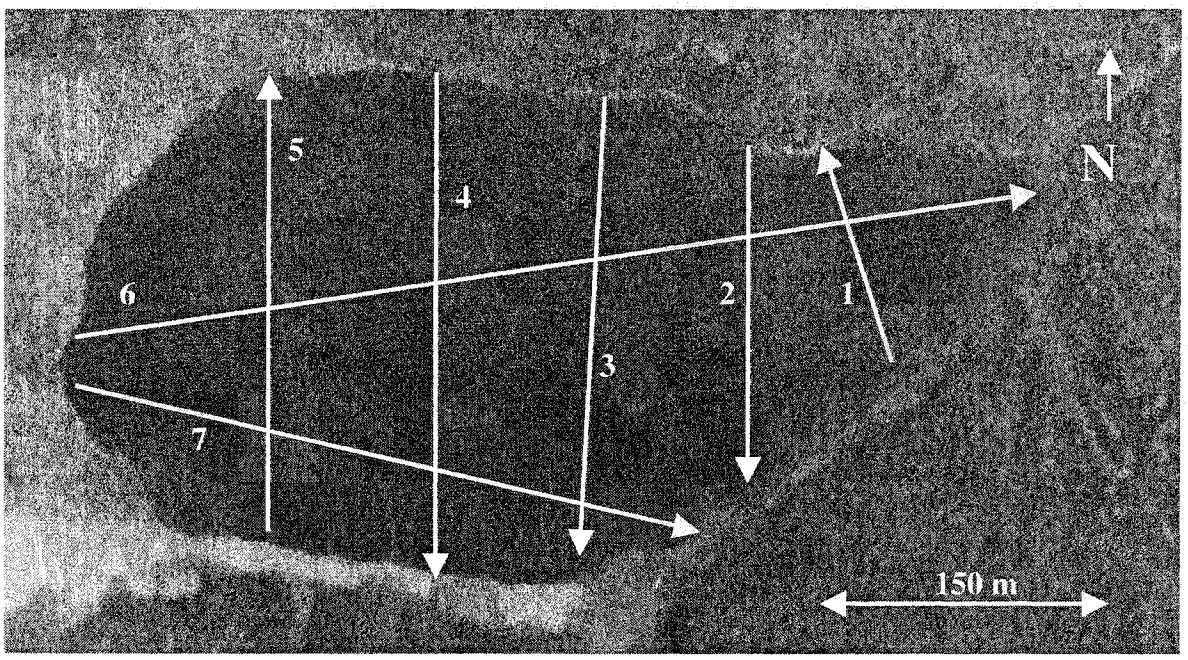


**Figure 6.** Sonar transects traveled on Otokomi Lake. Arrows indicate the direction of boat travel.

this, the sonar output was first used to generate spatial information on the lakebed in an XYZ coordinate system. These data were entered into the program Surfer®, in which a bathymetric map of the lake basin was created. This bathymetric map was then used as a tool to understand the sedimentation dynamics of Otokomi Lake.

### 3.1.4 Lake Temperature Profiling

A thermally stratified lake has different transportation and distribution mechanisms for fine-grained particulate matter than are found in thermally un-stratified lakes (Hilton et al., 1986). Identifying the presence of such stratification, and the depth at which it might occur, is of use when attempting to understand lacustrine sedimentation dynamics.

Temperature data were collected throughout the water column of Otokomi Lake through the use of a data-logging thermometer, known as a thermister. The thermister interfaced with a laptop computer through the program Boxcar®. Using this program, the thermister was programmed to record the temperature every five minutes. Five minutes was regarded as sufficient time for the air encased in the waterproof cylinder to equilibrate with the ambient water temperature. The thermister was then lowered through the water column, by one meter every five minutes, off of the side of an anchored dinghy. Each successive lowering was performed immediately after the thermister had taken a reading, allowing nearly a five full minutes for the thermister to adjust to the ambient water temperature at a particular depth. When the thermister cylinder came to rest on the lakebed, one last measurement was acquired before the thermister was retrieved. The data was later uploaded to a computer and imported into Microsoft Excel®, in which a temperature profile of the lake was generated.

### 3.1.5 Site Survey

Locating and characterizing inlet streams is an important part of lacustrine studies (Last and Smol, 2001). A survey of the land around Otokomi Lake was conducted in the summer of 2001 in order to locate stream inputs. Inlet streams, both ephemeral and flowing, were located around the lakeshore. Approximate stream gradients and cross sectional areas were determined, so that maximum stream discharges could be estimated using the Manning equation. Width, depth, and water velocity measurements were also conducted on Otokomi Lake's outlet creek, so that the capacity for sediment discharge from the basin could also be postulated. A survey of the modern plant community was conducted at the study site as well. The identity of this community, and of the environmental conditions responsible for its proliferation, would serve as a useful reference point when attempting to reconstruct past climates at Otokomi Lake.

## 3.2 Laboratory Methods

Several laboratory analyses were performed on the cores collected from Otokomi Lake. These included xradiography, core splitting and photography, core logging and sampling, tephra identification, combustion analysis, grain size analysis, magnetic susceptibility measurements, macrofossil identification and dating, and palynological analysis. These analyses, combined with information collected from the study site during the summer of 2001, were used to reconstruct the environmental and depositional history of the lake.

### 3.2.1 Xradiography

In order to examine bulk density differences in the percussion cores and resolve internal sedimentary structures, they were X-rayed at Western Inspection Ltd., Calgary

Alberta. While still frozen, the two cores were exposed to X-rays at a voltage of 110 KV and an amperage of 10 MA, for 2 minutes at a distance of 170 cm from the X-ray source. Xradiographs of interest were first scanned into a computer and the images later imported into Corel Draw®. Once in this program the grayscale values (1 – 256) of the xradiograph image were recorded along the centre line of each core section, at a spacing of one centimeter. These data were entered into Microsoft Excel®, where they were graphed for analysis.

### 3.2.2 Core Splitting and Photography

The frozen percussion core sections were taken to Core Laboratories Canada Ltd., Calgary, Alberta, where they were split along their long axes, using a circular saw equipped with a diamond blade. The orientation of the cut was such that the surface of the split core represented the same viewing perspective as the xradiograph images. The split core sections were placed under running water, where the waste from the sawing process was washed from their surfaces using a brush. The brushing was done perpendicular to the long axis of the core section, in order to minimize large stratigraphic displacements of loose core material. Once the core sections were cleaned, they were photographed using high-resolution digital photography. The core sections were then double-wrapped in plastic stretch wrap and stored in a freezer at the University of Calgary.

### 3.2.3 Logging and Sampling Core

For each of the two percussion cores, the selected sections were placed end-to-end on a table in the appropriate stratigraphic positions. A metric measuring tape and strip of paper were both affixed to the table next to the core. A log of sedimentary structures,

colors, textures and macrofossil locations was then recorded on the paper strip. For the small gravity core, a measuring tape was affixed to the side of the Plexiglas tube and a similar log was recorded on a separate piece of paper.

The percussion cores were thawed prior to sampling. Desiccation of the core halves was prevented by storing them in sections of 4-inch diameter PVC pipe that were capped airtight at each end. Sediment samples for palynological analysis, grain size analysis and combustion analysis were collected with a modified medicinal syringe. These samples each had a volume of 1 $cm^3$ and were taken along the long axis of the core at 1.4 cm intervals, with care taken to avoid sampling across obvious boundaries. A stainless steel spatula was periodically used to fill the syringe and/or level the sediment in it, to insure volumetric constancy. All tools were cleaned with water between samples to prevent cross contamination. A portion of the grain size analysis involved the incremental extraction of all remaining sediment in a core half. This was accomplished through the use of a thin plastic semi-circle, having the same diameter as the inside-diameter of the core sections. Starting 1 cm from the top of a core section, the semi-circle was inserted into the sediment, perpendicular to the long axis of the core. This process continued down the core section at 1 cm intervals, thereby isolating1 cm thick slices of sediment from the core.

Due to the high water content of the sediment in the gravity core, a different sampling procedure was employed. A circular rubber stopper was trimmed so that it had the same diameter as the inner diameter of the Plexiglas core tube. Using a PVC pipe, with a diameter slightly less than that of the core tube, the trimmed stopper was pushed up through the core tube. As the lacustrine sediment passed the upper edge of the

Plexiglas tube it was collected in 1 cm thick slices, using a 3-inch wide stainless steal spatula. These samples were placed in aluminum foil muffin trays and allowed to dry. In order to sub-sample this sediment for various analyses it was first wetted and then scooped into the modified 1 $cm^3$ syringe.

### 3.2.4 Tephra Identification

Three distinct sedimentary units within the longest percussion core were suspected of containing tephra. The contact relationships between these units and the bounding lake sediment were first studied with the aid of a 10 x hand lens. Small samples were then obtained of each unit, using a small stainless steel spatula. The samples were air-dried and inspected with a binocular microscope for the presence of glass shards. Upon confirmation of the presence of glass shards, each sample was chemically and morphologically analyzed with an electron microprobe for more accurate identification. Sampling for the microprobe analysis was not done volumetrically, because the units were of varying thickness and the analyses to be performed were generally not sensitive to sample size differences.

#### 3.2.4.1 Mineral Separation

The first stage in the preparation of the ash samples was a mineral separation procedure, which served to isolate the glass fraction. Each ash sample was dried and separated into three size fractions by sieving at both 120 and 170 mesh sizes. The intermediate size fraction, representing the silt-sized portion of the samples, was retained. Smaller grains were not retained because of size limitations posed by electron microprobe analysis, and larger grains may have been non-volcanogenic. Upon inspection under a binocular microscope, several of the retained grains appeared to be agglomerations of

smaller material. In order to disaggregate the agglomerations, they were placed in an ultrasonic water-bath for a period of thirty seconds. Following the ultrasonic treatment, the smaller grains were decanted off whereas the larger grains were dried and retained for further preparation. Each of the prepared ash samples were centrifuged in tubes containing a liquid mixture of Calgon and Decalin, having a density of 2.42 G. Through this process dense minerals, like magnetite and ilmenite, sink whereas the volcanic glass rises to the surface. After decanting, both fractions were washed with acetone and retained. For each ash sample these fractions were then mounted on separate microscope slides and carbon coated, in preparation for the electron microprobe analysis.

#### 3.2.4.2 Electron Microprobe Analysis

Electron microprobe analyses were conducted at the University of Calgary using a JEOL JXA-8200 Superprobe. The Superprobe contains five wavelength-dispersive spectrometers, making it a valuable tool for quantitative chemical analyses of trace elements. As well as for quantitative analyses, the Superprobe was also used to acquire backscattered electron images, detailing the morphology of the grains being studied.

##### 3.2.4.2.1 Volcanic Glass

The major oxides analyzed in the volcanic glass samples were $K_2O$, CaO, FeO, $Na_2O$, $TiO_2$, MnO, $Al_2O_3$, $SiO_2$ and MgO. The standards used to calibrate the Superprobe for each of the above oxides were orthoclase, anorthite, chromite, obsidian, rutile, rhodonite, anorthite, obsidian and diopside, respectively. The listed oxides are the primary chemical components of volcanic glass, in addition to trace amounts of water. Glass shards sourced from a particular volcano will be composed of characteristic

proportions of these oxides, making them a powerful diagnostic tool (Westgate and Gorton, 1981).

Glass shards were first identified on the basis of their morphology and the brightness of their appearance in the backscattered image. Care was taken to avoid analyzing shards containing inclusions of other minerals, like feldspars. These inclusions were identified by their morphology and their brightness in the backscattered image (Fig. 7). Once candidate glass shards were identified, the x-y coordinates of the area to be analyzed were entered into the Superprobe. When possible, 50 points were identified and analyzed on each slide, to ensure statistical accuracy in the measurements performed. Certain glass shards were large enough to be analyzed in two, or even three, areas, therefore making the total number of analyzed shards less than 50 per slide. The shards were analyzed with an accelerating voltage of 15.0 kV, a beam current of 10 nano-amps, and a beam width of 10 μm. The data were then subject to a ZAF Matrix Correction scheme, to account for bulk-compositional differences between the standards used and the sample being analyzed. The data generated from the Superprobe analysis were then imported into Microsoft Excel®, where they were edited. The oxide percentages, as determined by the microprobe analysis, were scrutinized at each analytical point. For a given slide, the chemical percentages displaying a significant deviation from the observed trend were re-evaluated by referring back to the backscattered electron image. Data that were affected by the interaction of the analyzing beam with inclusions or grain boundaries were identified and discarded.

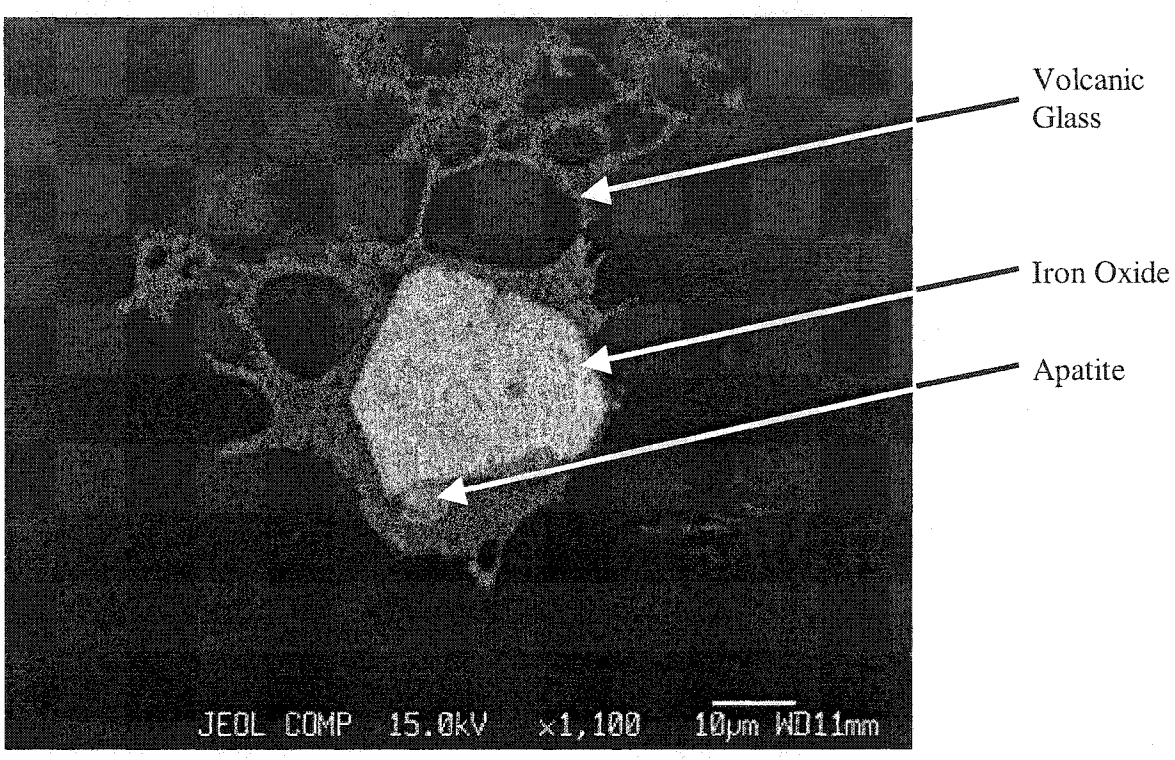


**Figure 7.** Backscattered electron image of an iron oxide/apatite phenocryst surrounded by volcanic glass. The volcanic glass was distinguishable, based on its dark tone and vesicular morphology.

#### 3.2.4.2.2 Magnetite and Ilmenite

The presence of magnetite and ilmenite grains was confirmed through the use of the Superprobe's energy-dispersive spectrometer. A quantitative analysis of $TiO_2$, FeO, $Cr_2O_3$, $Al_2O_3$, MgO and MnO was performed on these minerals, as an additional means to characterize the ash units. The standards used for the analysis were: ilmenite for $TiO_2$ and FeO, chromite for $Cr_2O_3$, $Al_2O_3$ and MgO, and rhodonite for MnO.

Because of the high atomic mass of magnetite and ilmenite, individual grains were identified by their extreme brightness in the backscattered electron image. Due to similarities in brightness and grain morphology, magnetite and ilmenite grains could not be distinguished from one another at this point. Because of this problem, 100 points were analyzed on each slide, where possible, in hopes that a statistically accurate number of measurements would be made on both magnetite and ilmenite grains. Large grains were analyzed in up to two or three areas, making the total number of analyzed grains less than 100 per slide. An accelerating voltage of 15.0 kV, a beam current of 10 nano-amps, a beam with of 10μm, and a ZAF correction scheme were used for these samples. An editorial process, similar to the one preformed on the glass data, was performed on the magnetite and ilmenite data. The only difference was that the data sets were separated into magnetite data and ilmenite data, based on $TiO_2$ concentrations. All valid measurements were then grouped for future analysis.

### 3.2.5 Combustion Analysis

Total organic and total inorganic carbon percentages were determined by combusting 1 $cm^3$ sediment samples at 550 °C and 950 °C, respectively. The procedure used followed the recommendations of Heiri et al. (2001), whereby sample size and

exposure time were kept constant, to insure result reproducibility and accuracy. Samples were first dried overnight at 100 °C to remove pore water. Each sediment sample was then broken up with a mortar and pestle to increase its surface area. The samples were each weighed, prior to being placed in a 550 °C furnace for four hours. Once ignited, the samples were cooled to room temperature and re-weighed. The samples were not cooled in a desiccator because an informal comparison of sample weights, between those samples placed in a desiccator and those not, yielded no measurable weight difference. The total amount of organic carbon in the samples was calculated using the following equation:

$$\%TOC = ((W_{100}-W_{550})/W_{100})*100$$

where %TOC represents percent of total organic carbon, $W_{100}$ represents the sample weight after drying at 100 °C and crushing, and $W_{550}$ represents the sample weight after combustion at 550 ° C.

The samples were then placed in a 950 °C furnace for two hours, cooled to room temperature and weighed again. The total amount of inorganic carbon in the samples was calculated using the following equation:

$$\%TIC = ((W_{550}-W_{950})/W_{100})*100$$

where %TIC represents percent of total inorganic carbon and $W_{950}$ represents the sample weight after combustion at 950 °C; the definition of the remaining terms remains unchanged. Organic and inorganic carbon values were plotted in Microsoft Excel® for analysis.

### 3.2.6 Grain Size Analysis

All three cores collected from Otokomi Lake were sampled for an analysis of their fine-grain (≤ 1 mm) sediment. The sampling procedure employed for this analysis involved the collection of 1 $cm^3$ plugs with a modified syringe, as described in section 3.2.3. The two percussion cores were also sampled for an analysis of their coarse-grain (> 1 mm) fraction. For this analysis the sampling procedure outlined in section 3.2.3, which involved the collection of 1 cm thick core slices, was adopted. Such large sample sizes were necessary, due to the large size of the clasts found in certain core sections.

#### 3.2.6.1 Fine-Grain (≤ 1 mm) Analysis

Fine-grain analyses were performed at the University of Calgary, using a Malvern Instruments® laser-scattering particle analyzer. The 1 $cm^3$ samples collected for analysis were first air dried, then individually powdered with a mortar and pestle and sieved to 1 mm. The ≤ 1 mm fraction was retained and split several times to achieve a weight between 0.15 g and 0.2 g. Because of the configuration of the particle analyzer, this was the requisite weight range for samples having a relatively high sand content. The samples were then placed in Pyrex beakers, into which 2 mL of 30% hydrogen peroxide was added in order to digest the organic fraction of the sediment. The following day, 10 mL of a 25g / L solution of Calgon was added to the beakers, in order to deflocculate any clay aggregates present in the samples, and allowed to sit overnight. The entire mixture was then poured into the particle analyzer, using distilled water to rinse the residue from the beaker into the machine. During this procedure if the obscuration reading on the machine fell below 5% or rose above 25% the samples were discarded and re-sampled at a more appropriate weight for analysis. The obscuration reading can be generally equated

to the concentration of the mixture being analyzed; very low or very high concentrations are not processed accurately. The data generated by the machine were imported into Microsoft Excel®, where they were graphed prior to interpretation.

### 3.2.6.2 Coarse-Grain (> 1 mm) Analysis

The 1 cm thick slices collected for the coarse-grain analysis were first dried at 100 °C overnight, in order to drive off pore water. After weighing the dry samples, they were each wet-sieved with a 1 mm sieve. The > 1 mm size fraction was retained, dried overnight at 100 °C and weighed. Hydrogen Peroxide was not used to digest the organic portion of the coarse material because the organic portion of the retained sediment was visibly minute. The weight percent of coarse material was determined using the following equation:

$$W\% = (W_c/W_t)*100$$

where W% represents the weight percent of the coarse fraction, $W_c$ represents the dry weight of the coarse fraction and $W_t$ represents the dry weight of the entire sediment slice. These data were entered into Microsoft Excel®, where they were graphed for analysis.

### 3.2.7 Magnetic Susceptibility

Magnetic susceptibility is simply defined at the degree to which a substance can be magnetized. In mathematical terms it is represented as the ratio of the intensity of the magnetization to that of the magnetic field responsible for creating it (Exploranium G.S. Ltd, 1995). Magnetic susceptibility measurements were performed using the handheld Exploranium KT-9 Kappameter, equipped with a 10 kHz oscillator. Measurements were

made while the Kappameter was connected to a laptop computer, interfacing with the DOS-based program, Scan 7®.

Magnetic susceptibility measurements were performed only on the un-sampled halves of the two percussion cores. The core catchers were first removed from each core with a saw. All of the core sections were then thawed to room temperature. The plastic stretch wrap was kept on the core sections, so that the Kappameter would not have to be cleaned between readings. Individual core sections were first raised 30 cm above the surface of the laboratory table, by placing them on Styrofoam blocks. All magnetically susceptible material was then removed from within 30 cm of the core section. Using the Scan 7® program, the Kappameter was programmed to record magnetic susceptibility measurements at a rate of 3 times/sec. An initial "zero" measurement was taken with the meter in free space, away from any magnetically susceptible material. Following this, the instrument was placed on the core section with the inductive coil resting on the long axis of the core, midway between the edges of the core tube. At each point the meter then gathered susceptibility data for ten seconds. This process was repeated at 5 mm intervals along the length of the core. The raw data were imported into Microsoft Excel®. All of the measurements from each analytical point were then averaged, prior to plotting then against core depth for analysis.

### 3.2.8 Coarse (> 1 mm) Organic Analysis

Macrofossils encountered at any time during the above analytical procedures were retained, labeled, and stored in water. Where possible, their identity was determined. Organic fragments having a dry mass greater than 10 mg were of particular interest because they could be carbon dated by accelerator mass spectrometry. The ages

of such fragments would serve as chronological markers for the layers of sediment from which they were extracted. In addition, the number of organic fragments encountered during the wet sieving portion of the coarse-grain analysis was recorded. Their concentration was used as a proxy for past plant productivity near Otokomi Lake.

### 3.2.9 Palynological Analysis

Palynological analyses were conducted on 1 $cm^3$ sediment samples that were collected at approximately 10 cm intervals from C1. Although a smaller sampling interval is desirable for many types of palynological analysis (Hills, 2000), the 10 cm interval was thought to be sufficient in order to outline the major patterns of vegetation change following deglaciation of the study site.

The samples were air dried, crushed with a mortar and pestle and then sieved at 1 mm, in order to remove large clastic grains containing no palynomorphs. The $\leq$ 1 mm fraction was then chemically processed, in order to isolate the pollen and spores present in the sediment. This procedure was a modified version of the methods outlined in *Palynology Preparation Technique, University of Calgary Micropaleontology Lab* (Bloom, unpublished literature). The samples were first placed in 10% HCl overnight to remove carbonate material. The samples were then subjected to a hot HF treatment, which digested any silicate minerals present. Unwanted organic material was subsequently oxidized from the samples by bathing them in Schulze solution for a period of thirty seconds. After this point, two tablets of *Lycopodium* spores were added to the wet samples and allowed to dissolve. These exotic marker grains were used as a means to calculate pollen influx rates in the basin. The samples were then sieved with 10 µm sieve

cloth and the > 10 μm fraction was retained for analysis. The isolated palynomorphs were not stained prior to being mounted on microscope slides for examination.

The prepared slides were scanned under 200 x magnification, with individual pollen and spore identifications being performed under both 400 x magnification and 1000 x oil immersion, when necessary. Reference to various palynological textbooks, reference slides, and to Dr. Len Hills himself facilitated identification of the palynomorphs. This identification was accurate only to the level of genus for many of the palynomorphs present. In order to generate statistically valid data, an attempt was made to count 300 grains per slide. For samples with low native-pollen concentrations, the number of native palynomorphs present on the entire slide was recorded. The pollen data were then plotted for analysis.

# 4. Results

## 4.1 Site Description and Survey

Otokomi Lake in Glacier National Park, Montana was chosen as the study site for this project (Fig. 8). The climate of Glacier National Park is considered a transition between a northern pacific coastal climate and a continental climate. Average annual precipitation on the east side of the continental divide can reach 260 cm / yr. This area of the park has highly variable winter temperatures, with alternating arctic and pacific airflows. Throughout all areas of the park the prevailing wind direction is from the west (Finklin, 1986).

Access to the site is via the Rising Sun Campground, from which a 9 km long trail makes its way alongside Rose Creek to the lake itself. This area of Glacier National Park lies on west-dipping, thrust-faulted meta-sedimentary and meta-volcanic strata of the Proterozoic-aged Belt-Purcell Supergroup. The lake itself rests on argillites, quartzites and siltites from the Grinnell and Appekunny formations, whereas the mountains above the lake also contain some argillites and siltites from the Empire Formation. The lake has a surface area of approximately 10 hectares, a maximum depth of 54 m, a secci depth of 5.9 m, a "tear-drop" shape, and is located at 48° 42' 50" N, 113° 35' 53" W, at an elevation of 1976 m asl There is one main outlet, Rose Creek, draining to the northeast, with a late-summer discharge of approximately 4.52 $m^3$/min. One small inlet stream enters the lake from the southwest, sourced from a small pond perched on bedrock cliffs west of the lake. There are also several ephemeral inlet streams located around the lake's perimeter. The most prominent of these streams enters the lake from the south and has an estimated maximum flood-velocity of approximately 2.9 m / s; such a velocity is capable

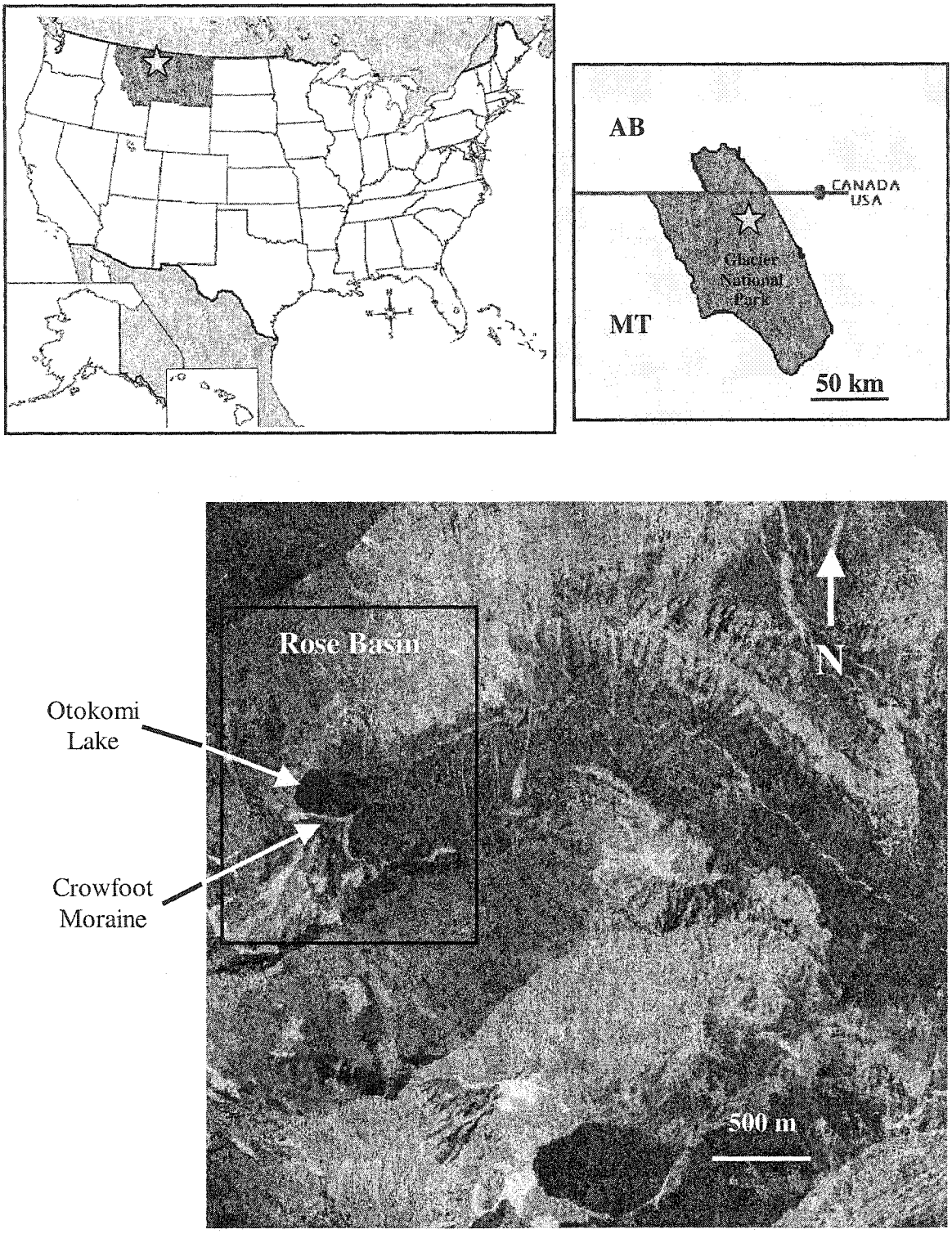


**Figure 8.** Location of Glacier National Park, Montana, Rose Basin and Otokomi Lake. Photo courtesy of the U.S. Department of the Interior.

of transporting pebble-sized clasts as bed load (Prothero and Schwab, 1996). The north shore and eastern margins of the lake are bordered by scrubby forest and herbaceous lakeshore vegetation, whereas the west end of the lake meets bedrock cliffs. A small talus slope, sourced from these cliffs, builds into the northwest end of the lake.

To the south of the lake is a cirque, with an average headwall elevation of 2401 m asl that now holds only a small amount of perennial ice. At the bottom of the cirque, in contact with the southern shore of the lake, is a vegetated Crowfoot moraine, which is approximately 10 m tall and 200 m long. Two lateral moraine ridges connect to the terminal moraine, which borders the lake (Fig. 9). A pit, dug into the crest of the terminal moraine, confirmed the presence of glacial till. No obvious LIA moraine was deposited upstream of this older moraine; only hummocky terrain, comprised of glacial diamict, was seen.

The elevation of Otokomi Lake is below modern day tree line, which is approximately 2244 m asl in Rose Basin, and up to 2378 m asl on the south-facing slopes of nearby mountains. Conifer trees, such as Subalpine Fir, White Pine and White Spruce are common in the study area. Shrubby vegetation at the site includes Gooseberry, Honeysuckle, Willow and Shrubby Penstemon. Native herbaceous plants include Cut Leafed Anemone, Grass of Pernasis (among other grasses), Sow Thistle, Glacier Lilly, Arnica, Timothy, St Johnswort, Cowparsnip, Fireweed, Monkey Flowers, Pussy Toes and several other species for which field-identification was difficult. This plant community is typical of the sub-alpine environments on the east side of the park (Shaw and On, 1979). Included in this community are species adapted to the cool, dry conditions of exposed mountain slopes and also those characteristic of wetter and more sheltered

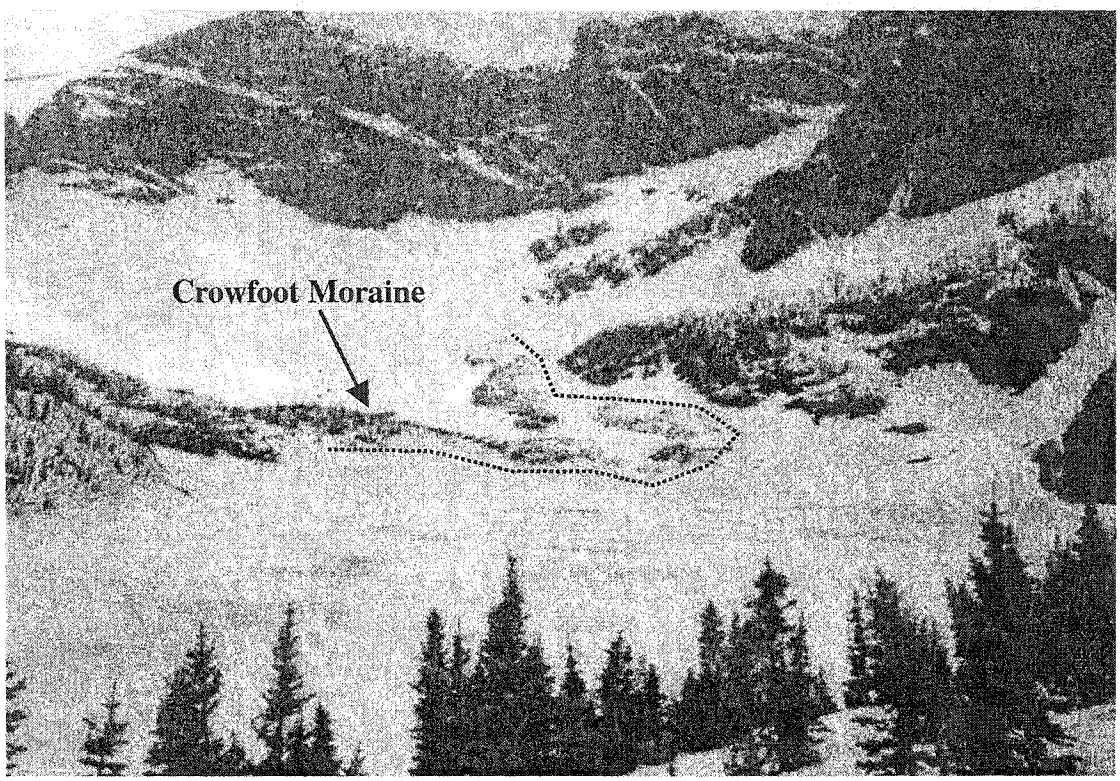


**Figure 9.** View of Otokomi Lake, looking southwest. The Crowfoot moraine can be seen bordering the lake's southern shore. The dashed line outlines terminal and lateral portions of the moraine and is located on the distal side of the moraine crest.

environments, like those found along the margins of Rose Creek and Otokomi Lake (Shaw and On, 1979; Spurr and Barnes, 1980; Ringius and Sims, 1997).

**4.2 Sonar Profiling**

An example of one of the sonar profiles obtained from Otokomi Lake, and a schematic representation of its interpretation, can be seen in Figure 10; the six other sonar profiles can be seen in Appendix A. The sonar data obtained from the four north-south transects reveal a simple basin profile with a symmetrical funnel shape. In these profiles the basin has a slope of approximately 30° and a maximum profundal zone width of 50 m. The sonar profile taken along the long axis of Otokomi Lake did not reveal any irregularities in the morphology of the profundal zone, such as bedrock protuberances or ridges separating the main basin into sub-basins. Because of this, and the fact that the basin appears quite symmetrical in north-south cross-section, core collection sites would ideally be located along the long axis of the lake, equidistant from the north and south shores. Such sites would allow core penetration into the flat-lying profundal sediment at the basin's centre, where sediment accumulation and preservation are maximized. Because the lakebed is not flat over most of its extent, the sonar signal was often reflected at an angle off of the lakebed, before returning to the transceiver. This effect causes distortion in the data that is generated and may misrepresent the true slope-angle of the lakebed reflector (Jones, 1999). In light of this distortion, the data can be "corrected" through migration. When a sample time migration was performed on an individual profile, the true angle of the lakebed was found to be near 35°. The difference between the true and apparent dip angles was not considered significant in terms of its effect on interpretation of sediment transport and deposition processes in the lake basin,

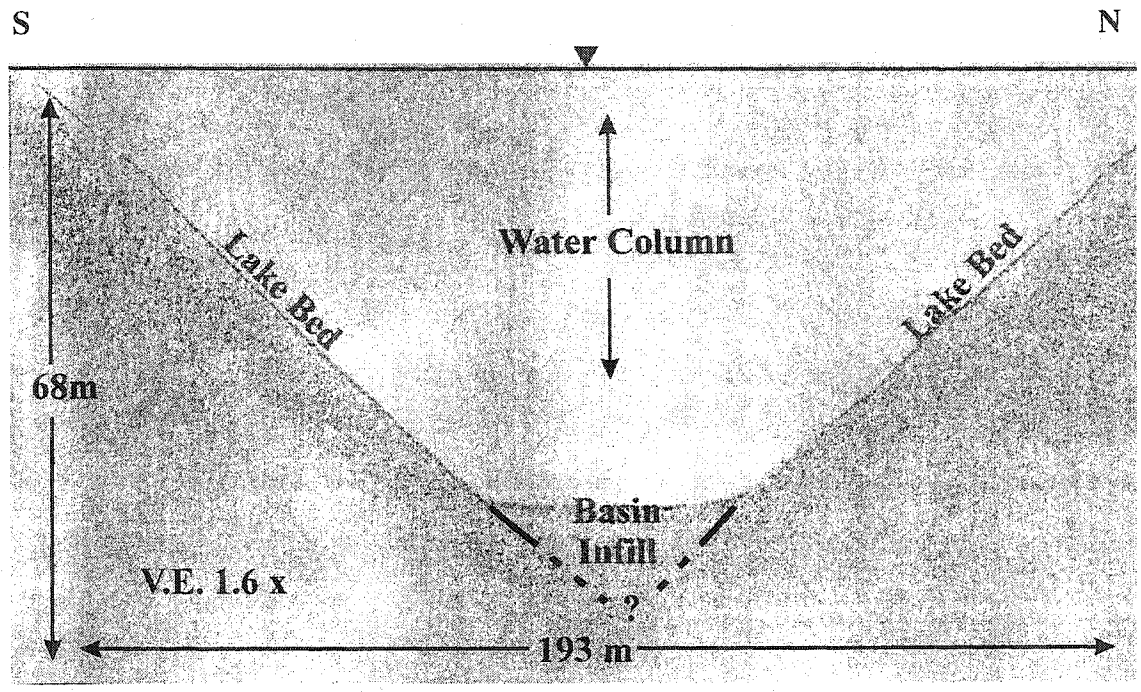


**Figure 10.** Sample interpretation of a north-south sonar profile taken from Otokomi Lake. The faint line, which can be seen below the lakebed reflector, is likely an artifact of the collection technique and not the underlying bedrock.

therefore the remainder of the sonar data were not migrated. The bathymetric map created from the sonar data can be seen in Figure 11. Although this map is a valuable interpretive tool, it is only a generalization made from the sonar data, and the true basin morphology may contain features that were not resolved.

**4.3 Lake Temperature Profile**

The temperature data that were obtained from Otokomi Lake are presented in Figure 12. The lake exhibits thermally stratified water in the summer months, with a thermocline depth of approximately 14 m. This thermocline separates the warm waters of the epilimnion from the cold waters of the hypolimnion. The presence of such stratification likely affects the transportation and distribution of fine particulates within the basin (Håkanson and Jansson, 1983).

**4.4 Xradiography**

Because of the amount of sediment recovered in C1, X-ray images of from this core were scanned and analyzed. Of the two core orientations that were imaged, the 90° x-ray image was chosen for scanning (Fig. 13). This was due to the fact that the cores were subsequently split-open along the 0° plane and, as a consequence, the cut-surface and the 90° x-ray image both represented views from the same perspective. When plotted in Excel®, the grayscale values of the X-ray image were generally found to decrease with depth (Fig. 14). Almost all sample points from the top of the core to a depth of 40 cm had a grayscale value of 200, which was the highest value recorded for the entire core. Two main deviations from the general trend of decreasing grayscale values with depth were seen (Fig. 15); one was over the depth range of 107 cm – 124 cm, where grayscale values were lower than those expected from the general trend; the other was between depths of

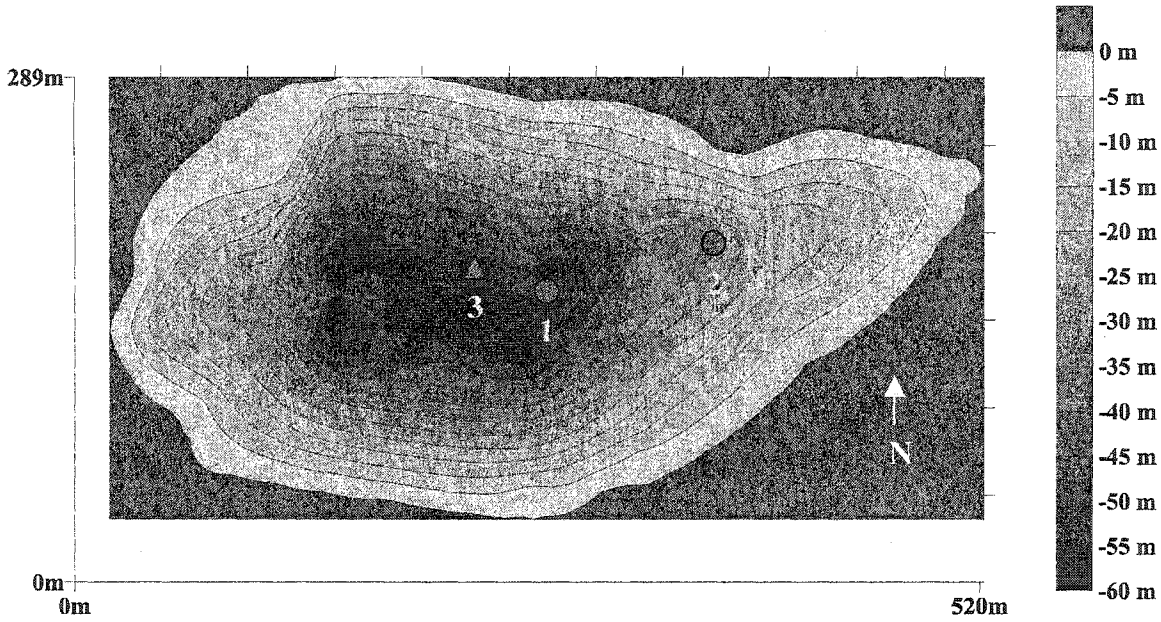


**Figure 11.** Bathymetric map of Otokomi Lake, generalized from data obtained on six sonar transects. The lake has a simple funnel shape, which is slightly disrupted by sediment influx from a talus slope in the lake's NW corner. Core locations and numbers are indicated on the map; percussion cores represented by circles, and the gravity core by a triangle.

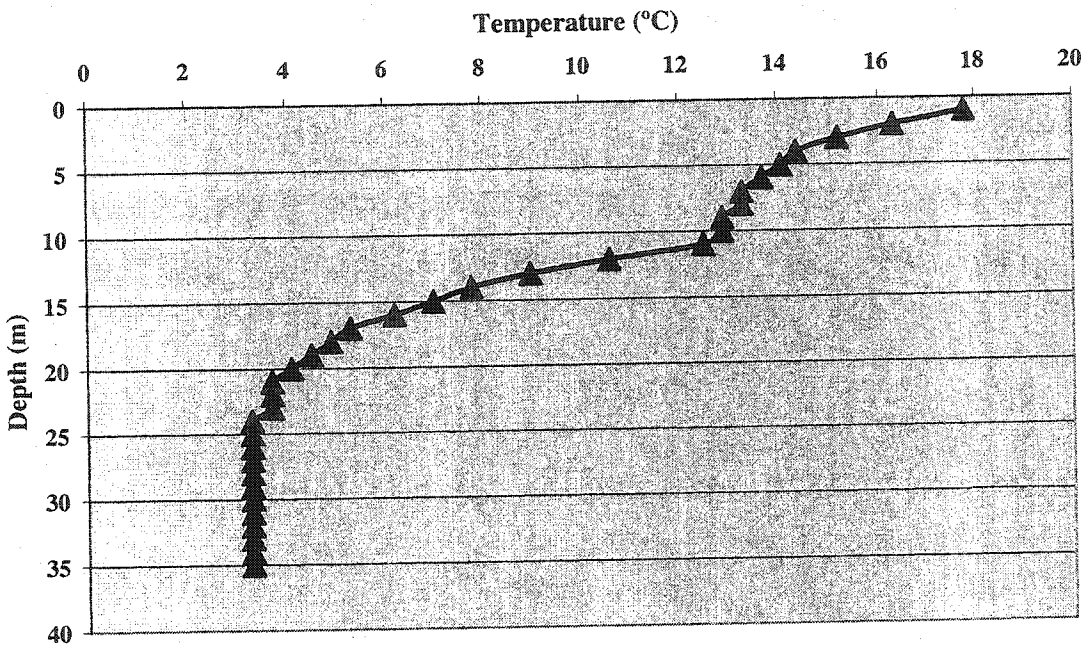


**Figure 12.** Temperature profile for Otokomi Lake showing thermal stratification, with a thermocline depth of approximately 14 m.

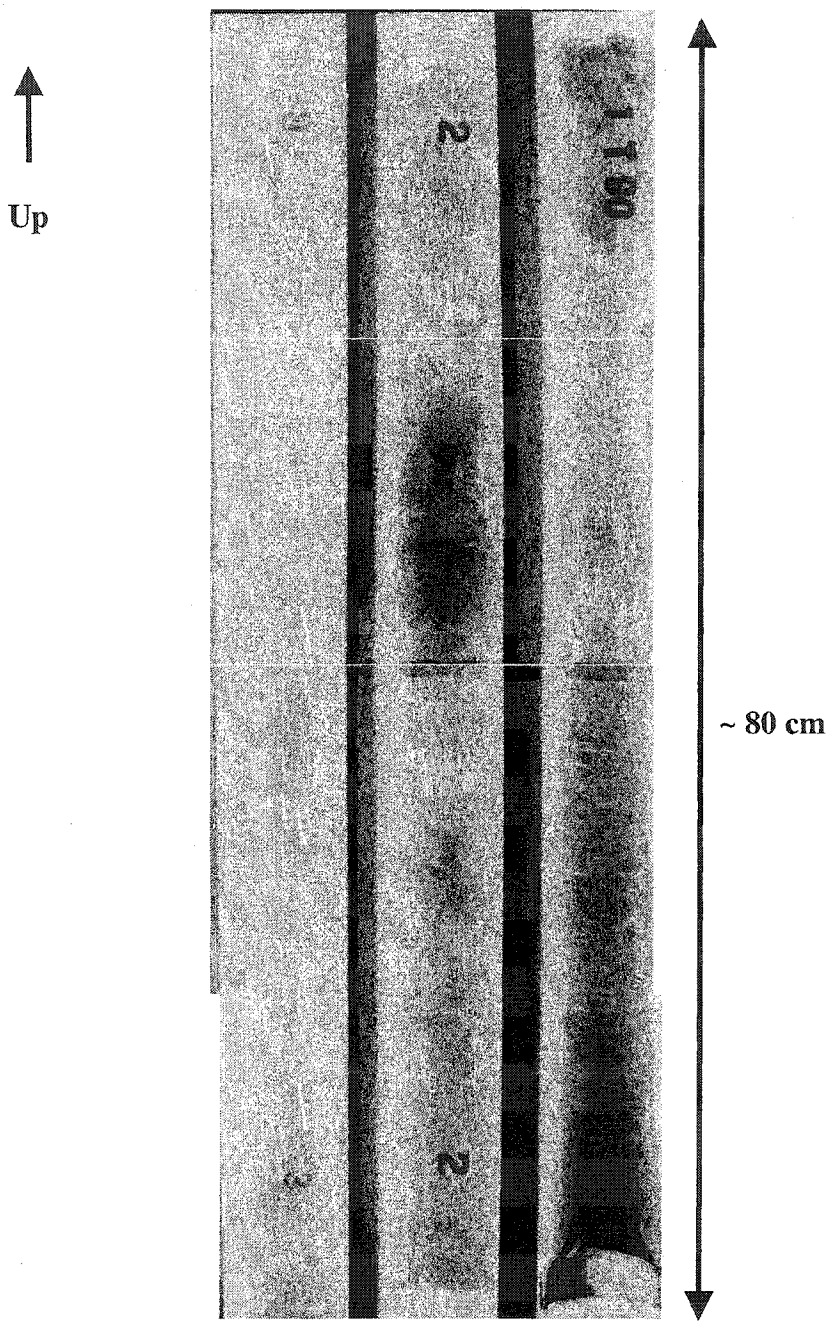


**Figure 13.** 90° composite X-ray image of percussion core C1. Of the three sections, the left represents the top of the core, the centre section represents the middle of the core and the section on the right represents the bottom of the core. Note the metal core catcher located at the bottom of the right section.

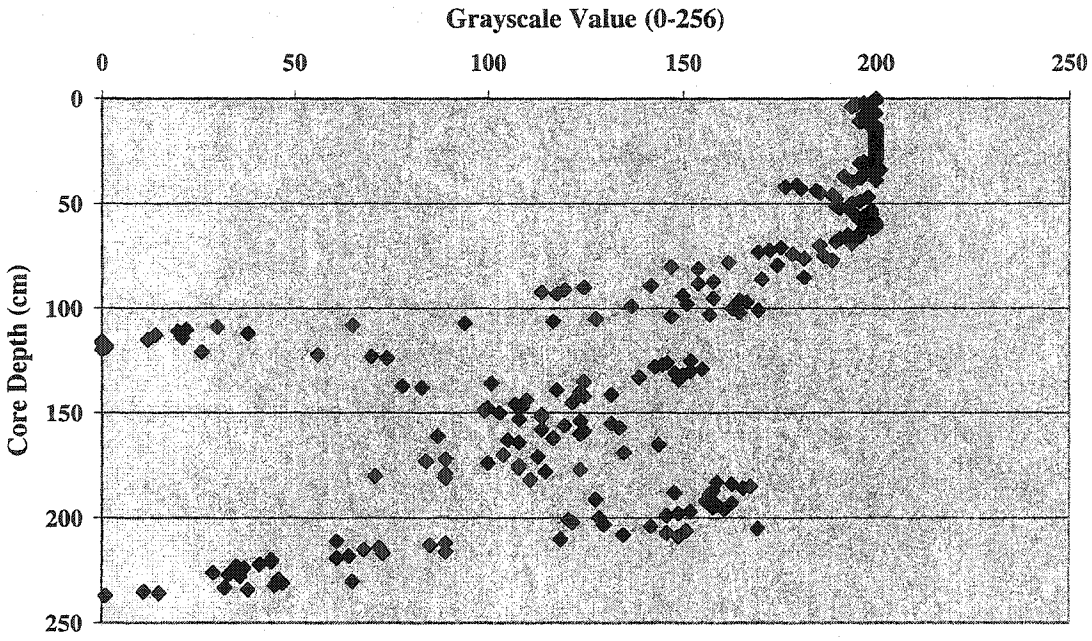


**Figure 14.** Plot of xradiograph grayscale values vs. depth for Otokomi Lake core C1.

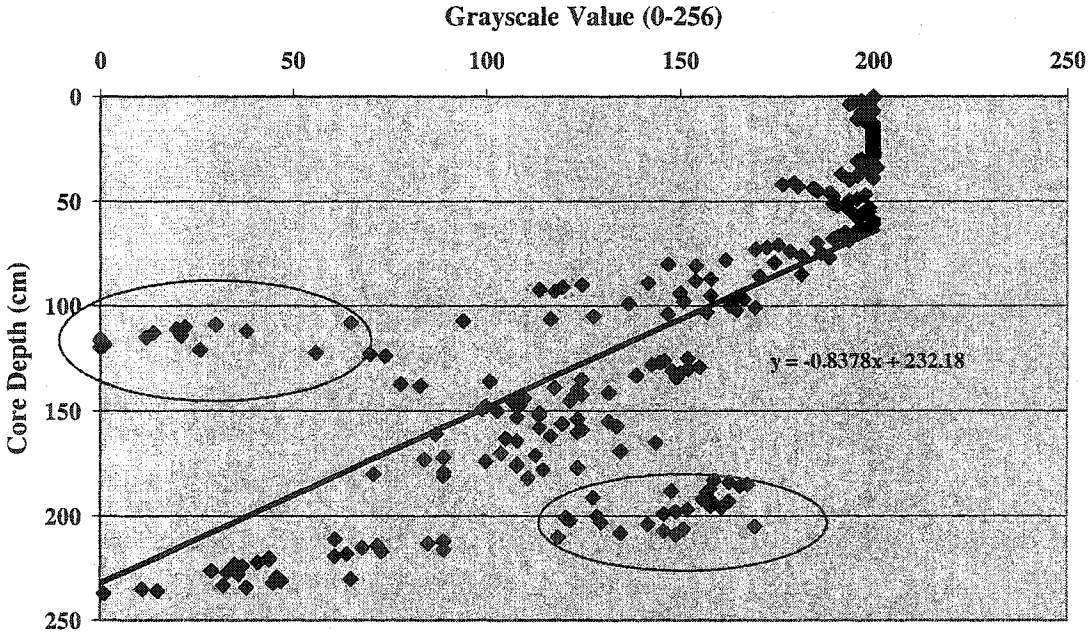


**Figure 15.** Plot of xradiograph grayscale values vs. depth for Otokomi Lake core C1 with trend line added. Areas with the largest deviations from the trend are circled.

183 cm and 209 cm, where the grayscale values were higher than would be expected from the overall trend. Although xradiograph images were also taken of C2, the grayscale values from these images were not tabulated because the core was not thought to contain the sedimentary layers of primary interest to this project.

## 4.5 Descriptive Stratigraphy

### 4.5.1 Percussion Cores

Just over 240 cm of sediment was retrieved from the bottom of Otokomi Lake in C1, whereas C2 contained approximately 120 cm of sediment upon recovery. Visual inspection of each core revealed very little organic matter, save a few centimeters of organic-rich sediment at the top of C1. The dominant sediment color in each core ranged from pink to shades of brown and red. All of the sediment layers in the two cores exhibited a concave-down parabolic appearance, which is attributed to the friction experienced between the sediment and the sides of the core barrel during core collection. In C1 these layers were not symmetrical, but appeared to be drawn-down to a greater extent on one side of the core barrel. The apex of these asymmetrical curves was also slightly off-centre.

During the retrieval of C1, coarse pebbles in a clay-rich matrix were observed adhering to the inside of the core barrel below the core catcher. This material fell from the core tube during handling and was not retained for analysis. From the core catcher to a depth of 205 cm in C1 there was a zone of laminated clay-rich sediment containing occasional pebbles. Directly above this zone, centered at depths of 204.2 cm and 200.9 cm were two volcanic ash layers, with thicknesses of 4 mm and 10 mm respectively. Above these layers the core changed dramatically to a dark brown silty-clay matrix

containing many scattered pebbles. At a depth of 170 cm the core matrix changed to light red silty-clay, although the scattered pebbles remained. This matrix was interrupted at 124 cm by a 15 cm thick zone of very coarse pebbles containing no fine-grained matrix. The top half of this zone contained a matrix of volcanic ash. Directly above the pebble zone was a globular lens of volcanic ash, approximately 10 cm thick. The light red silty-clay matrix with scattered pebbles resumed above this lens to a depth of 86 cm, above which only the matrix color changed, becoming dark red. This dark red sediment was overlain by a 5 cm thick layer of organic rich sediment at the top of the core.

Between the depths of 108 cm and 113 cm in C2 there was a zone of very coarse pebbles containing no fine-grained matrix. This was overlain and underlain by volcanic ash, similar to the manner in which the coarse pebble zone was associated with volcanic ash in C1. Above the ash, to a depth of 67 cm, there was a zone of light brown silty-clay with many scattered pebbles. Overlying this zone was a one-centimeter thick layer of volcanic ash, which was connected to the lower ash layer via a thin ash conduit located at the edge of the core barrel. This ash was overlain by a 4 cm thick void space. From a depth of 62 cm to the top of the core was a zone containing a dark red silty-clay matrix and scattered pebbles. Almost no organic-rich sediment was seen at the top of C2.

Both percussion cores contained many conspicuous minerogenic horizons. The majority of these horizons consisted of pebbles, ranging in thickness from a few millimeters to several centimeters. Clast alignment in the pebble horizons was often parallel to bedding and most clasts appeared to be matrix supported. A few pebble horizons appeared to be the basal portion of graded beds. In C1 there were also a few silt-dominated minerogenic horizons, and one clay horizon. The coarse minerogenic horizons

and scattered pebbles in C1 appeared above 185 cm, with the exception of one very thin pebble layer at 221 cm. Many minerogenic horizons were also found along the length of C2, with all of them containing pebbles. In addition to minerogenic horizons, five layers containing small black organic fragments were seen in C2.

### 4.5.2 Gravity Core

The single gravity core collected from Otokomi Lake (C3) was 19 cm in length. The top 5 cm of the core contained highly organic dark-brown gyttja with visible plant fragments. Between 5 cm and 11 cm there was a brown organic-rich silty clay zone with scattered pebbles. A pink, clay-rich zone with scattered pebbles and fine laminations was observed between 11 cm and 19 cm. Descriptions of core stratigraphy, locations of minerogenic and organic horizons, and possible stratigraphic correlations between all three cores are shown in Figure 16.

## 4.6 Tephra Identification

All three of the suspected volcanic ash layers in C1 appeared to have glass shards in them when analyzed under a binocular microscope at 100 x magnification. The upper and lower boundaries of the 200.9 cm and 204.2 cm ash layers in C1 appeared sharply defined and were laterally continuous. The ash lense centered at 103.7 cm was laterally discontinuous and had convoluted upper and lower contacts. The ash layer centered at 204.2 cm appeared off-white and was composed of fine-sand sized grains. The ash layer centered at 200.9 cm had a banded appearance, with alternating off-white and black bands, giving the layer a "salt and pepper" look. This layer was also composed to fine-sand sized grains. The layer centered at 103.7 cm had a gray appearance, with no banding, and was composed of fine-grained sand.

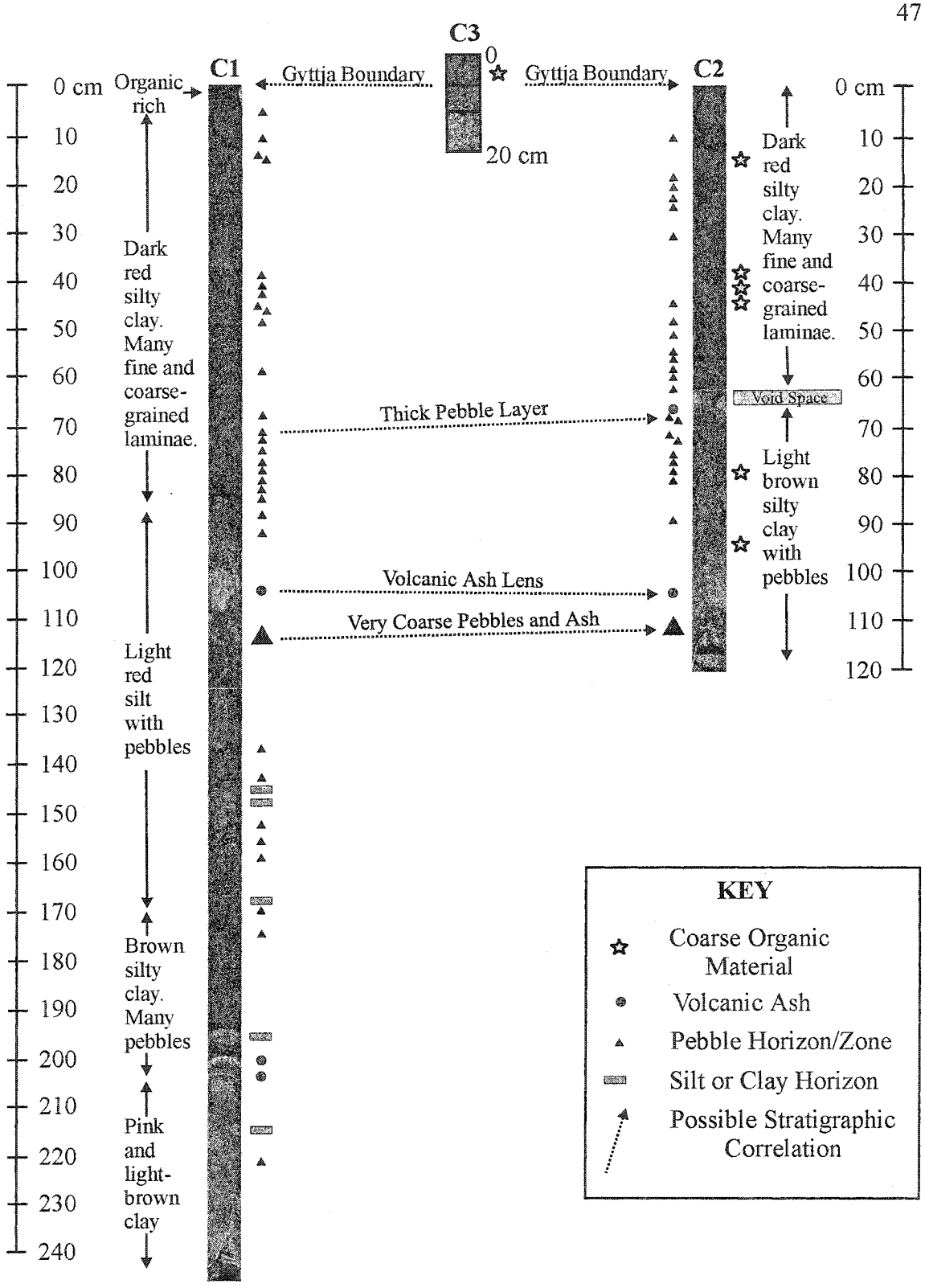


**Figure 16.** Generalized stratigraphy for Otokomi Lake cores C1, C2 and C3. Note that color and grain size descriptions are not presented for C3, as the sedimentary zones are too close together for such text to fit. See **4.5.2** for descriptions.

### 4.6.1 Microprobe Analysis

#### 4.6.1.1 Volcanic Glass

The SEM images of the < 2.42 G "light" fraction of each ash layer revealed the presence of many vitreous, vesicular shards. The shards in each sample appeared platy and included elongate, furrowed, and curved varieties. In each sample there were also examples of Y-shaped shards and many large, complex, vesicular masses (Fig. 17). The glass shards also contained phenocrysts, which differed from the glass in their geometry, brightness and lack of vesicles. The abundance of vesicles in the three ash samples varied; the layer centered at 204.2 cm contained the most vesicles, followed by the layer centered at 200.9 cm, and lastly by the ash lens centered at 103.7 cm. The shards from the ash layer centered at 200.9 cm were, on average, the largest of the three samples, with the other two samples having shards of approximately the same size. A summary of the various grain-size measurements conducted on the three ash samples can be seen in Table 1. The 103.7 cm sample contained shards of two distinct photographic tones; approximately one third of the shards had a light tone and the remaining two thirds of the shards had a dark one (Fig. 18).

The 200.9 cm and 204.2 cm ash samples had chemically very similar glass fractions, whereas the 103.7 lens was chemically distinct (Table 2).

#### 4.6.1.2 Magnetite and Ilmenite

The chemical data obtained for the 103.7 cm sample revealed only low $TiO_2$ percentages, characteristic of magnetite grains. Therefore, ilmenite was either scarce or not present at all in the analyzed sample of that ash deposit. For the other two ash layers the ilmenite compositions were quite similar. The magnetite data for all three ash

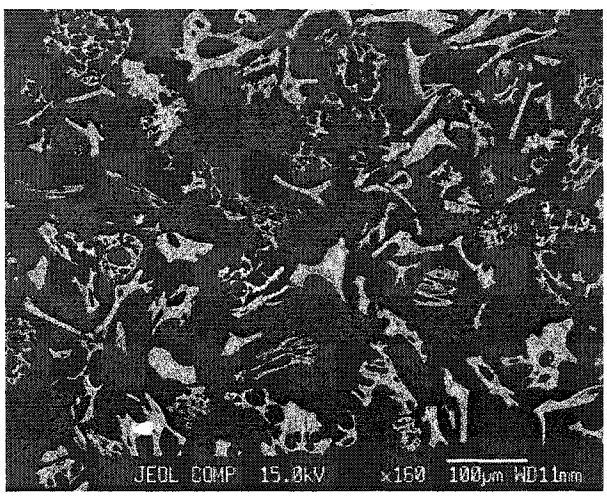


Ash Lens
Depth: 103.7 cm

Ash Layer
Depth: 200.9 cm

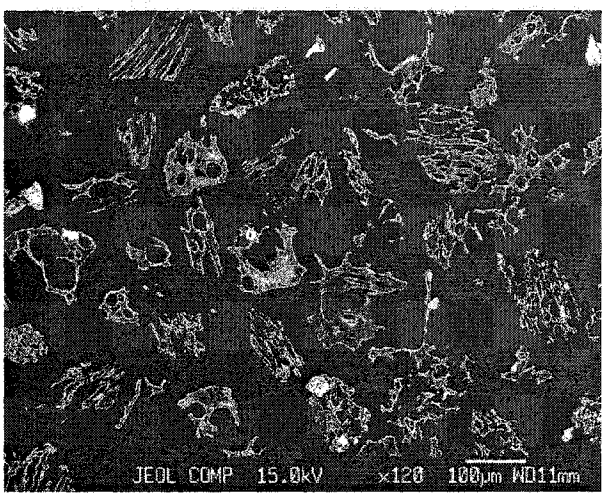


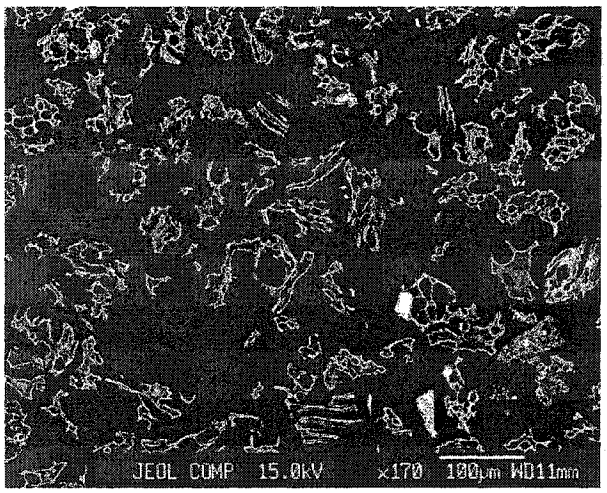


Ash Layer
Depth: 204.2 cm

**Figure 17.** SEM images of the < 2.42 G fraction of the three volcanic ash units found in Otokomi Lake C1. Note the scarcity of vesicles in the 103.7 cm sample.

**Table 1.** Grain size measurements for the three volcanic glass samples collected from Otokomi Lake C1.

| Ash Sample | Mean Grain Area ($\mu m^2$) | Mean Long Axis Length ($\mu m$) | Median Long Axis Length ($\mu m$) | Mean Perimeter ($\mu m$) | Mean Roundness | Sample Size (n) |
|---|---|---|---|---|---|---|
| **103.7 cm** | 1268.90 | 74.55 | 72.36 | 292.46 | 0.22 | 80 |
| **200.9 cm** | 3523.92 | 106.55 | 100.32 | 531.76 | 0.20 | 56 |
| **204.2 cm** | 1323.75 | 70.13 | 65.38 | 327.89 | 0.19 | 73 |

**Table 2.** Average chemical composition of the three volcanic glass samples collected from Otokomi Lake C1. All values corrected to a total of 100%. Original totals ranged from 94.1% - 97.5 %, with the remaining fraction assumed to be water. The number of sample points (n) used in each analysis is presented in the last column. *Total iron expressed as FeO.

| | $K_2O$ (%) | CaO (%) | *FeO (%) | $Na_2O$ (%) | $SiO_2$ (%) | $TiO_2$ (%) | MnO (%) | $Al_2O_3$ (%) | MgO (%) | Total (%) | n |
|---|---|---|---|---|---|---|---|---|---|---|---|
| **103.7 cm (All Grains)** | 2.69 | 1.90 | 2.24 | 5.27 | 71.76 | 0.50 | 0.06 | 14.95 | 0.62 | 100.00 | 49 |
| **103.7 cm (Dark Grains)** | 2.82 | 1.58 | 1.86 | 5.33 | 72.88 | 0.43 | 0.05 | 14.58 | 0.47 | 100.00 | 36 |
| **103.7 cm (Light Grains)** | 2.34 | 2.81 | 3.29 | 5.12 | 68.67 | 0.69 | 0.07 | 15.96 | 1.05 | 100.00 | 13 |
| **200.9 cm (All Grains)** | 3.55 | 1.16 | 0.97 | 3.93 | 77.22 | 0.19 | 0.03 | 12.71 | 0.23 | 100.00 | 56 |
| **204.2 cm (All Grains)** | 2.49 | 1.35 | 1.17 | 3.92 | 77.21 | 0.18 | 0.02 | 13.37 | 0.27 | 100.00 | 46 |

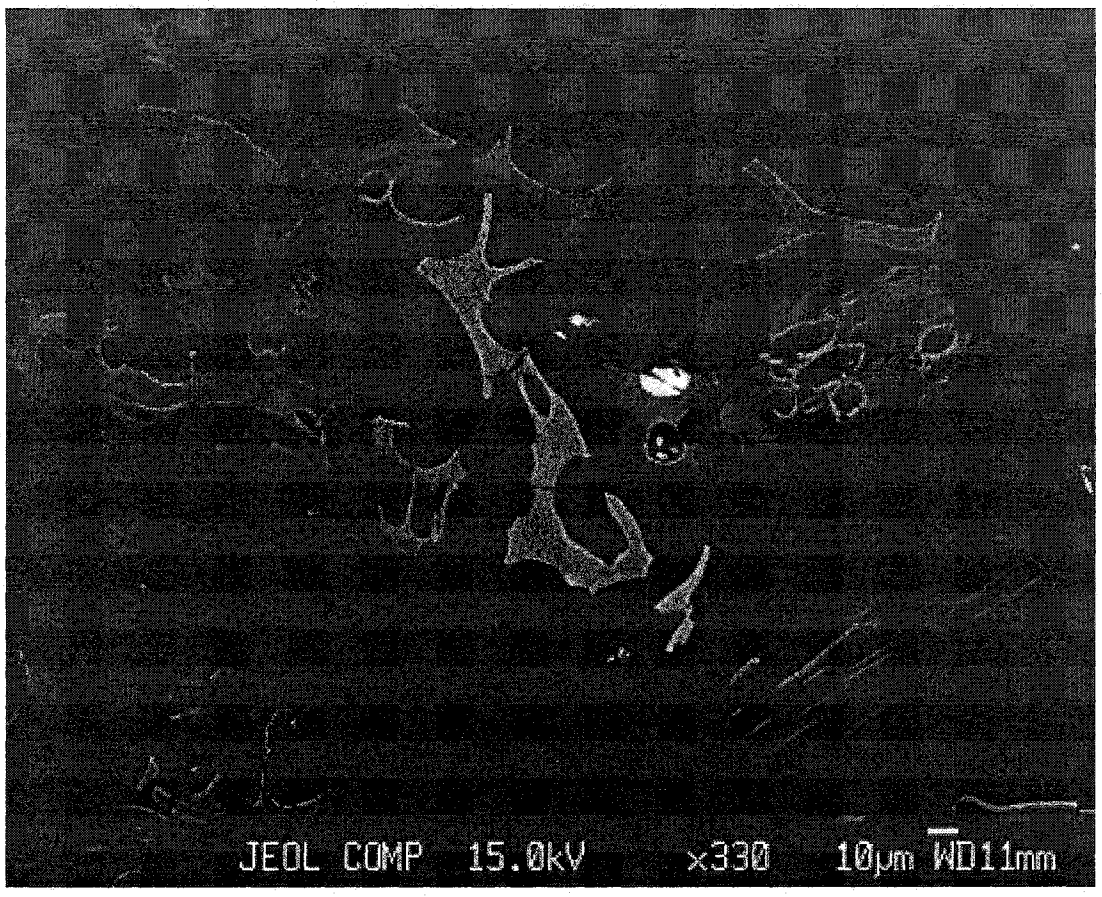


**Figure 18.** SEM image of glass shards isolated from the 103.7 cm tephra lens. Note the light tone of the shard in the centre of the image, compared to that of the surrounding shards.

samples, along with the ilmenite data for the 200.9 cm and 204.2 cm samples, are presented in Table 3.

For the magnetite and ilmenite analyses, the total percentage of chemical species present in each sample ranged between 99% and 91%. The samples having the lowest total percentages may have contained certain chemical species that were not accounted for in the microprobe analysis. These species could have been hydroxides, for which the water of hydration is unquantifiable through microprobe analysis or reduced compounds such as pyrite. As such, the magnetite and ilmenite data were considered unreliable and not formerly compared with the literature.

### 4.7 Combustion Analysis

#### 4.7.1. Organic Carbon

Organic carbon values in Otokomi Lake C1 ranged from 1.5% to 12.3% by weight. From the bottom of the core to a depth of 126 cm organic carbon values remained quite close to 3%, above which depth the values generally increased but showed more variability. No combustion data were generated for the 97 cm – 124 cm interval because of the extremely coarse nature of the sediment.

Organic carbon values in Otokomi Lake C2 ranged from 3% to 9.5% by weight. The trend was generally linear with an average value of 5%. The one major deviation from this trend was a sharp increase in organic carbon between depths of 51 cm and 53 cm. In general, the organic carbon data from C2 displayed less variability than that from the same interval in C1.

**Table 3.** Average chemical composition of the magnetite and ilmenite grains isolated from the three volcanic ash layers found in Otokomi Lake C1. Note that no ilmenite data is presented for the 103.7 cm sample, due to the absence of these grains on the prepared slide. The number of sample points (n) used in each analysis is presented in the last column.

| | | $TiO_2$ (%) | FeO+ $Fe_2O_3$ (%) | $Cr_2O_3$ (%) | $Al_2O_3$ (%) | MgO (%) | MnO (%) | Total (%) | n |
|---|---|---|---|---|---|---|---|---|---|
| **103.7 cm** | Magnetite | 7.04 | 81.04 | 0.01 | 2.47 | 2.68 | 0.44 | 93.69 | 19 |
| **103.7 cm** | Ilmenite | N/A | N/A | N/A | N/A | N/A | N/A | N/A | 0 |
| **200.9 cm** | Magnetite | 6.33 | 85.83 | 0.08 | 2.03 | 1.32 | 0.37 | 95.96 | 65 |
| **200.9 cm** | Ilmenite | 37.84 | 58.34 | 0.02 | 0.24 | 2.13 | 0.45 | 99.02 | 32 |
| **204.2 cm** | Magnetite | 6.46 | 81.05 | 0.05 | 2.03 | 1.29 | 0.32 | 91.20 | 75 |
| **204.2 cm** | Ilmenite | 38.06 | 53.87 | 0.01 | 0.22 | 2.19 | 0.42 | 94.77 | 22 |

In Otokomi Lake C3, organic carbon values ranged from 6% to 17.5% by weight. The highest values were found at the top of the core and the lowest value at a depth of 11.5 cm. The organic carbon data for all three cores can be seen in Figure 19.

### 4.7.2 Inorganic Carbon

Inorganic carbon values in C1 ranged from 0% to 3.6% by weight. Values were the highest at the top and bottom of the core, with the lowest values occurring between depths of 78 cm and 151 cm.

Inorganic carbon values for C2 ranged from 0.34 % to 5.7% by weight. Values were at their lowest at the bottom of the core and increased to their maximum value of 5.7% at 50 cm depth, after which they decreased towards the core-top to a low of 2.1%.

In C3 the inorganic carbon values ranged from 2.4% to 6.3% by weight. From the bottom of the core to a depth of 6.5 cm the values remained very close to 3%, after which point they increased steadily to their maximum value of 6.3% at the top of the core. The inorganic carbon values for all three cores can be seen in Figure 20.

## 4.8 Grain Size Analysis

### 4.8.1 Fine-Grain (≤ 1 mm) Analysis

The percentage of clay in C1 ranged from 0% to 33.4%, with the highest clay percentages near the core bottom. Clay percentages were near zero over the interval of 118 cm –92 cm and also from 54 cm to the core top. In C2 the clay percentages ranged from 7.7% - 0%, with an average value of about 1%. Clay percentages remained near this average throughout the length of the core. In C3 the percent of clay in the samples ranged from 0% - 11.5%, with the highest values found near the core bottom. Figure 21 displays the percentage of clay in the ≤ 1 mm fraction of the sediment in cores C1, C2 and C3.

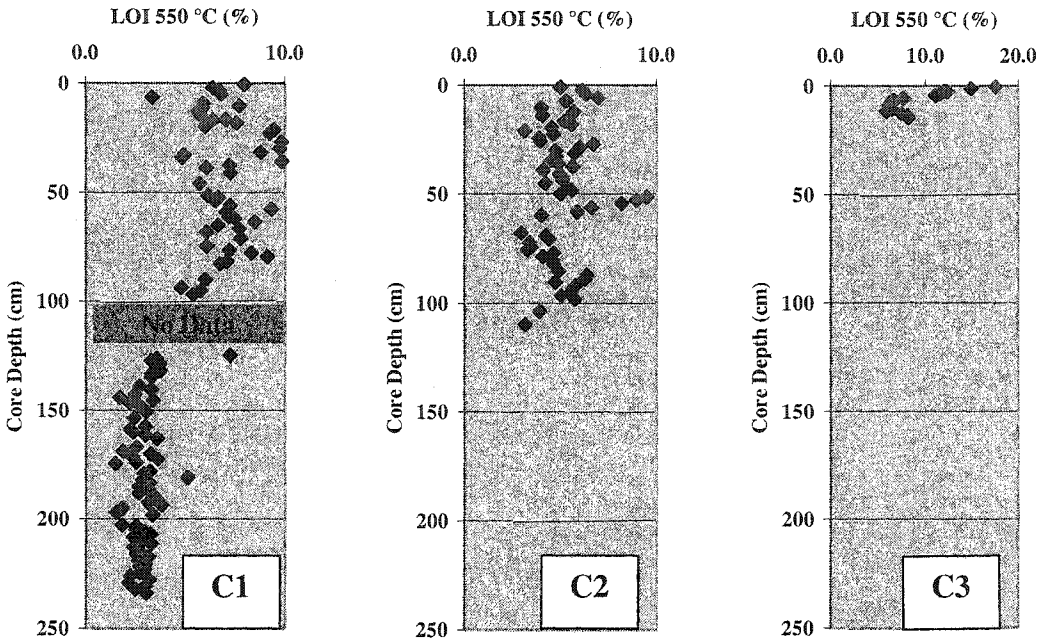


**Figure 19.** Organic carbon values for Otokomi Lake cores C1, C2 and C3.

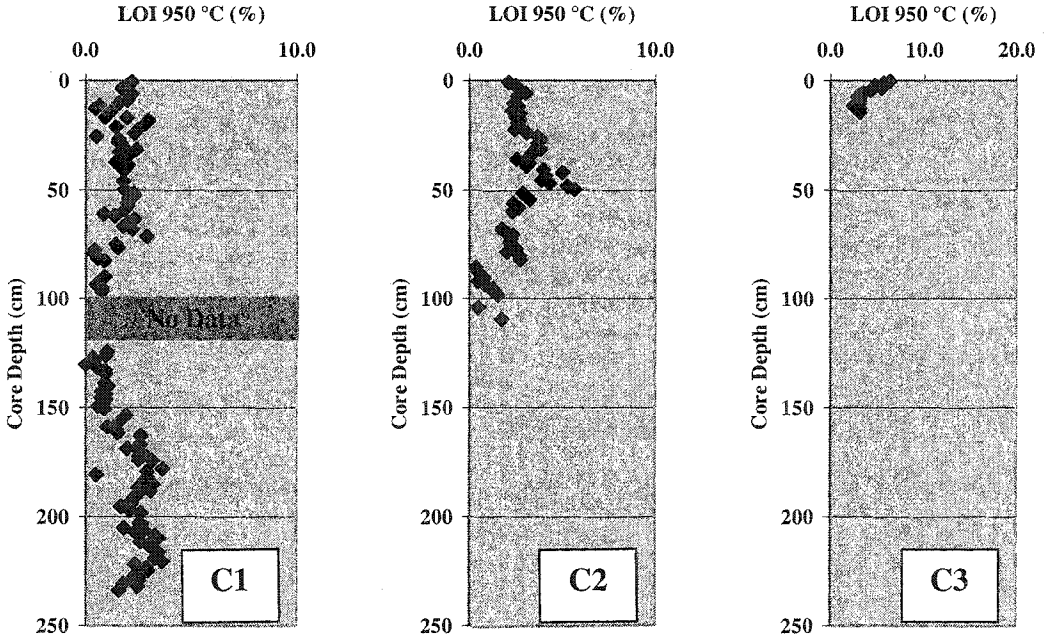


**Figure 20.** Inorganic carbon values for Otokomi Lake cores C1, C2 and C3.

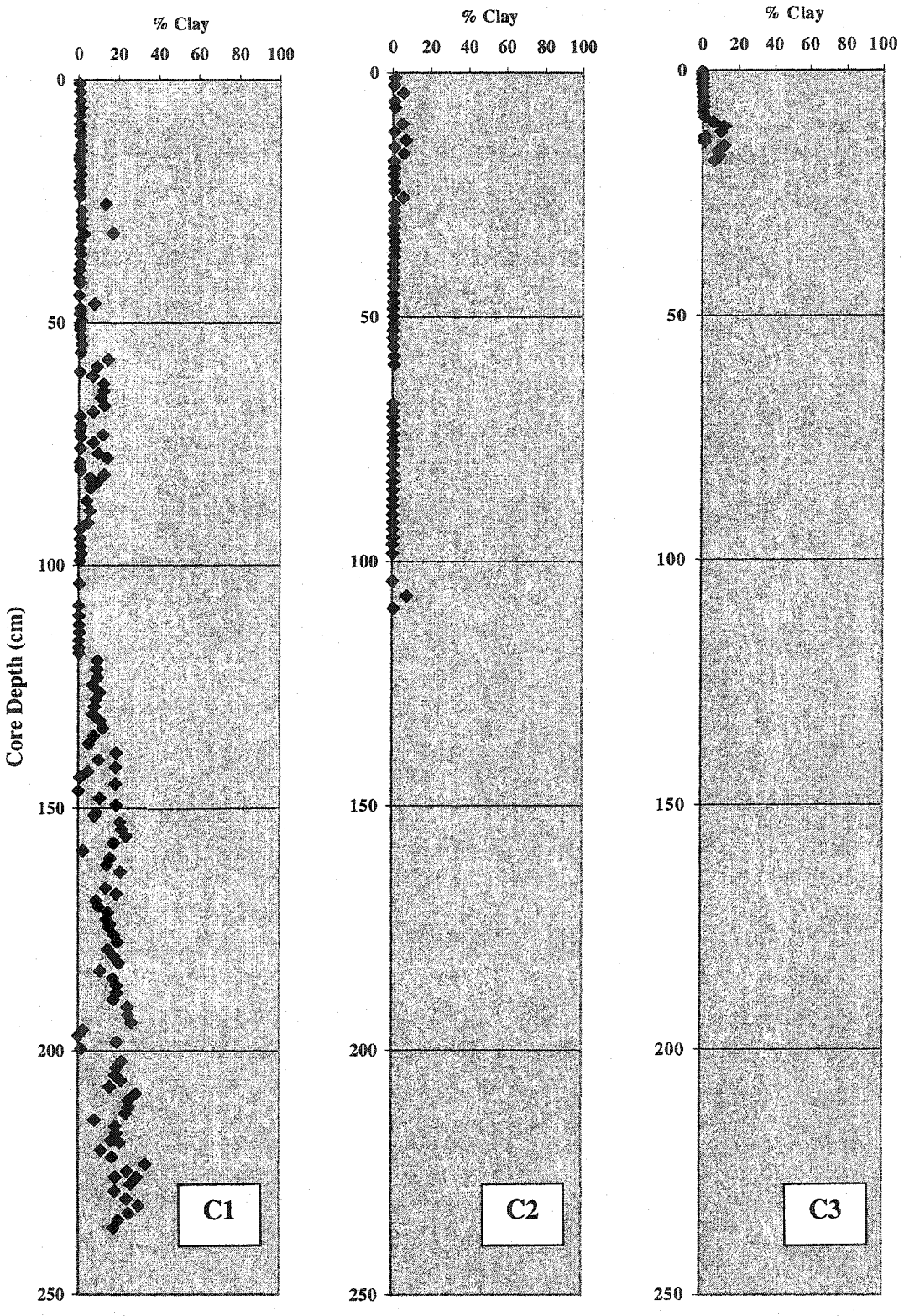


**Figure 21.** Percent clay in the ≤ 1 mm fraction of Otokomi Lake cores C1, C2 and C3.

The silt content in C1 ranged from 10% to 97% with the highest silt values near the top and bottom of the core, and relatively lower silt values over the interval of 40 cm – 190 cm. In C2 the silt content ranged from 30% to 89%, with values generally increasing towards the core bottom. In C3 silt values ranged from 33% to 78%, with the lowest values at the core top. Figure 22 displays the percentage of silt in the ≤ 1 mm fraction of the sediment in cores C1, C2 and C3.

The percentage of sand in C1 ranged from 5.5% to 89%. In contrast to the silt content of C1, the sand values were low near the top and bottom of the core and relatively higher over the interval of 35 cm – 202 cm. The sand content of C2 ranged from 9.6% to 70% and displayed a general increasing trend with depth, although the data set exhibited a lot of variation. The sand content of C3 ranged from 19% to 67%, with the highest values at the top of the core. Figure 23 displays the percentage of sand in the ≤ 1 mm fraction of the sediment in cores C1, C2 and C3. In addition to the data presented in Figures 21 – 23, cumulative percentages of clay, silt and sand in cores C1, C2 and C3 are presented in Figure 24.

### 4.8.2 Coarse-Grain (> 1 mm) Analysis

In C1 the coarse fraction of the sediment ranged between 1.3% and 83% by weight. Values were low near the top and bottom of the core and were relatively higher over the interval of 67 cm – 183 cm, with the highest percent of coarse material found near 115 cm depth. In C2, the coarse fraction ranged between 1.6% and 66% by weight. The data displayed a large degree of variability with no broad trend. Figure 25 shows the weight percent of coarse material in Otokomi Lake cores C1 and C2.

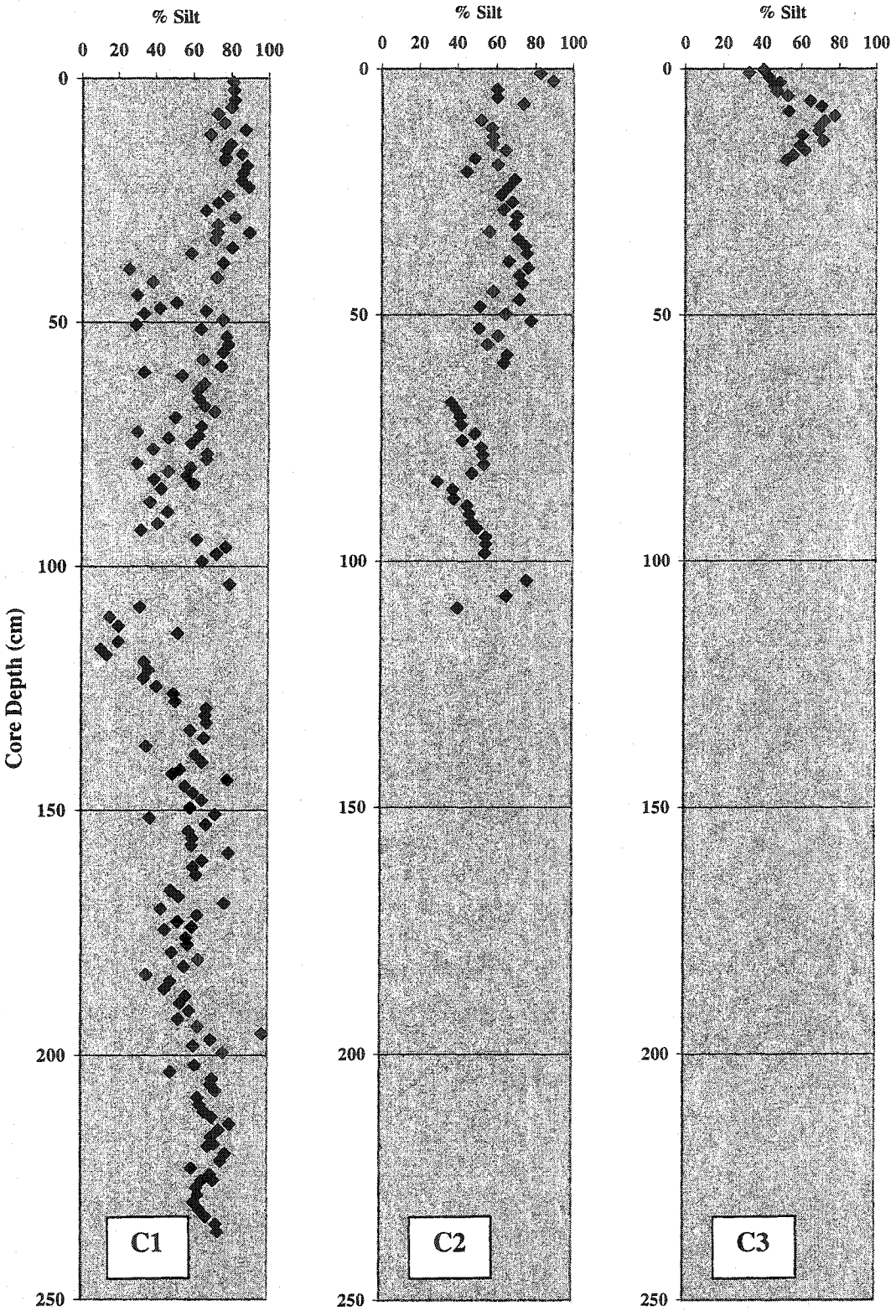


**Figure 22.** Percent silt in the ≤ 1 mm fraction of Otokomi Lake cores C1, C2 and C3.

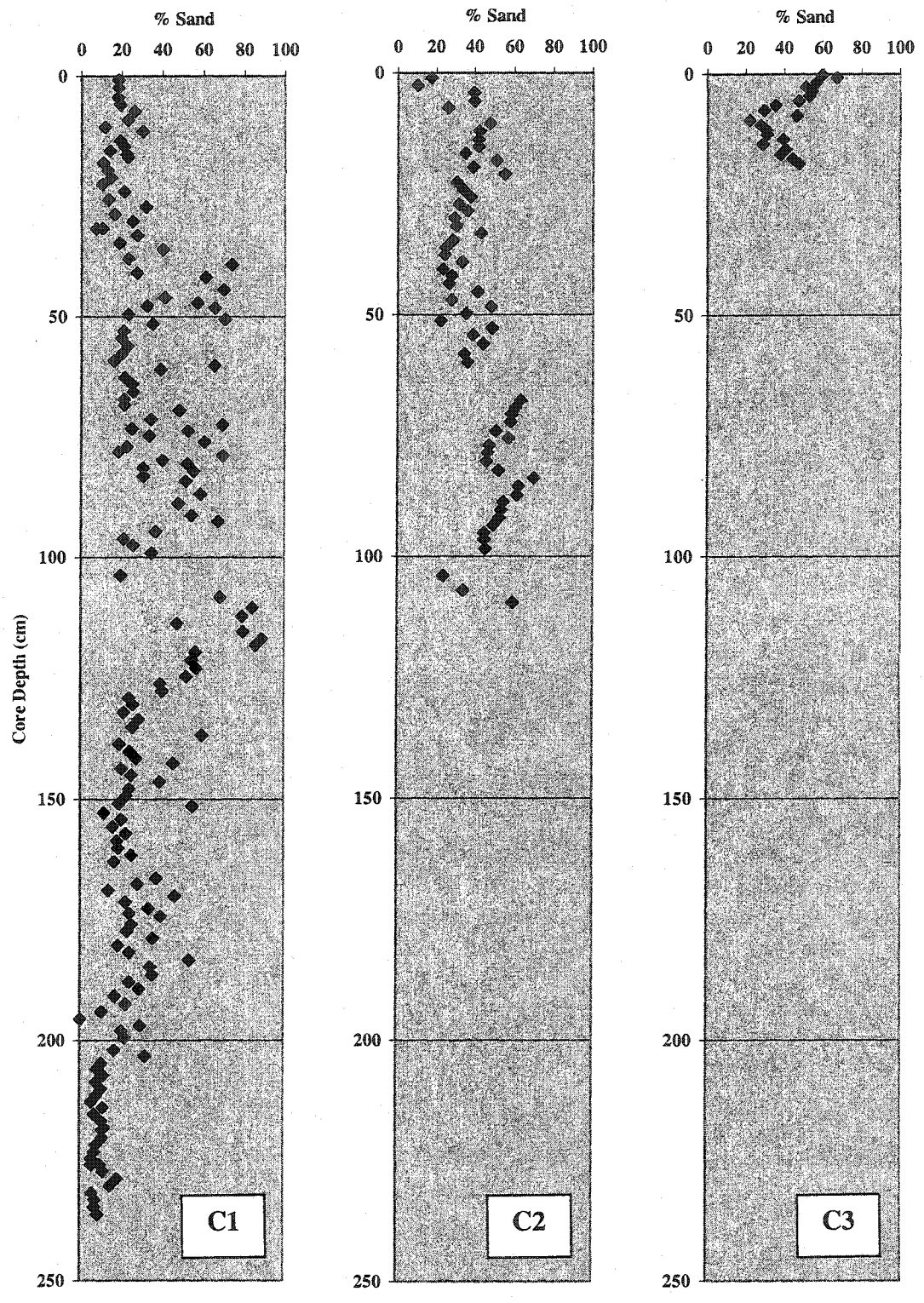


**Figure 23.** Percent sand in the ≤ 1 mm fraction of Otokomi Lake cores C1, C2 and C3.

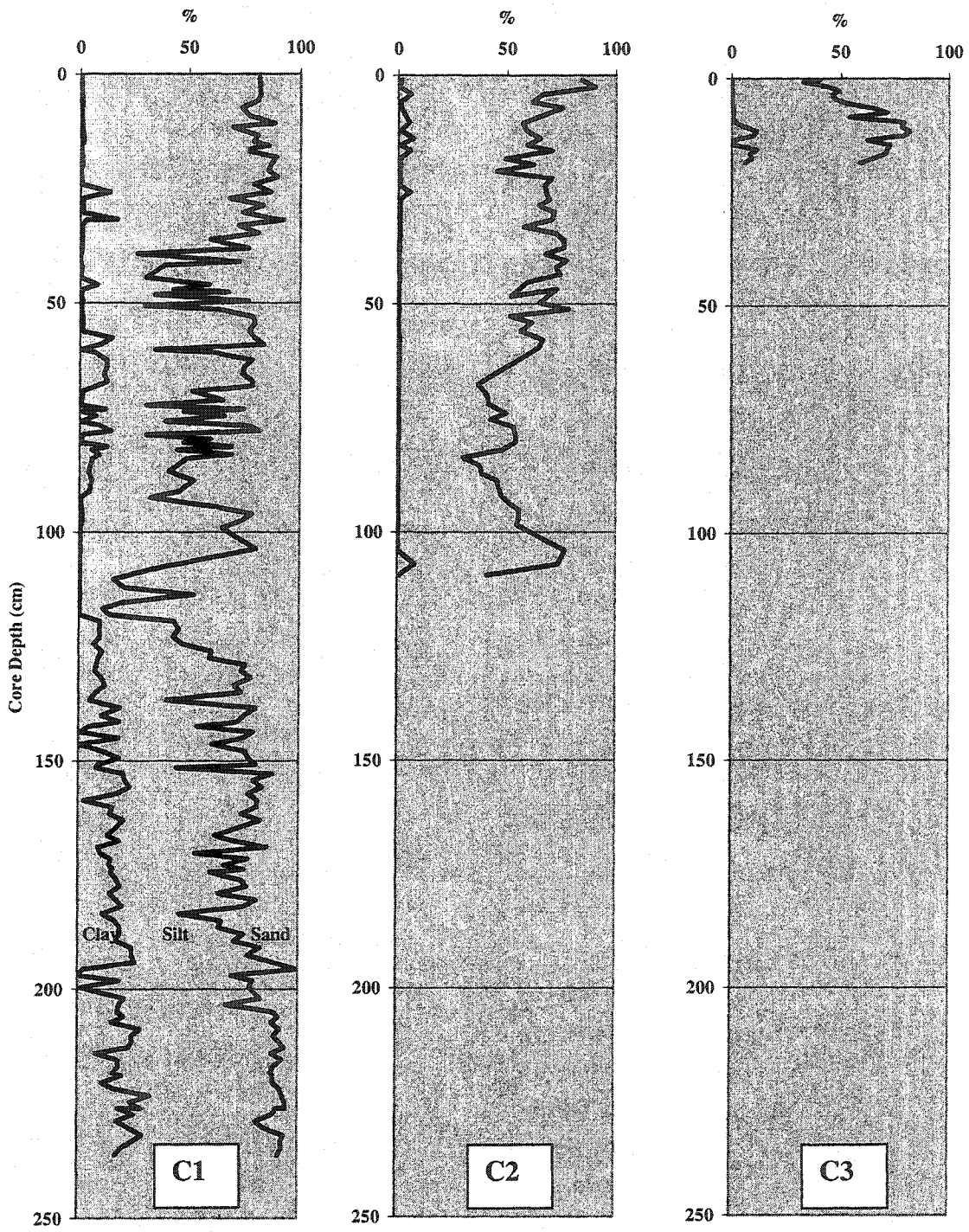


**Figure 24.** Cumulative percentages of clay, silt and sand within the ≤ 1 mm fraction of Otokomi Lake cores C1 C2 and C3. All size fractions total 100% for any given depth. Clay content is on left, silt in the middle and sand to the right.

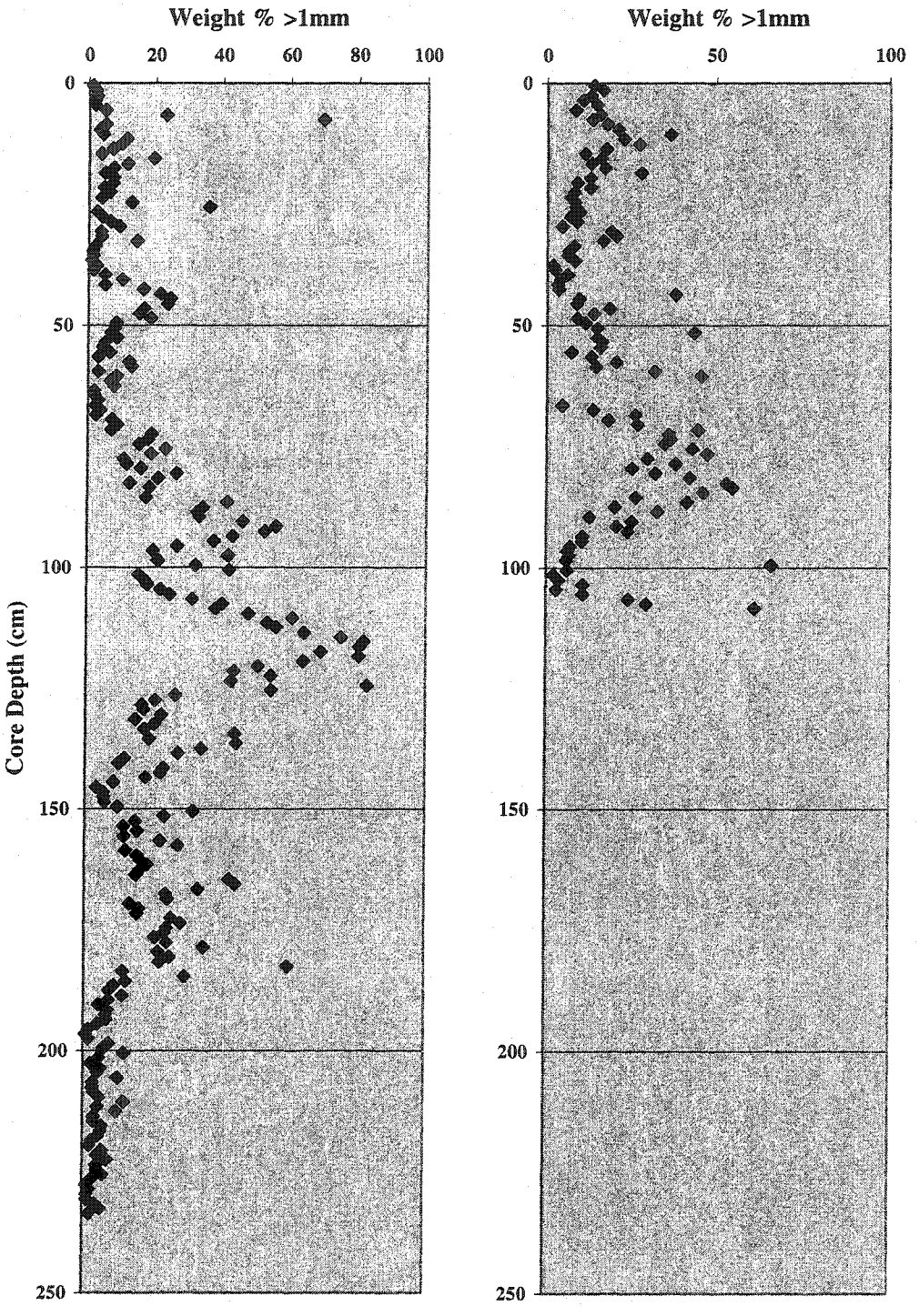


**Figure 25.** Weight percentages of the coarse (> 1 mm) fraction of the sediment in Otokomi Lake cores C1 and C2.

**4.9 Magnetic Susceptibility (Fig. 26)**

The magnetic susceptibility values for Otokomi Lake C1 ranged from 0.01 – 1.82, with a general trend of magnetic susceptibility increasing with depth. Over the length of the core, six distinct areas were seen that displayed lower magnetic susceptibility values than adjacent sediments. These areas corresponded to the ends of the six core sub-sections that were analyzed. The magnetic susceptibility values would drop noticeably as the instrument would near the end of these core sections. It is presumed that these "edge effects" were the cause of the low magnetic susceptibility values, and not the nature of the sediment at these points. There were also three peaks where values deviated positively from the general trend. The peaks centered at 201 cm and 102 cm corresponded to depths where volcanic ash was identified. The third and smallest peak was centered at 181 cm.

The magnetic susceptibility values for C2 displayed a trend that was very similar to the trend seen in the top portion of C1. The main difference was that the values for C2 were slightly higher than the values for C1, at any given depth. The range in magnetic susceptibility values for C2 was from 0.4 to 7.4. The maximum value corresponded to a peak centered at 103 cm.

**4.10 Coarse (> 1 mm) Organic Fragments (Fig. 27)**

The type of organic fragments isolated from Otokomi Lake C1 and C2 included small black flakes of unknown origin, small twigs, pieces of conifer cones, woody fragments and organic agglomerations. It is unknown what portion of the black organic material was charcoal, as opposed to partially decomposed plant material. In C1 the majority of the visible organic fragments were found in the top 100 cm, although

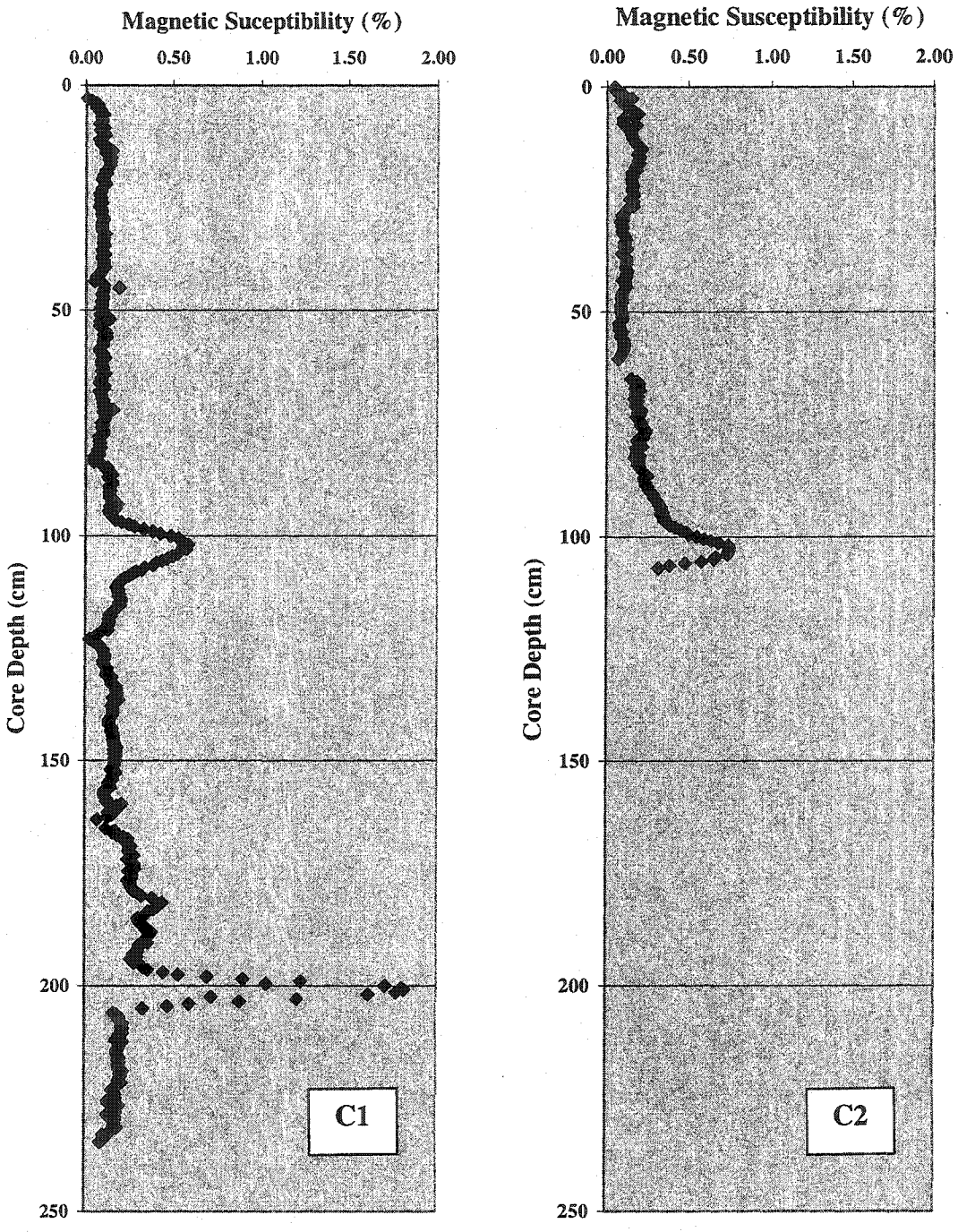


**Figure 26.** Magnetic Susceptibility values for Otokomi Lake cores C1 and C2.

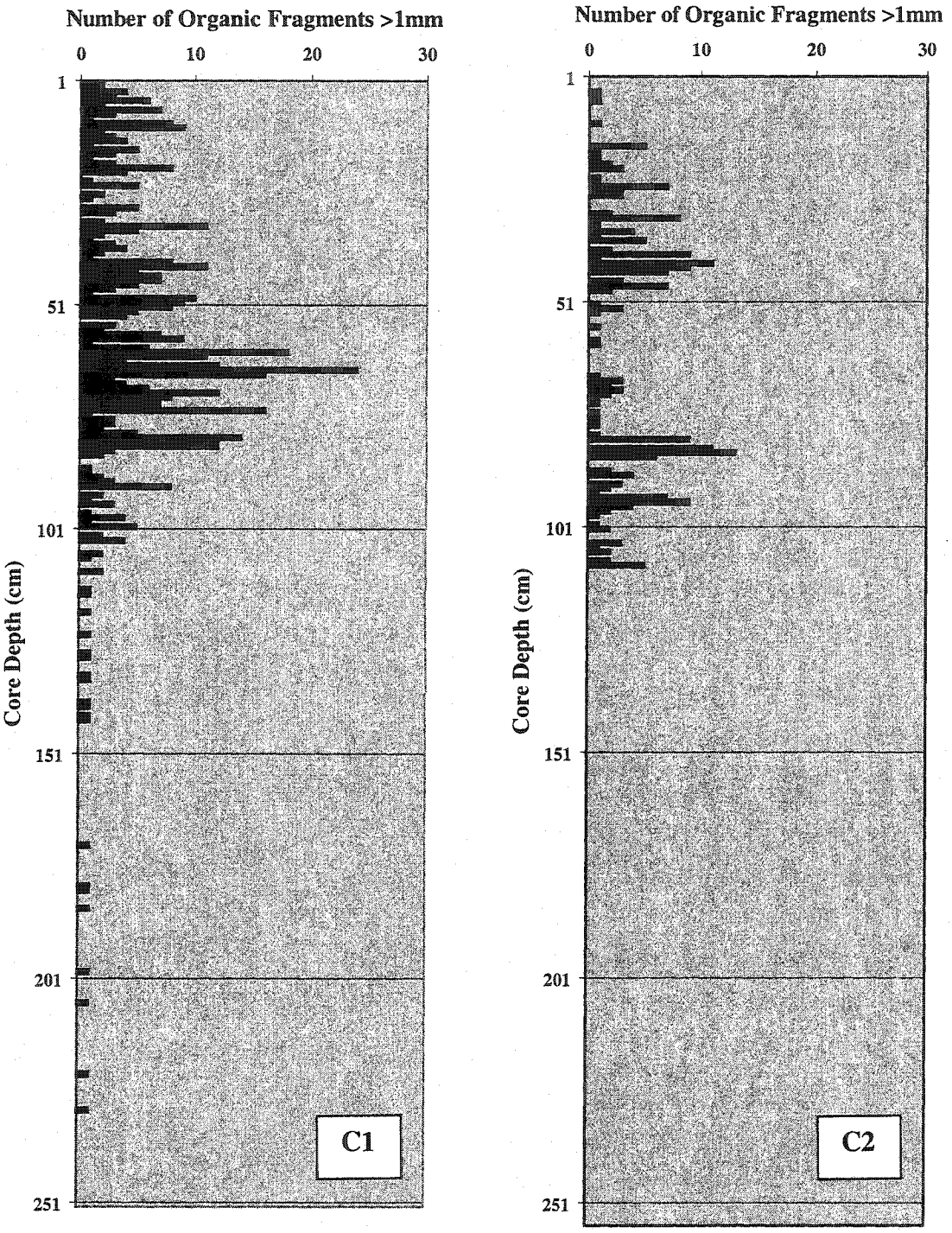


**Figure 27.** Number of coarse (> 1 mm) organic fragments per cm in Otokomi Lake cores C1 and C2.

fragments were found at depths as great as 230 cm. The number of visible fragments in this core ranged from 0 to 24 per cm. The largest number of fragments was from a depth of 65 cm. The number of organic fragments per cm in C2 ranged from 0 to only 13 per cm, despite earlier observations of organic banding in that core. Between 42 cm and 84 cm there was a lack of coarse organic material in C2, which contrasts with the high concentration of such material over the same interval in C1. It is important to note that coarse organic material was not expected in C2 between the depths of 63 cm – 67 cm because of the void space present in that portion of the core.

Three organic fragments were radiocarbon dated using accelerator mass spectrometry. The samples were collected from depths of 128.5 cm, 127.5 cm and 72.7 cm and were identified as an organic fragment of possible plant or animal origin, a small twig and a chip of wood, respectively. The conventional radiocarbon ages of the samples were 2530 +/- 40 BP (128.5 cm), 2590 +/-40 BP (127.5 cm) and 2180 +/- 40 BP (72.7 cm).

**4.11 Palynological Analysis**

With the exception of certain readily identifiable grains, the majority of the pollen counts were tentative due to the poor state of preservation. The various degrees of degradation visible in the protein coats of the palynomorphs were an indication that the majority of the samples were over-oxidized during their chemical preparation. The inability to properly identify palynomorphs introduced a level of uncertainty into many of the conclusions that, otherwise, may have been accurately drawn from the palynological data. However, the pollen data are still being presented in hopes that some meaningful relationships or trends may be identified. The grain types in which identifications were

made with relative certainty included periporate grains and species of pine, spruce, fir, alder, hazel, ragweed and horsetail.

Out of the 28 pollen slides analyzed for Otokomi Lake C1, 8 contained less than 300 native pollen grains. One of these slides was from 126.4 cm, whereas the other seven included all of the samples collected between 193.6 cm and 239.7 cm. Furthermore, five of the slides with low native pollen counts had less than 100 native grains per slide.

A major change in the palynomorph assemblage was seen at approximately 193.6 cm depth; the relatively high pollen percentages exhibited, up to that point, by many of the shrubs, herbs and spores decreased significantly (Fig. 28). As previously mentioned, it is also above 193.6 cm that the pollen counts were high enough to yield more statistically accurate data. Above this depth the ratio of native pollen grains to exotic grains, which serves as an indicator of productivity, began to increase from a low of 0.02 to a value of approximately 0.5. This productivity ratio remained above 0.5 throughout the remainder of the core. Various pine and spruce species remained the dominant palynomorphs above the depth of 193.6 cm, with relative percentages reaching maximum values of 75% and 41% respectively. At depths of 143.2 cm, 124.8 cm, and 32.3 cm relative pine and spruce percentages dropped, the productivity ratio dropped, and palynomorphs such as alder and ragweed showed relative increases. This relationship was most pronounced at 32.3 cm, where the relative pine percentage dropped to 20% and the relative alder percentage jumped to its maximum value of 16%. Additional trends in the palynological data from depths exhibiting low native pollen totals, or evident only within species where identification was uncertain, were not characteristic of environmental conditions affecting the site.

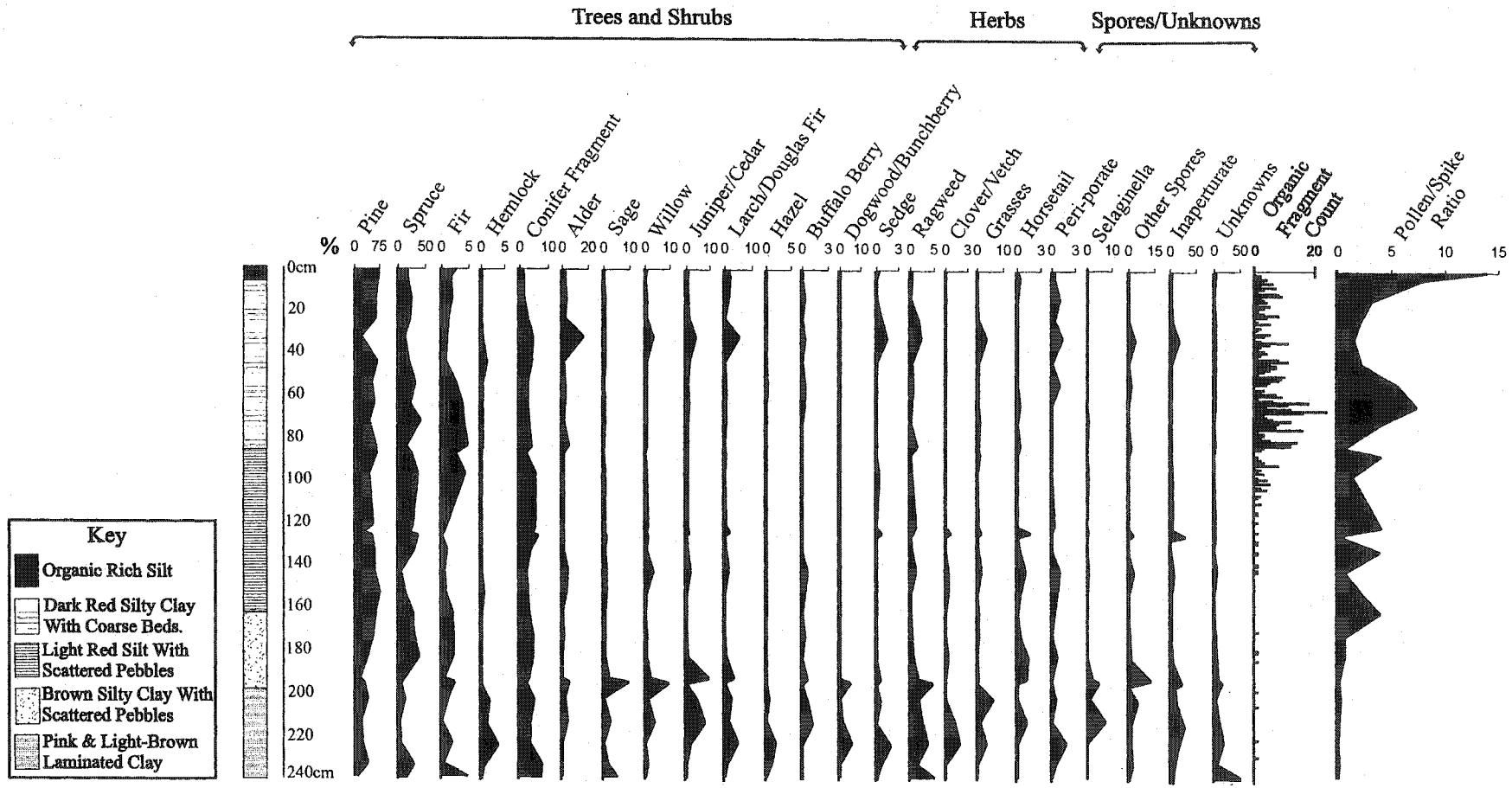


**Figure 28.** Pollen diagram for Otokomi Lake C1, showing relative pollen percentages at 10 cm intervals. Generalized core stratigraphy and the count of coarse organic fragments are also included in this diagram for comparative purposes.

# 5. Interpretation and Discussion

## 5.1 Mechanisms of Sedimentation in Otokomi Lake

Otokomi Lake can be characterized as a dimictic, oligotrophic alpine lake. In such a lake, the thermal stratification seen in the August temperature profile is coupled with reverse thermal stratification in the winter months (Håkanson and Jansen, 1983). Mixing within the water column in the spring and fall facilitates the transition between the two types of thermal stratification. This mixing is an important mechanism for resuspending and redistributing fine-grained material within shallow lakes having thermoclines located near the lake bottom (Evans, 1994). With a relatively shallow thermocline and a deep basin profile, Otokomi Lake likely experiences little resuspension of fine particulate matter during turnover events (Larsen and MacDonald, 1993). However, because the thermocline represents a boundary between low and high-density water masses, suspended particulates entering the lake may be dispersed throughout the basin along this boundary. This may be an important distribution mechanism during periods of prolonged ice cover or drought, when incoming water volumes and sediment loads are low.

The measured secci-disc transparency of 5.9 m indicates low levels of lake productivity at present (Håkanson and Jansen, 1983). Otokomi Lake appears to have been unproductive throughout much of its past as well; in cores C1 and C2 almost every sample analyzed by loss on ignition had less than 10% organic carbon by weight. It is important to note that the organic component of Otokomi sediment is a combination of allochthonous and autochthonous material. The allochthonous portion was discovered and quantified during the wet-sieving portion of the coarse-grain (> 1 mm) analysis. Therefore, for any given sample, the weight percent of autochthonous organic sediment

represents only a fraction of the total weight percent of organic sediment, as determined by loss on ignition. This emphasizes the highly oligotrophic nature of Otokomi Lake through time. Since very little organic sediment has been transported to, or produced within, Otokomi Lake over time, the majority of its profundal sediment must be minerogenic.

The small surface area of Otokomi Lake provides little fetch for the generation of large waves. Even in the presence of 75 km / h winds, an effective fetch of 500 m can only produce waves having a height of 40 cm (Håkanson and Jansen, 1983). In addition, the steep basin morphology, coupled with a narrow shoreline, allows only a small portion of the nearshore zone to be disturbed by wave action. Therefore, the resuspension and redistribution of sediment through wave processes is thought to play a minimal role in the sedimentation dynamic of Otokomi Lake.

Although wind may not play a large role in transporting *lacustrine* sediment, it may play an important role in getting sediment to the lake in the first place. Otokomi Lake is located east of the continental divide and is subject to prevailing westerly winds (Finklin, 1986). When the ground in Rose Basin is ice-free and dry enough to be eroded by wind, particles as large as fine-sand (Allen, 1979) may be blown into Otokomi Lake.

Besides wind transportation, the only mechanism for getting clastic sediment into Otokomi Lake is overland transport, including alluvial, fluvial and mass-movement processes. The talus slope on the lake's northwest corner is capable of introducing large clasts into the lake. The bathymetric map of Otokomi Lake (Fig. 11) shows the effect of the talus slope on basin morphology; a shelf can be seen building into the lake's northwest corner, where the majority of the coarse colluvium is being deposited at the

water's edge. The loading and oversteepening of the sloping lake-bottom by this accreting shelf may cause periodic slumping. The turbidity currents created by this slumping would transport coarse material basin wards (Allen, 1979). In fact, with such a large portion of the lake basin dipping at an angle near 30°, periodic sub-aqueous slumping of the slope is expected in many areas. As this dip angle is very near the angle of repose, a cohesive force exceeding that achieved from the frictional interaction of grains is required to stabilize the slope. The cohesive interaction of clay particles could stabilize such a slope, however clay deposition is more likely in the low energy environment of the basin centre. Sediment entering the lake from inlet streams or through mass wasting activity could also lead to slumping in affected areas. The moraine that borders the lake's entire southern edge is composed of unconsolidated glacial till, is 10 m tall, and is very near the angle of repose. Sediment shed from this source into the lake may also be a leading cause of slumping on the steeply dipping slopes of the lake basin.

Snow avalanches are expected to commonly occur on the steep slopes above the lake. In order for snow avalanches to deliver sediment into Otokomi Lake they must reach the lake itself. Judging from the statistical "runout ratio" method employed by Nixon and McClung (1993), avalanches originating south and northwest of Otokomi Lake commonly reach the lake. Therefore, any clastic sediment entrained within the avalanche debris on the lake surface would enter the lake during the spring melt. The ability of snow avalanches, particularly wet-snow avalanches, to erode the ground surface and incorporate clastic material into their deposits has been documented (Luckman, 1975; Gardner, 1983).

One perennial, and several ephemeral inlet streams also deliver sediment to Otokomi Lake. The periodicity and degree to which the inlet streams flood are major factors in controlling the volume and rate of sediment influx into the basin from these sources. During dry periods of the summer the only source of overland water input is the small inlet stream on the lake's western edge, which travels over bedrock before entering the lake. During periods of low flow this stream runs very clear and carries very little sediment into the basin. Thus, at times like this, Otokomi Lake has very little sediment input from fluvial sources. During these dry times, sedimentation rates in the lake are likely minimal, with the dominant sediment inputs being the result of aeolian processes and episodic mass movement events. Mid-winter conditions, in which freezing temperatures persist for extended periods, would also be associated with low stream discharges and reduced sediment transport. With the exception of intrabasin events, like basin slumping, clay deposits in the basin centre likely result from the low-energy depositional conditions associated with nominal fluvial activity.

Otokomi Lake's outlet has a limited capacity to transport suspended sediment out of the lake. Water flows into the outlet stream over the top of a shelf at the lake's eastern end. Therefore only the surface waters flow out of the lake, even during times of high discharge. This gives the majority of the water in Otokomi Lake a high residency time, allowing for effective sedimentation of suspended particulates.

**5.2 Understanding the Sedimentary Record**

An initial comparison of the sedimentary data trends from C1 and C2 with those from C3 revealed a correlation between the sediment 6 cm below the surface of C3, with the sediment at the surface of C1 and C2 (Fig. 29). This was taken to be an indication that

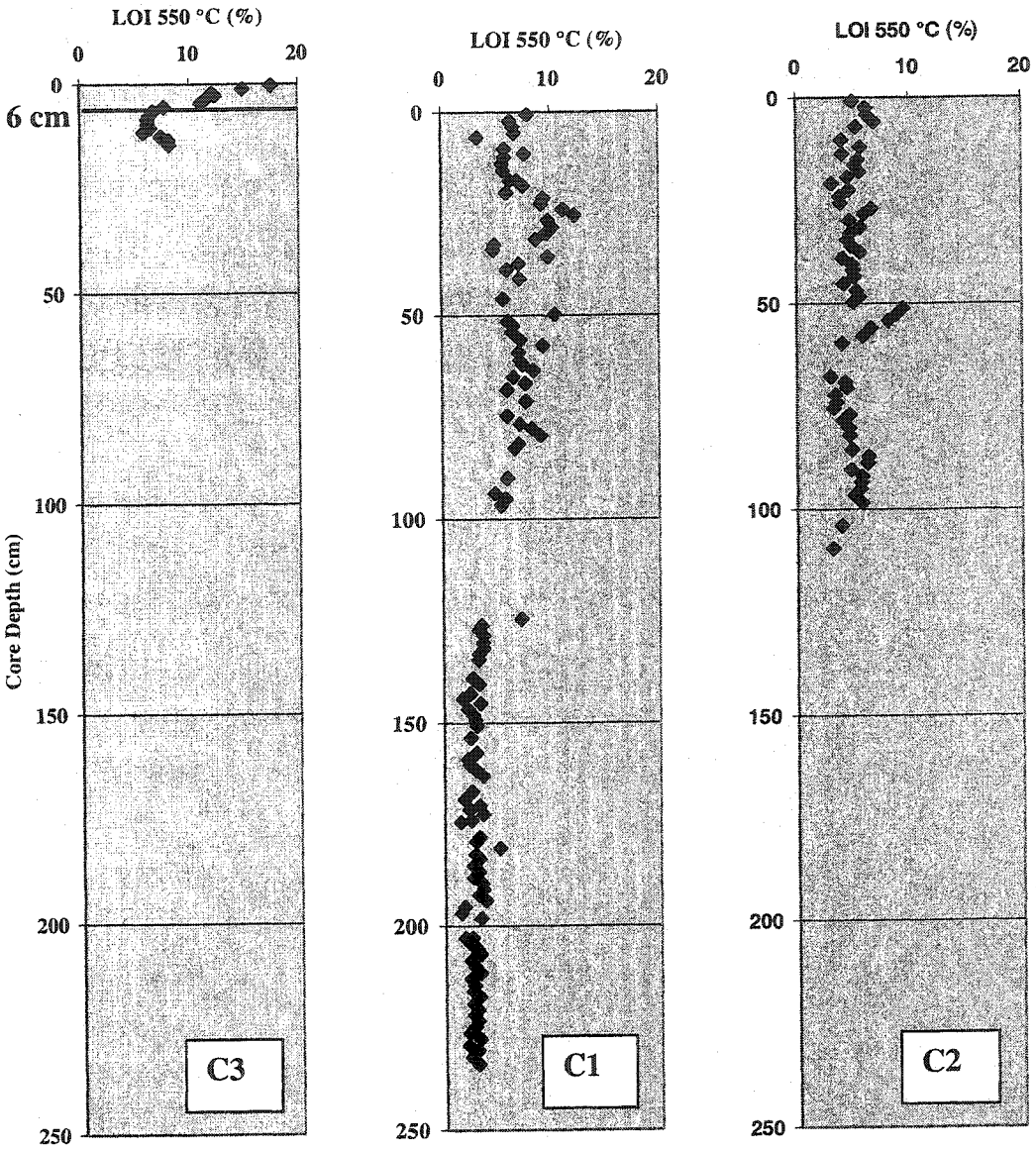


**Figure 29.** Stratigraphic correlation between Otokomi Lake cores C1, C2 and C3. The L.O.I. values in C3 only approach those of C1 and C2 below a depth of 6 cm.

approximately 6 cm of sediment was lost from the top of both C1 and C2 during the core collection procedure. When necessary, this lost sediment was taken into account during the calculation of sedimentation rates for C1 and C2.

### 5.2.1 Color and Coarseness

The two most striking characteristics of the percussion cores collected from Otokomi Lake were their vivid color and the amount of coarse clastic sediment within them. The pinkish red color of the core sediment was evidence of the Precambrian rock source, whereas the coarse clasts found in each core were evidence of high-energy sediment transport mechanisms. It is likely that more than one mechanism is responsible because of the different textures associated with the coarse material.

If the pebbles visible in the percussion cores were carried to the basin centre as fluvial bed load, the pebble-laden water would have to have retained its flow velocity from the lake's edge to the basin deeps. This is unlikely, as flow expansion would take place as the water entered the lake, thereby reducing its velocity and its ability to transport large clasts. In this case deposition would have occurred at the mouth of the inlet stream and not in the basin centre.

The bathymetric map of Otokomi Lake shows that the basin begins to slope steeply downward not far from the water's edge. Therefore any coarse clasts deposited near this underwater scarp may be transported down the basin slope during sub-aqueous slumping events. The turbidity current associated with this slumping would create a graded deposit (Allen, 1979). However, if a variety of fine and coarse-grained material were carried onto lake ice by a snow avalanche, this material could also settle to the bottom of the lake in a fining upwards sequence during the spring melt. These two types

of depositional mechanisms may be distinguished from one another based on the orientation of the coarse grains within them (Smith, 2000); graded deposits from turbidity currents would have clasts aligned parallel to the lakebed, whereas graded deposits resulting from snow avalanche activity would have clasts aligned vertically. However, for the purposes of this discussion the most important consideration is that these two mechanisms both deposit a graded sequence of sediment in a short period of time. Therefore the graded minerogenic beds identified in the percussion cores are interpreted to be the result of either sub-aqueous slumping or snow avalanche activity.

A different mechanism must be responsible for selectively depositing coarse clasts into the fine-grain matrix of the core. It is known that lacustrine shoreline sediment is affected by wave action during times of open water. This wave action is capable of transporting fine grains into deeper water. Over time, the fine-grain fraction of the shoreline sediment may become depleted. Consequently, during periods of ice cover, shorefast ice would only be capable of incorporating coarse sediment. Ice rafting processes, as described by Smith (2000) and Luckman (1975), could then transport this coarse material the centre of lake basin. This is one process that may explain the presence of matrix-supported pebbles in C1 and C2. A problem with this theory is that when lake ice begins to melt in the spring it is often first observed to melt around the lake's perimeter, creating a moat of water (Gilbert, 2001). As a result, the shorefast ice would consequently deposit its sediment load at or close to the very spot it acquired it. This effect undoubtedly reduces the amount of ice rafting in lake environments. Continued melting during the spring season likely involves the fracturing of the ice "pan" at the basin centre, as it moves about in response to wind and wave action. The dynamic

movement of ice fragments at this time, coupled with the freezing and thawing cycles common in spring, is believed to facilitate a small amount of ice rafting in lakes such as Otokomi Lake. With lacustrine deposition rates commonly averaging several millimeters per decade (Andrews et al., 1982), even a very modest amount of ice rafting could achieve the scattering of pebbles seen in the Otokomi cores. Therefore, ice rafting is thought to play a role in the redistribution of coarse sediment within Otokomi Lake.

It seems unlikely that infrequent and localized sedimentation from ice fragments is capable of depositing *layers* of pebbles at the bottom of Otokomi Lake. The presence of these layers may indicate that the magnitude of ice rafting in the basin is temporally variable or that a different mechanism is active in transporting these large clasts. Snow avalanches traveling over frozen ground, or traveling over a ground surface deflated by wind or runoff activity, may entrain only coarse material into their deposits. If these deposits reach the frozen surface of the lake they could be deposited as layers on the lakebed. Therefore the isolated pebble layers in the percussion cores may either be the product of heightened ice rafting activity or erosion by snow avalanches.

Lastly, the large mass of coarse sand and pebbles in the middle of C1 is interpreted strictly as a single massive avalanche deposit. The main characteristic of core sediment containing ice rafted debris appears to be coarse clasts in a fine matrix. Because this large mass in C1 consists of only coarse clasts, is present in both cores, and is found in the low energy environment of the basin centre, a high-energy mechanism capable of distributing large volumes of coarse material over a broad area is required. A snow avalanche carrying coarse material onto lake ice is such a mechanism.

### 5.2.2 The Fine-Grain Story

Using C1 as an example, a congruency can be seen between the sand data in the fine-grain analysis and the data from the coarse-grain (> 1 mm) analysis (Fig. 30). With the exception of slightly more scatter in the sand data, the coarse-grain data trends mimic those of the sand data. Both show relative increases and decreases at the same depths and of similar magnitudes. The silt data set, on the other hand, is the mirror image of the two coarser data sets. The silt data set shows relative increases at depths where the two coarser data sets show relative decreases and vice versa. A possible explanation for the positive relationship between the sand and coarse-grain data sets would be that the same mechanisms that are transporting and distributing the coarse material within the basin are also responsible for the transport and distribution of the sand sized grains. When these processes are more active, whether they be ice rafting, snow avalanching, basin slumping or extra-basinal mass movement events, the sedimentary record is biased towards grains sand sized and larger. When these processes are not as active, the slower processes of fine-grain sedimentation dominate, characterized by silt and clay deposition.

A comparison of the silt and clay data sets shows that the fine-grain sedimentation regime is itself dynamic. There is little similarity between these two data sets. Silt is present throughout C1 in much higher percentages than clay, and the trends of the two data sets do not match. The high percentage of silt in C1, as opposed to clay, reflects both the high-energy nature of the site and the low availability of clay in the catchment area of the lake. The high-energy nature of the drainage basin is reflected by its sparsely vegetated steep alpine slopes. The ephemeral stream activity in this basin likely involves flow regimes readily capable of entraining and transporting silt grains. Only low-gradient

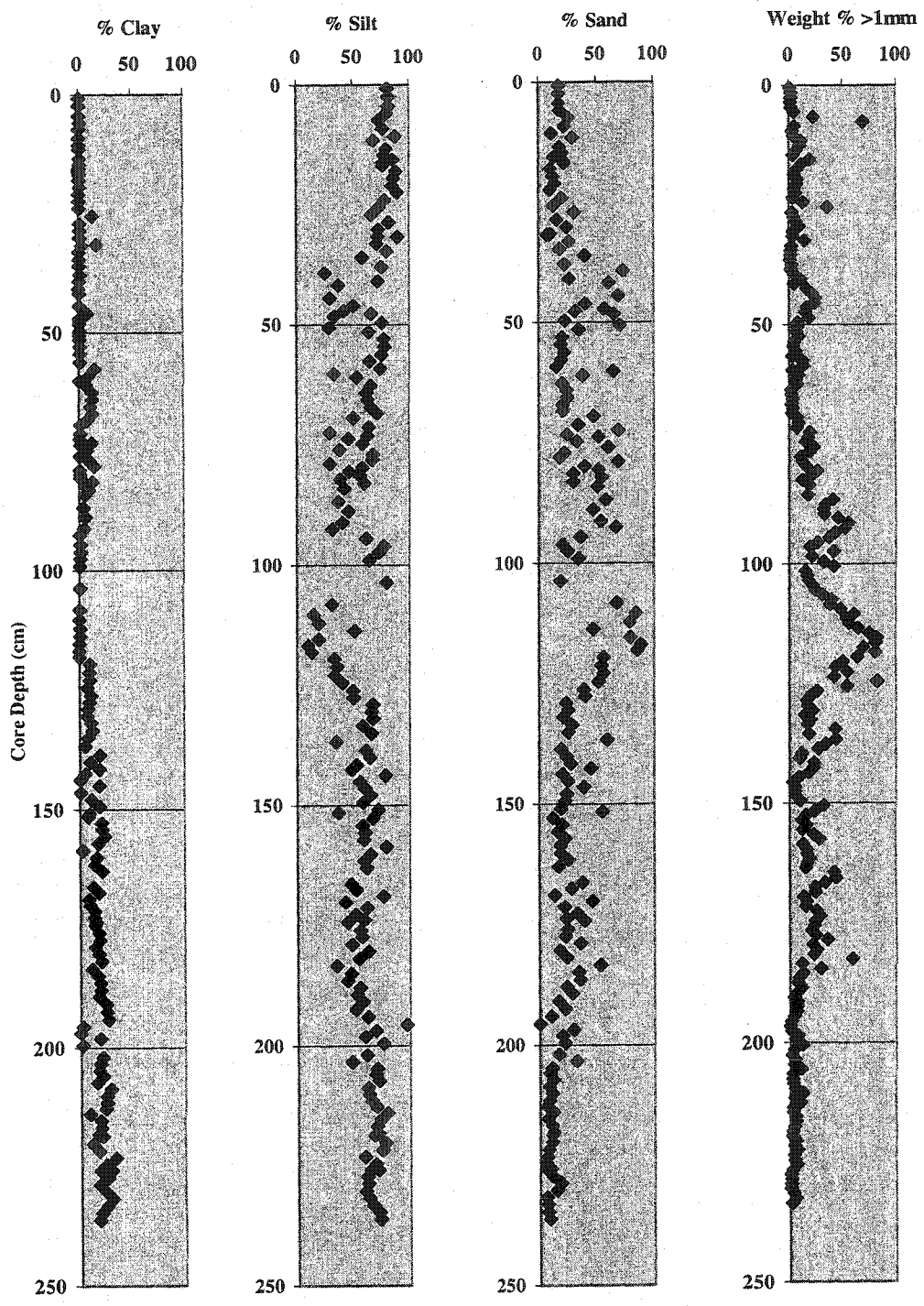


**Figure 30.** Coarse and fine grain size data for Otokomi Lake C1.

stream channels would facilitate flow deceleration and fine-grain deposition. With this in mind, there appears to be no reason why clay material would not also be incorporated into the flows of Otokomi Lake's inlet streams. Therefore the variations in clay concentration throughout C1 might only relate to changes in clay availability in the sediment source areas. Immediately following Wisconsinan deglaciation, Rose Basin would have likely contained a cirque glacier and a veneer of recently exposed glacial till. The erosive activity of the cirque glacier would have produced clay-sized material at its base, which could have washed into the basin with the glacial meltwater. In addition to active glaciation in Rose Basin at this time, the recently exposed glacial till in other portions of the catchment would have had a clay component that was readily available for erosion and transport by runoff. Clay availability in the basin would have diminished once active glaciation ceased and the clay had been washed from the surface of the local till. This is evident in the clay data from C1, where percentages are highest at the bottom of the core, and steadily drop to almost 0% at the top of the core.

### 5.2.3 Core Chronology and Sedimentation Rates

Three prominent late Quaternary ash deposits have been identified in northwestern Montana. The youngest of the three is the Mazama ash (ca. 6730 B.P.), which is underlain by a Glacier Peak G (ca. 11,200 B.P.) / St Helens Jy (ca. 11,400 B.P.) ash couplet (Lemke at al., 1975; Carrara, 1989; Franklin et al., 1993). Traditionally, discrimination between these three ash layers has been based on chemical analyses of the glass shards (there was no mention in the literature of separate light and dark glass shards being recognized in the Mazama ash, therefore the analysis in which they were grouped together was used as the comparator from this study). Each ash layer identified in this

study has a glass chemistry that correlates well with one of the three ash layers mentioned above (Fig. 31). The large lens of ash centered at 103.7 cm in C1 is chemically similar to Mazama ash, the 200.9 cm layer to Glacier Peak G ash, and the 204.2 cm layer to Mount Saint Helens Jy ash. In addition to their glass chemistry, the three ash layers in this study have the same relative stratigraphic position, thickness and texture as the late Quaternary ashes mentioned above (Lemke et al., 1975; Osborn, 1985; Carrara, 1989; Carrara and Trimble, 1992). Therefore, based on agreement between the chemical and stratigraphic data of this study and that of the literature, the three ash units in C1 are interpreted to be Mazama (103.7 cm), Glacier Peak G (200.9 cm) and Mount Saint Helens Jy (204.2 cm). Although the volcanic ash identified in C2 was not chemically analyzed with the Superprobe, its texture, volume and approximate stratigraphic position were consistent with those of the Mazama ash.

Anderson et al. (1984) demonstrated that volcanic ash is capable of sinking through uncompacted lake sediment, creating stratigraphic time displacements of several hundred years. White and Osborn (1992) also recognized the potential for ash migration in the sediments of Copper Lake, Alberta. A possible explanation for up-core ash migration is that sediment liquefaction is initiated by core-barrel vibration during the collection process. This liquefaction would facilitate the upward movement of the ash because of its relatively low density. In both C1 and C2, the Mazama ash appeared to have migrated up-core from its original stratigraphic position. In C1 the bulk of the ash had the appearance of a laterally discontinuous globular lens, centered at 103.7 cm. This lens was continuous with ash that was intermixed with the underlying avalanche debris, having a lower boundary within the debris at 114 cm. In C2 the Mazama ash was also

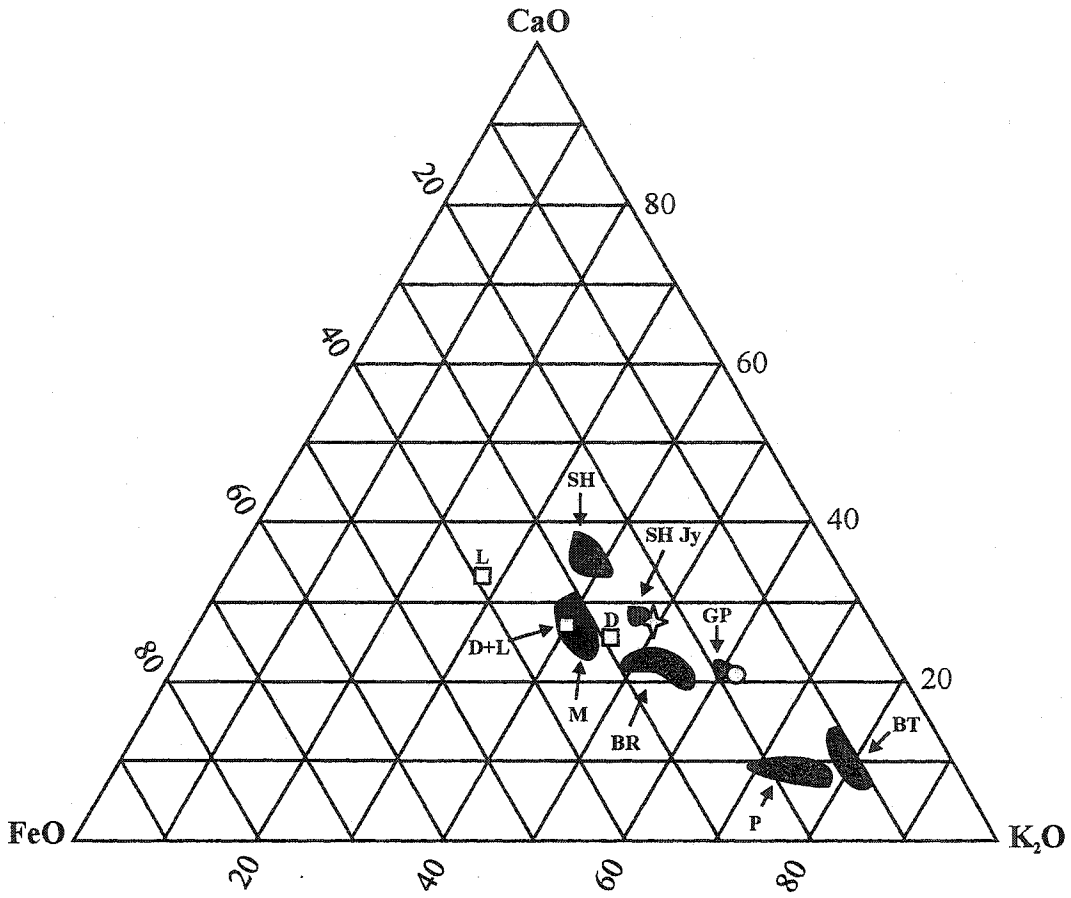


**Figure 31.** A comparison of the relative abundance of FeO, CaO and $K_2O$ in the three volcanic glass samples analyzed in this project with accepted relative abundances for some widespread western North America tephra layers. Squares represent the 103.7 cm ash sample, with analyses for the dark (D), light (L) and dark+light (D+L) grains included. The circle represents the 200.9 cm layer and the star represents the 204.2 cm layer. M=Mazama, GP= Glacier Peak set G, SH= St Helens, BR=Bridge River, P=Pearlette and BT= Bishop Tuff. All comparative data obtained from Westgate and Gorton (1981) except St Helens Jy data, obtained from Carrara (1989).

associated with coarse debris located between 108 cm and 113 cm and was connected, via a thin conduit, to an ash layer 41 cm above it. Because the lower boundary of the Mazama ash was near 114 cm in each percussion core, in contrast with its variable upper boundaries, the ash is interpreted to have traveled up-core, via liquefaction, from a stratigraphic position of approximately 114 cm. However, it seems highly unlikely that the ash layer was initially deposited *within* the avalanche debris, where the lower boundary is found, because the debris was deposited over a very short period of time. Additionally, if ash deposition postdated the avalanche event it would not likely have traveled down-core into the dense avalanche deposit. Ash deposition immediately predating the avalanche event would have a stratigraphic position of 124 cm, based on the lower bound of the avalanche deposit in C1. By this interpretation, the Mazama ash was initially deposited at a depth of 124 cm, got displaced soon thereafter by an avalanche event to a depth of 114 cm, and then migrated up-core in both C1 and C2 during the coring process.

The two lower ash units do not appear to have migrated from their original stratigraphic position. Although they were only present in C1, they appeared laterally continuous and had conformable contacts with the bounding sediment. Based on observations of the Mazama ash migration in C1 and C2, the Glacier Peak G and Saint Helens Jy ash layers would not have maintained their characteristic thickness, texture and relative stratigraphic positions if they had migrated during the coring process, or at any other time. It appears that only the Mazama ash, possibly because of its high volume and relatively high stratigraphic position, was able to exert enough force to travel up-core during core collection.

Sedimentation rates in Otokomi Lake appear to be highly variable, with many rapid deposition events separating periods of fine-grain deposition. Therefore, prior to calculating sedimentation rates, the depth and thickness of all horizons that were interpreted as being deposited instantaneously were first determined. These horizons represent zero time in a stratigraphic sense and therefore serve to over-represent sedimentation rates. The depth at any given point could then be corrected by subtracting the total thickness of overlying sediment that was deposited instantaneously. This correction process was limited by the ability of the observer to accurately identify and interpret intervals of rapid deposition. Because of the extremely coarse nature of the core, periods of rapid deposition that produced thin layers, or layers of intermediate grain size, may have been overlooked. This sort of error would have resulted in an overestimation of sedimentation rates. Using the above correction procedure, the St Helens Jy ash layer had an equivalent depth of 144.4 cm. If the rate of sedimentation for the overlying material were constant it would be equivalent to 1.32 cm / 100 yr. Using this sedimentation rate, the predicted depth for Mazama deposition (6845 B.P.) would be 90.3 cm. However, based on core observations, the corrected depth for Mazama deposition appears to be 84 cm. The difference between these numbers may be attributed to the errors associated with the depth correction technique, as well as variations in the sedimentation rate over such a large stratigraphic interval. Overall, the general agreement between the two numbers may indicate that the Mazama tephra was in fact deposited at a core depth close to 124 cm before being displaced.

The presence of approximately 35 cm of sediment below the St Helens Jy ash suggests that deglaciation of Rose Basin significantly predated 11,400 B.P. Using the

previously calculated sedimentation rate of 1.32 cm / 100 yr, the bottom of C1 (240 cm) corresponds to an age of approximately 14, 100 B.P. Although there is no glacial diamict "plug" at the bottom of C1, coarse pebbles were discovered on the inside of the core barrel, below the core catcher, at the time of recovery. If this material, which likely impeded further core penetration into the lake, represents the basal till layer in Otokomi Lake, then 14,100 B.P. represents a time estimate for the initial deglaciation of Rose Basin. Other cores collected from more productive alpine lake basins in the North American Cordillera have encountered basal till at depths between 250 cm and 310 cm (Spooner et al., 1997; Spooner et al., 2002; Mazzucchi et al., (in press); Reasoner et al. 1994). Therefore it seems possible that the basal till layer in such an unproductive alpine lake could be found below 240 cm of sediment. The basal date of 14,100 B.P. for Otokomi Lake, however, may actually be a *minimum* estimate. Fine-grain sedimentation rates during the early stages of lake development are often lower than the rates at higher stratigraphic levels (Fergusson and Hills, 1985; Reasoner et al., 1994; Gerloff et al., 1995). Therefore the sedimentation rate below 204 cm in C1 may have been lower than the 1.32 cm / 100 yr rate calculated from higher stratigraphic levels. However, a basal date of $\geq$ 14,100 B.P. is significantly older than some of the oldest estimates for deglaciation in the North American Rockies; Fergusson and Osborn (1981) dated snail shells from postglacial sediments in Elk Valley, British Columbia at ca. 13,430 B.P.; Kearney and Luckman (1987) reported a date of ca 13,500 B.P. for organic material at the bottom of Maligne Lake in Jasper National Park; Fulton (1984) suggested that retreat of the Cordilleran Ice Sheet was underway by 13,000 B.P. This discrepancy could be explained if the post-glacial sedimentation rates in Otokomi Lake were in fact quite high.

However, this explanation contradicts the low post-glacial sedimentation rates predicted by Fergusson and Hills (1985) and others. If, on the other hand, the ≥ 14,100 B.P. estimate for deglaciation in Rose Basin is appropriate it may be related to the relatively low latitude of Glacier National Park relative to many of the sites described above, or the proximity of Rose Basin to the eastern margin of the mountain ice fields that covered the park (Carrara, 1989). These factors would have contributed to a relatively early deglaciation in the Glacier National Park region and the consequent exposure of Rose Basin soon after its initiation.

The notion that the clay rich sediment at the bottom of C1 represents the early stages of sedimentation in Otokomi Lake is corroborated by the LOI, pollen and organic fragment data for that core (Fig. 32). Over the 204 cm – 240 cm interval the LOI values are at their lowest, reflecting the low levels of lake productivity expected in a recently de-glaciated alpine lake. In addition, the relative absence of organic fragments over the same interval is likely a product of terrestrial plant scarcity in Rose Basin at that time. In the pollen data, the productivity ratio between native pollen species and the exotic *Lycopodium* grains was by far the lowest over the 214 cm – 240 cm interval. Although this ratio was highly variable throughout the core, the low values encountered over the 214 cm – 240 cm interval were not seen at higher stratigraphic levels. These low ratios are likely related to a lack of pollen-producing plants near Otokomi Lake at that time. The pollen that was deposited over this interval may have had a more distal source. Plant communities establishing themselves in the valley bottoms of Glacier National Park could have produced the pollen that was subsequently blown up to alpine areas, like Rose Basin.

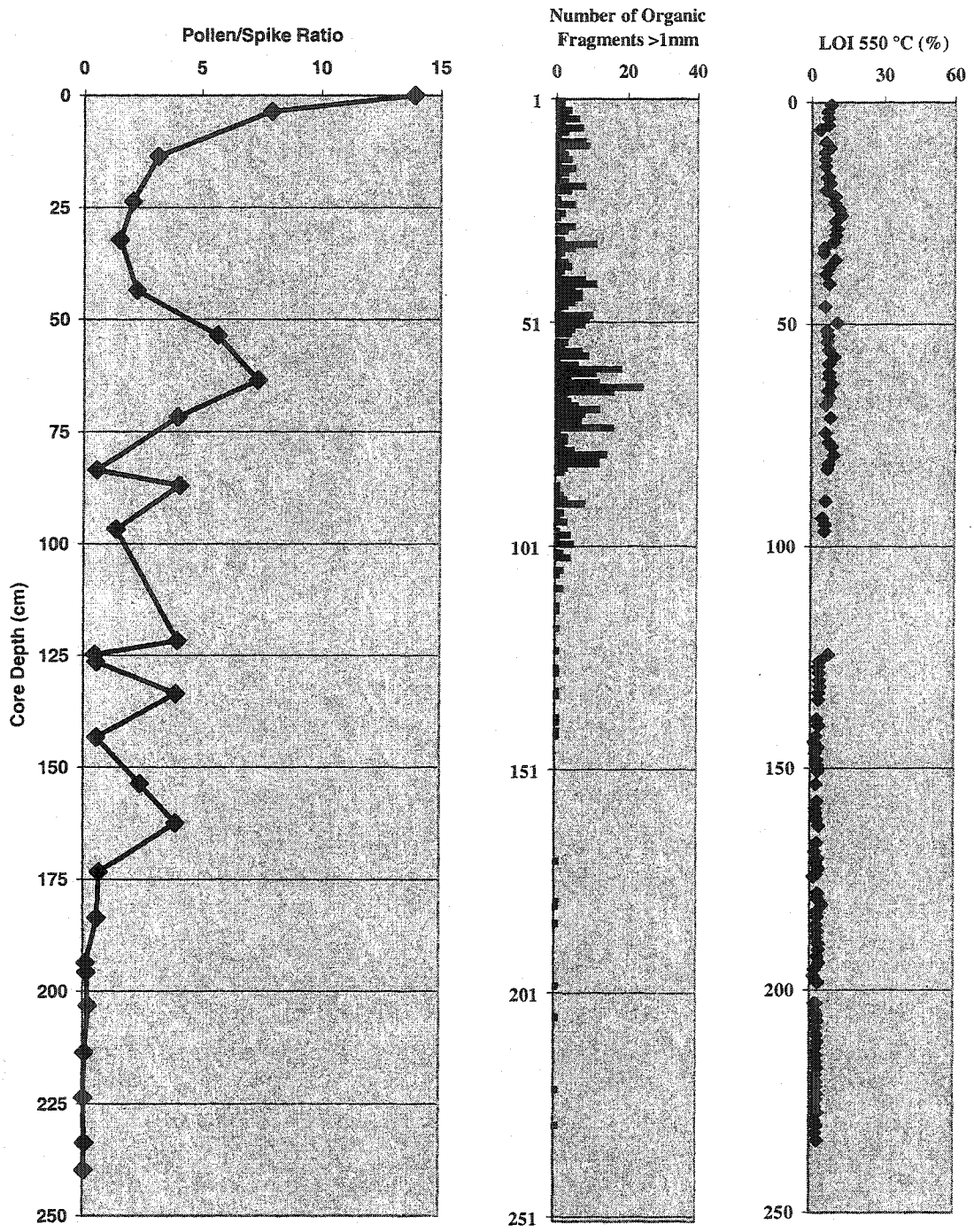


**Figure 32.** Comparison between Pollen Ratio, Coarse (> 1 mm) Organic Fragment Count, and LOI data sets for Otokomi Lake C1. All three data sets show low values over the 204 cm - 240 cm interval

The Holocene pollen assemblage for areas of western Montana, northern Idaho and southwestern Alberta is reportedly dominated by pine pollen, with additional amounts of spruce, fir, sage, grass and alder varying by site (Mack et al., 1978; Carrara et al., 1986; Mehringer et al., 1977; Fergusson and Hills, 1985; Mack et al., 1983). Consistent with this trend, various pine species dominated the pollen record of Otokomi Lake. The high percentage of pine pollen throughout most of C1 indicates that, once established, pine trees remained in Rose Basin through the Holocene. In addition, the dramatic increase in the amount of pollen above 195 cm may indicate that a plant community, similar to that which exists there today, established itself in Rose Basin soon after the deposition of the Glacier Peak G Tephra (ca 11,200 B.P.). The inferred timing of these changes is consistent with conclusions made by Carrara (1989), that portions of the continental divide near Glacier National Park were de-glaciated by 11,400 B.P. and that deglaciation of the entire park was 90% complete by 11,200 B.P. (Carrara, 1986). This consistency supports the conclusion that the two lower ash units are accurate time stratigraphic markers for C1.

The three dated plant fragments recovered from C1 provide the only data that contradicts the chronology that has been established thus far. Although all three dates are problematic, two dates pose the greatest concern and are addressed herein. Based on the proposed chronology, the sediment immediately below the avalanche debris should be isochronous with Mazama ash deposition. However, the two carbon dates for material collected immediately below the avalanche debris are 2530 +/- 40 B.P. and 2590 +/- 40 B.P. A possible explanation for these dates is that the Mazama ash had somehow migrated up-core into sediments approximately 2560 B.P. in age. This contrasts with the

previous interpretation, whereby the ash migrated up-core from a depth of approximately 124 cm. Presumably, if such a voluminous ash deposit had migrated up-core from a much lower stratigraphic level, there would be some evidence of its migration or its initial position. No Mazama ash was visibly encountered at any lower stratigraphic position in C1. In addition, as volcanic ash exhibits a high magnetic susceptibility, any hidden ash conduits or obscure ash horizons should be resolved through analysis of the magnetic susceptibility data. The only anomalously high magnetic susceptibility values below the avalanche debris in C1 are associated with stratigraphic levels characterized by abundant coarse sediment (Fig. 33). Visual inspection of C1 also revealed high densities of coarse sediment at these depths. In addition, during the wet sieving of sediment from C1 no sediment having the texture of ash was seen or felt in the samples from 124 cm – 201 cm.

The core chronology that would be associated with Mazama ash deposition at a much lower stratigraphic level is also problematic. For example, if the 181 cm magnetic susceptibility spike were related to the initial deposition of Mazama ash, the stratigraphic position of the organic fragments would still be inconsistent. In addition, the proximity of the Mazama ash to the lower ash couplet would result in an extremely compressed early Holocene sedimentary record compared with those in the literature (Reasoner et al., 1994; Gerloff et al., 1995; Spooner et al., 2002; Mazzucchi et al., (in press)). Correcting for this effect would invoke retracting the conclusion that the lower ash couplet had not migrated from its initial position, or the conclusion that C1 represents the entire sedimentary record of Otokomi Lake. As both of the above conclusions have been substantiated with data from this project and the literature, their retraction does not seem reasonable.

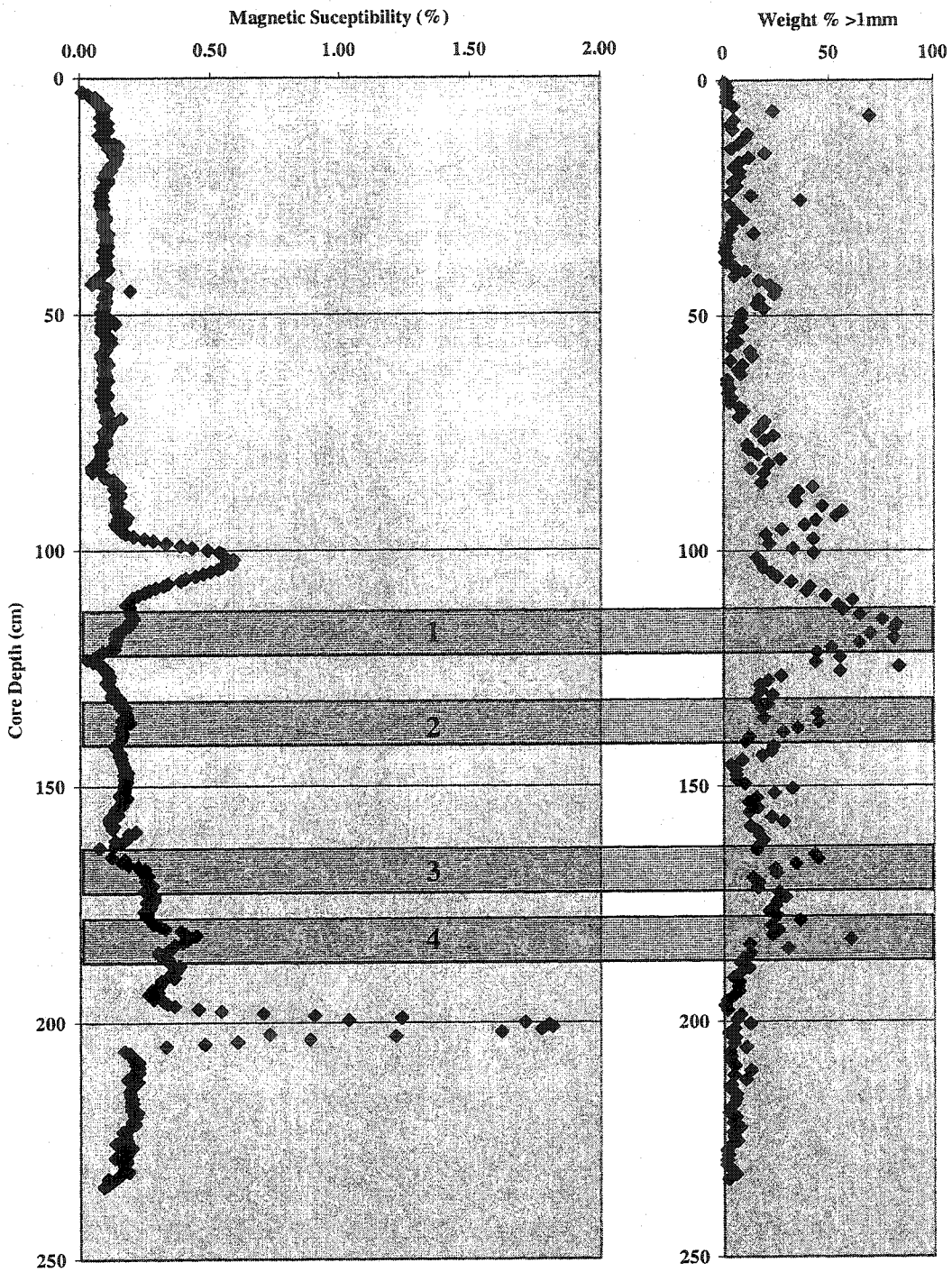
Magnetic Suceptibility (%)
0.00
0.50
1.00
1.50
2.00
Weight % >1mm
0
50
100
Core Depth (cm)
0
50
100
150
200
250
1
2
3
4

**Figure 33.** Shaded bars highlighting depths where magnetic susceptibility highs are correlated with high volumes of coarse sediment in Otokomi Lake C1. The minor magnetic susceptibility peak near the top of bar 1 is immediately below a susceptibility high associated with the 103.7 cm volcanic ash lens and immediately above a susceptibility low associated with the edge of one of the six core sections that were analyzed. A susceptibility peak can clearly be seen in the centre of bar 2, along with its corresponding peak on the coarse sediment graph. The relatively high susceptibility within the lower portion of bar 3 is immediately below a susceptibility low associated with the edge of one of the core sections that were analyzed. The magnetic susceptibility peak within bar 4 is clearly associated with an increase in coarse sediment at 185 cm in C1. Note that the magnetic susceptibility high near 200 cm in C1 is related to the volcanic ash couplet found at that depth, and not to an increase in coarse sediment.

It is possible that the carbon-dated organic fragments were removed from their original stratigraphic positions during core collection, as a result of friction between the penetrating core barrel and the lake sediments. However, most of the organic fragments encountered at a given depth should not have been displaced to any great degree because only the perimeter of the sediment "cylinder" entering the core barrel experiences this friction. In turn, the likelihood of isolating and dating *two* highly displaced organic fragments seems even lower. The only remaining explanation for the equivocal nature of the carbon dates would be related to errors in sample collection or possible contamination with younger carbon. Although the possibility of human error in the collection and labeling of samples cannot be discounted, it can neither be confirmed because there was no conscious deviation from the accepted experimental protocols at any time during the project. C1 was first thawed in the summer of 2001, however the organic fragments were not dated until the following year. Much of the core sediment remained moist for over a year in the enclosed tubes described in Chapter 3. During this time the split core sections were open to microbial growth. Although no obvious growth was visible on the surface of the cores at the time of wet sieving, the possibility that the organic fragments were host to microbial colonization exists. In an e-mail letter received from a technician at the carbon dating facility it was stated that any such carbon contamination would not have a pronounced affect on the radiocarbon age of the samples. The anomalously young organic fragments from 127.5 cm and 128.5 cm in C1 remain a mystery, one that may only be resolved through the acquisition of additional carbon dates below these depths in C1. The remainder of this discussion will be based on the assumption that the carbon

dates do not accurately represent the age of the sediment they were collected from, and that the ash layers preserved in C1 more accurately represent the core chronology.

### 5.2.4 Evidence of Moraine Emplacement

Provided that C1 contains nearly the entire post-glacial sedimentary record of Otokomi Lake, the sedimentary signature for the emplacement of the Crowfoot moraine should be present at some level in the core. This signature would be one associated with cold conditions and would presumably have a texture resulting from the sedimentary effects of sudden moraine emplacement along the lake's south shore.

Many of the data sets generated from the sedimentary analysis of C1 show a distinct change above 185 cm (Fig. 34). Although this is by no means the only notable deviation from the observed data trends, this deviation it is consistent across the data sets and appears to bear the hallmark of a sedimentary change associated with glacial advance and moraine emplacement.

Going up-core, the weight percent of coarse material in C1 jumps approximately 15 % at 185 cm. This quantifies the visible coarsening that was apparent above this point in C1. Because higher sediment densities are related to low X-ray grayscale values, the general decrease in grayscale with depth in C1 is consistent with the expectation of higher bulk densities at lower stratigraphic levels (Last and Smol, 2001). The sudden decrease in grayscale values above 185 cm opposes this general trend, and represents a sudden increase in the sediment density above that depth. As lithified rock fragments generally have a higher density than unconsolidated sediment, an increase in the percentage of rock fragments would likely increase the average sediment density at a given depth. Therefore, the observed deviation in the X-ray data can be also attributed to

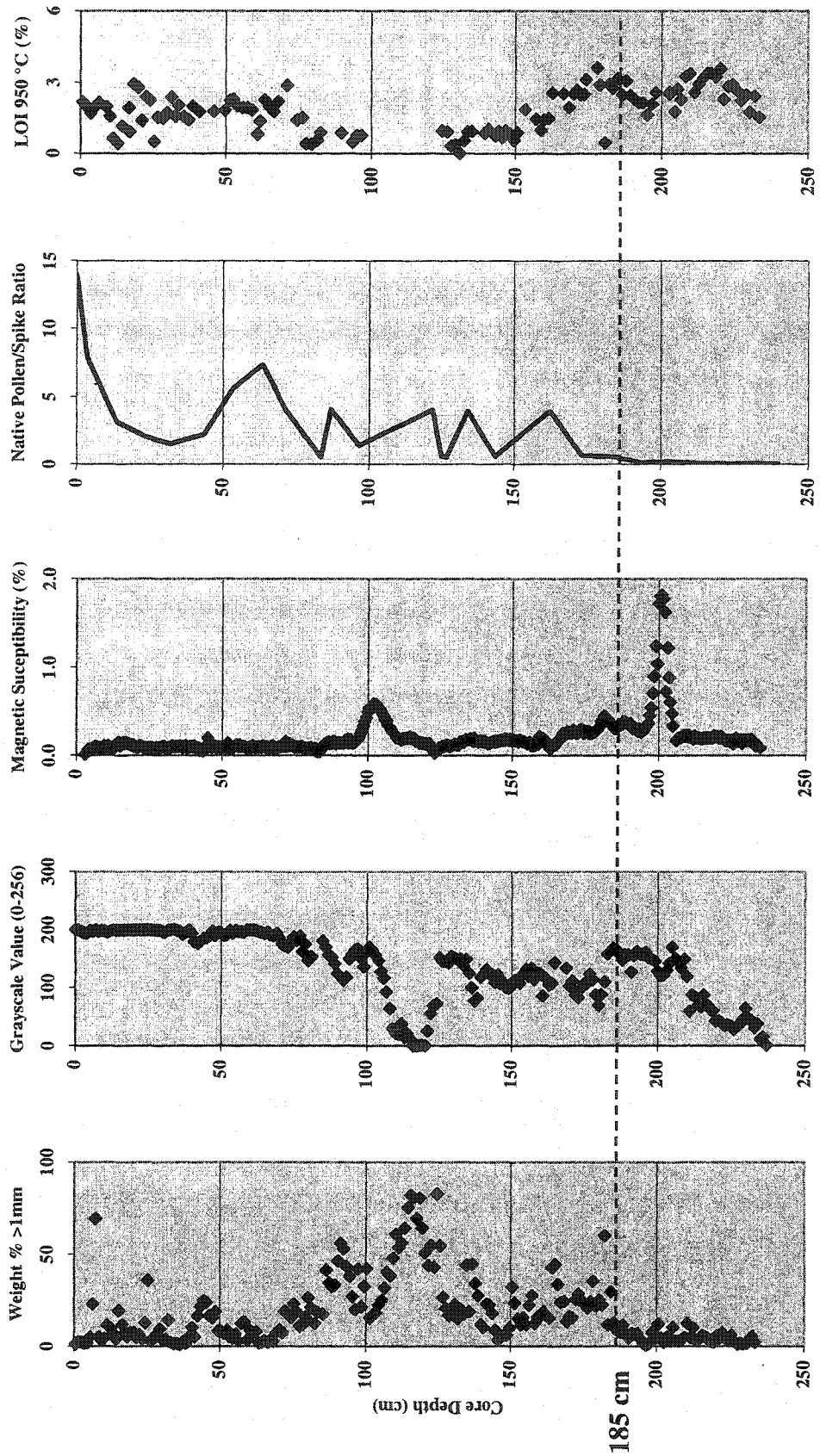


**Figure 34.** A comparison of coarse (> 1mm) grain size, X-ray, magnetic susceptibility, pollen productivity, and LOI data for Otokomi Lake C1. A distinct change, attributed to moraine emplacement, is evident above 185 cm for all of the data sets.

the increased density of coarse rock fragments above 185 cm. Similar to X-ray data, magnetic susceptibility data can also be thought of as a proxy for sediment density (Colorado School of Mines, 2003). The increase in magnetic susceptibility values above 185 cm is therefore attributed to the sediment density increase already established from the previous data sets. As with the X-ray data, the general up-core decrease in magnetic susceptibility is likely a result of the increasing organic and water content of the sediment.

Moraine emplacement can be used to explain the increased density of coarse rock fragments in C1 above 185 cm. The appearance of a 200 m long and 10 m high mound of unconsolidated glacial till along the shore of Otokomi Lake would likely intensify the coarse sediment transportation and deposition mechanisms acting within the basin. Although the moraine would not have affected the frequency or magnitude of snow avalanches in Rose Basin, its emplacement at the water's edge created an abundant source of coarse sediment that remains to this day. Small mass movement events or stream activity could easily have moved coarse sediment from the flank of the moraine to the nearshore environment of the lake. Ice rafting and subaqueous slumping could then have transported this coarse material to the basin centre. Inorganic sediment, often characterized by having a relatively coarse grain size, has also been attributed to upstream glacial activity in other studies (Engstron et al., 1990; Reasoner et al., 1994; Menounos an Reasoner, 1997).

Warming of lake water is often associated with increased calcium carbonate precipitation (Håkanson and Jansson, 1983). This causes an enrichment of the inorganic carbon content of associated sediments. Likewise, increases and decreases in the pollen

productivity ratio may also be attributed to increases and decreases in plant productivity in the areas where pollen is sourced. In this study, both the inorganic carbon and pollen ratio data sets show an interesting up-core trend whereby they increase up-core below 200 cm, decrease up-core to a depth of 194 cm and then increase up to, and past, the 185 cm reference depth. These parallel trends may represent the initial post-glacial warming of Glacier National Park, which gets interrupted by a cooling event, and then resumes shortly thereafter. These data would put the height of the cooling at 194 cm, at which depth both the pollen ratio and inorganic carbon values are low. This is not necessarily inconsistent with the coarse sediment influx into the Lake above 185 cm. Although the cool conditions needed for glacial activity and moraine emplacement may have existed at the time the 194 cm sediments were deposited, the environmental conditions necessary for mobilizing the moraine sediment may not. The warming trend that followed the 194 cm cooling event may have created the ice-free conditions necessary for effective transport of moraine sediment into the lake. Once these sediments began entering the lake, time would have been required for the associated processes of ice rafting and basin slumping to become accelerated. These time lags may explain the 9 cm offset between sediment associated with the cooling event and sediment which first records coarse influx into the basin. Based on the approximate 1.32 cm / 100 yr sedimentation rate, the 194 cm cooling event, responsible for moraine deposition, would have occurred at 10,590 B.P. This date is within the established range for Younger Dryas cooling.

If the sedimentary trends in the lower portion of C1 are not associated with climatic cooling, and subsequent moraine emplacement, then several questions remain:

**If moraine emplacement happened earlier in the lake's history, why is there no record of this in the lake sediment?**

Surely the initial post-glacial warming experienced in Rose basin would have mobilized some moraine sediment if a moraine were present. Instead, we primarily see clay-rich silt being deposited in Otokomi Lake up to the 185 cm mark.

**If moraine emplacement post-dates the coarsening we see at 185 cm, then what can explain this change in lake sedimentation?**

A simple increase in avalanche frequency above 185 cm would not account for the coarsening, because a large portion of the coarse sediment does not have the texture previously associated with avalanche deposits. In addition, the cold, sparsely vegetated, recently de-glaciated landscape associated with the lowermost sediment in C1 seems a likely environment for high avalanche activity. However, very little coarse material is seen in this portion of the core.

**If moraine emplacement post-dates the coarsening seen at 185 cm, then at what point was the moraine deposited?**

Since the moraine is pre-Mazama in age, sediments associated with its emplacement must be found below the 104 cm Mazama tephra lens, if not deeper. No obvious and consistent trends are seen in the sedimentary data over this interval that could be associated with both climatic cooling and moraine deposition. If any of the influxes of coarse sediment highlighted in Figure 36 are in fact indicative of moraine emplacement, they still do not explain the abrupt coarsening at 185 cm and they lack correlative trends in the pollen and inorganic carbon data.

## 6. Conclusions

- Sedimentation in Otokomi Lake is characterized by both low and high-energy transport and distribution mechanisms. Low energy mechanisms, associated with aeolian and low-flow fluvial inputs, are responsible for depositing clay and silt within the lake basin. High-energy mechanisms, such as turbidity currents, ice rafting and drainage basin mass-movements, deposit sand to pebble sized clasts within the lake basin.
- Based on the chronological control offered by three volcanic ash layers in C1, deglaciation of Rose Basin has a minimum bracketing age of 11,400 B.P., although 14,100 B.P. is the estimated basal date for the core.
- The 14,100 B.P. basal date estimate for Otokomi Lake indicates that deglaciation for this portion of western North America may have been significantly earlier than previous estimates.
- Correlative shifts in the pollen, loss on ignition, coarse (> 1 mm) grain size, magnetic susceptibility and X-ray grayscale data for C1 were all related to a sedimentary change in Otokomi Lake brought about by the emplacement of the adjacent Crowfoot moraine.
- The estimated emplacement date for the Crowfoot moraine is 10,590 B.P., which is within the Younger Dryas interval. This information supports the hypothesis that the Crowfoot moraine family represents a regional response in western North America to Younger Dryas cooling.
- The Mazama ash contains two chemically distinct glass fractions. This finding has implications for the ability of people to characterize the Mazama ash through its

glass chemistry. If researchers indiscriminately analyze different proportions of these two glass species, chemical analyses will neither be consistent nor comparable between or within studies.

**References**

Alden, W.C., 1953. Physiography and Glacial Geology of Western Montana and adjacent areas. U.S. Geological Survey Professional Paper **231**. 200 pp.

Allen, J.R.L., 1979. Physical Processes of Sedimentation. George Allen and Unwin Ltd., London, England.

Alley, R.B., D.A. Meese, C.A. Shuman, A.J. Gow, K.C. Taylor, P.M. Grootes, J.W.C. White, M. Ram, E.D. Waddington, P.A. Mayewski and G.A. Zielinski, 1993. Abrupt Increase in Greenland Snow Accumulation at the End of the Younger Dryas Event. *Nature* **362:** 527-529.

Anderson, R.Y., E.B. Nuhfer and W.E. Dean, 1984. Sinking of Volcanic Ash in Uncompacted Sediment in Williams Lake, Washington. *Science* **225:** 505-508.

Andrews, J.T., H. Nichols, S.K. Short, R. Stuckenrath and P.W. Birkeland, 1982. Alpine Lake-Sediment Studies, Front Range Colorado: A Contribution to Long-Term Ecological Research (LTER) Program. *Abstracts with Programs – American Quaternary Association* **7:** 61.

Barnosky, C.W., 1989. Postglacial Vegetation and Climate in the Northwestern Great Plains of Montana. *Quaternary Research* **31:** 57-73.

Beget, J.E., 1983. Radiocarbon-dated evidence of worldwide early Holocene Climate Change. *Geology* **11:** 389-393.

Beierle, B.D., 1997. Early Holocene Climate of Southwestern Alberta, Canada, Reconstructed from Lake Sediment Cores. M.Sc. Thesis, University of Calgary. 115 pp.

Bennett, K.D., S.A. Haberle and S.H. Lumley, 2000. The last Glacial-Holocene Transition in Southern Chile. *Science* **290:** 325-328.

Bloom, L. (ed), (Unpublished Literature) Palynology Preparation Technique, University of Calgary Micropaleontology Lab. University of Calgary, Alberta, Canada.

Bradley, R.S., M.J. Retelle, S.D. Ludlam, D.R. Hardy, B. Zolitschka and S. Lamoureux, 1996. The Taconite Inlet Lakes Project: a Systems Approach to Paleoclimatic Reconstruction. *Journal of Paleolimnology* **16:** 97-110.

Briner, J.P., D.S. Kaufman, A. Werner, M. Caffee, L. Levy, W.F. Manley, M.R. Kaplan and R.C. Finkel, 2002. Glacier Readvance during the Late Glacial (Younger Dryas?) in the Ahklun Mountains, Southwestern Alaska. *Geology* **30, 8:** 679-682.

Brown, D.G., and S.J. Walsh, 1992. Relationships Between the Morphometry of Alpine and Subalpine Basins and Remotely Sensed Estimates of Lake Turbidity, Glacier National Park, Montana. *Physical Geography* **13, 3:** 250-272.

Carrara, P.E., 1986. Late Pleistocene Deglaciation and Reforestation of the Glacier National Park Region, Montana. *Programs and Abstracts, American Quaternary Association Conference* **35a, 9:** pp. 122.

Carrara, P.E., S.K. Short and R.E. Wilcox, 1986. Deglaciation of the Mountainous Region of Northwestern Montana, U.S.A., as Indicated by Late Pleistocene Ashes. *Arctic and Alpine Research* **18, 3:** 317-325.

Carrara, P.E., 1987. Holocene and Latest Pleistocene Glacial Chronology, Glacier National Park, Montana. *Canadian Journal of Earth Sciences* **24:** 387-395.

Carrara, P.E., 1989. Late Quaternary Glacial and Vegetative History of the Glacier National Park Region, Montana. *U.S. Geological Survey Bulletin 1902.* 64 pp.

Carrara, P.E., and R.G. McGimsey, 1988. Map Showing Distribution of Moraines and Extent of Glaciers from the Mid-19$^{th}$ Century to 1979 in the Mount Jackson area, Glacier National Park, Montana. *U.S. Geological Survey- Miscellaneous Investigations Series.*

Carrara, P.E., and D.A. Trimble, 1992. A Glacier Peak and Mount Saint Helens J Volcanic Ash Couplet and the Timing of Deglaciation in the Colville Valley area, Washington. *Canadian Journal of Earth Sciences* **29:** 2397-2405.

Colorado School of Mines, 2003. http://www.mines.edu/fs_home/tboyd/GP311/MODULES/MAG/NOTES/suscept.html.

Dansgaard, W., J.W.C. White and S.J. Johnsen, 1989. The Abrupt Termination of the Younger Dryas Event. *Nature* **339:** 532-533.

Davis, P.T., and G. Osborn, 1987. Age of Pre-Neoglacial Cirque Moraines in the Central North American Cordillera. *Géographie Physique et Quaternaire* **40, 3:** 365-375.

Dirszowsky, R.W., and J.R. Desloges, 1997. Glaciolacustrine Sediments and Neoglacial History of the Chephren Lake Basin, Banff National Park, Alberta. *Géographie Physique et Quaternaire* **51, 1:** 41-53.

Eden, D.N., and M.J. Page, 1998. Palaeoclimatic Implications of a Storm Erosion Record from late Holocene Lake Sediments, North Island, New Zealand. *Palaeogeography, Palaeoclimatology, Palaeoecology* **139:** 37-58.

Engstrom, D.R., B.C.S. Hansen and H.E. Wright Jr., 1990. A Possible Younger Dryas Record in Southeastern Alaska. *Science* **250:**1383-1385.

Evans, R.D., 1994. Empirical Evidence of the Importance of Sediment Resuspension in Lakes. *Hydrobiologia* **284:** 5-12.

Exploranium G.S. Ltd., 1995. User's Guide, KT-9 Kappameter. Exploranium G.S. Ltd., Mississauga, Ontario, Canada. 71 pp.

Ferguson, A., and G. Osborn, 1981. Minimum age of Deglaciation of Upper Elk Valley British Columbia. *Canadian Journal of Earth Sciences* **18:** 1635-1636.

Ferguson, A., and L.V. Hills, 1985. A Palynological Record, Upper Elk Valley, British Columbia. *In:* Harington, C.R. (ed), *Climatic change in Canada; 5, Critical periods in the Quaternary climatic history of northern North America,* pp. 355-369. National Museum of Natural Sciences, Ottawa, Canada.

Finklin, A.I., 1986. A Climatic Handbook for Glacier National Park- With Data for Waterton Lakes National Park. *United States Forest Service Technical Report INT-204.* 124 pp.

Franklin, F.F. Jr., P.J. Mehringer Jr. and J.C. Sheppard, 1993. Age, Distribution, and Stratigraphy of Glacier Peak Tephra in Eastern Washington and Western Montana, United States. *Canadian Journal of Earth Sciences* **30:** 535-552.

Friele, P.A., and J.J. Clague, 2002. Younger Dryas Readvance in Squamish River Valley, Southern Coast Mountains, British Columbia. *Quaternary Science Reviews* **21:** 1925-1933.

Fulton, R.J., 1971. Radiocarbon Geochronology of Southern British Columbia. Geological Survey of Canada, Paper **71-37:** 28 pp.

Fulton, R.J., 1984. Quaternary Glaciation, Canadian Cordillera. *In:* Fulton, R.J. (ed), *Quaternary Stratigraphy of Canada.* Geological Survey of Canada Paper **84-10:** 39-48.

Gardner, J.S., 1983. Observations on Erosion by Wet Snow Avalanches, Mount Rae Area, Alberta, Canada. *Arctic and Alpine Research* **15, 2:** 271-274.

Gerloff, L.M., 1994. Holocene and Latest Pleistocene Paleoenvironments of the Mission Mountains, Northwestern Montana. M.Sc. Thesis, University of Calgary. 97 pp.

Gerloff, L.M., L.V. Hills and G.D. Osborn, 1995. Post-Glacial Vegetation History of the Mission Mountains, Montana. *Journal of Paleolimnology* **14:** 269-279.

Gilbert, R., and J. Shaw, 1981. Sedimentation in Proglacial Sunwapta Lake, Alberta. *Canadian Journal of Earth Sciences* **18:** 81-93.

Gilbert, R., J.R. Desloges and D.S. Lemmen, 1997. Palaeoenvironmental Assessment from the Physical Properties of Lacustrine and Marine Sediments; a Canadian Contribution to IGCP 374. *Journal of Paleolimnology* **17:** 295-296.

Gilbert, R., 2001. Personal Communication.

Glew, J.R., 1991. Miniature Gravity Corer for Recovering Short Sediment Cores. *Journal of Paleolimnology* **5:** 285-287.

Gosse, J.C., E.B. Evenson, J. Klein, B. Lawn and R. Middleton, 1995. Precise Cosmogenic $^{10}$Be Measurements in Western North America: Support for a Global Younger Dryas Cooling Event. *Geology* **23:10** 877-880.

Håkanson, L., 1977. The Influence of Wind, Fetch, and Water Depth on the Distribution of Sediments in Lake Vänern, Sweden. *Canadian Journal of Earth Sciences* **14:** 397-412.

Håkanson, L., and M. Jansson, 1983. Principles of Lake Sedimentology. Springer-Verlag, New York. 316 pp.

Hallett, D.J., L.V. Hills and J.J. Clague, 1997. New Accelerator Mass Spectrometry Radiocarbon ages for the Mazama Tephra layer from Kootenay National Park, British Columbia, Canada. *Canadian Journal of Earth Sciences* **34:** 1202-1209.

Harris, S.A., and J.A. Howell, 1977. Chateau Lake Louise Moraines- Evidence for a new Holocene Glacial event in Southwest Alberta. *Bulletin of Canadian Petroleum Geology* **25:** 441-455.

Heine, J.T., 1996. Evidence for a Global Younger Dryas Event on Mount Rainier Volcano, Washington? *Abstracts with Programs- Geological Society of America* **77:46** Suppl. F31

Heine, K., 1994. The Late-Glacial Moraine Sequences of Mexico; is there Evidence for The Younger Dryas Event? *Paleogeography, Paleoclimatology, Paleoecology* **112:1-2** 113-123.

Heine, K., and J.T. Heine, 1996. Late Glacial Climatic Fluctuations in Ecuador; Glacier Retreat During Younger Dryas Time. *Arctic and Alpine Research* **28:4** 496-501.

Heiri, O., A.F. Lotter and G. Lemcke, 2001. Loss on Ignition as a Method for Estimating Organic and Carbonate Content in Sediments: Reproducibility and Comparability of Results. *Journal of Paleolimnology* **25:** 101-110.

Hills, L.V., 2000. Personal Communication.

Hilton, J., J.P. Lishman and P.V. Allen, 1986. The Dominant Processes of Sediment Distribution and Focusing in a Small Eutrophic, Monomictic Lake. *Limnology and Oceanography* **31, 1:**125-133.

Jones, E.J.W., 1999. Marine Geophysics. John Wiley and Sons Ltd., Toronto. 466 pp.

Kearney, M.S., and B.H. Luckman, 1987. A mid-Holocene Vegetation and Climate Record from the Subalpine Zone of the Maligne Valley, Jasper National Park Alberta, Canada. *Paleogeography, Paleoclimatology, Paleoecology* **59:** 227-242.

Kovanen, D.J., 2002. Morphologic and Stratigraphic Evidence for Allerød and Younger Dryas age Glacier Fluctuations of the Cordilleran Ice Sheet, British Columbia, Canada and Northwest Washington, U.S.A. *Boreas* **31:** 163-184.

Kudras, H.R., H. Erienkeuser, R. Vollbrecht and W. Weiss, 1991. Global Nature of the Younger Dryas Cooling Event Inferred from Oxygen Isotope Data from Sulu Sea Cores. *Nature* **349:** 406-408.

Lambert, A., and K.J. Hsü, 1979. Non-annual Cycles of Varve-like Sedimentation in Walensee, Switzerland. *Sedimentology* **26:** 453-461.

Larsen, C.P.S., and G.M. MacDonald, 1993. Lake Morphometry, Sediment Mixing and the Selection of Sites for Fine Resolution Palaeoecological Studies. *Quaternary Science Reviews* **12:** 781-792.

Last, W.M., and J.P. Smol (eds), 2001. *Tracking Environmental Change Using Lake Sediments* **1-4.** Kluwer Academic Publishers, Dordrecht, Netherlands.

Lemke, R.W., M.R. Mudge, R.E. Wilcox and H.A. Powers, 1975. Geologic Setting of the Glacier Peak and Mazama Ash-Bed Markers in West-Central Montana. United States Geological Survey Bulletin **1395-H:** 31 pp.

Lewis, T., R. Gilbert and S.F. Lamoureux, 2002. Spatial and Temporal Changes in Sedimentary Processes at High-Arctic Proglacial Bear Lake, Devon Island, Nunavut, Canada. *Arctic, Antarctic, and Alpine Research* **34, 2:** 119-129.

Luckman, B.H., 1975. Drop Stones Resulting from Snow-Avalanche Deposition on Lake Ice. *Journal of Glaciology* **14, 70:** 186-188.

Luckman, B.H., and M.S. Kearney, 1986. Reconstruction of Holocene Changes in Alpine Vegetation and Climate in the Maligne Range, Jasper National Park, Alberta. *Quaternary Research* **26:** 244-261.

Luckman, B.H., and G. Osborn, 1979. Holocene Glacier Fluctuations in the Middle Canadian Rocky Mountains. *Quaternary Research* **11:** 52-57.

Luckman, B.H., 1988. 8,200 year old Wood from the Athabasca Glacier, Alberta. *Canadian Journal of Earth Sciences* **25:** 148-151.

Mack, R.M., N.W. Rutter and V.M. Bryant Jr., 1978. Reexamination of Postglacial Vegetation History in Northern Idaho: Hager Pond, Bonner Co. *Quaternary Research* **10:** 241-255.

Mack, R.M., N.W. Rutter and S. Valastro, 1983. Holocene Vegetational History of the Kootenai River Valley, Montana. *Quaternary Research* **20:** 177-193.

Mankeiwicz, D., J.R. Steidtmann and L.E. Borgman, 1975. Clastic Sedimentation in a Modern Alpine Lake. *Journal of Sedimentary Petrology* **45, 2:** 462-468.

Matthewes, R.W., L.E. Heusser and R.T. Patterson, 1993. Evidence for a Younger Dryas-Like Cooling Event on the British Columbia Coast. *Geology* **21:** 101-104.

Mazzucchi, D., I.S. Spooner, R. Gilbert and G. Osborn, (In Press). Reconstruction of Holocene Climate Change using Multi-proxy Analysis of Sediments from Pyramid Lake, B.C., Canada. *Arctic, Antarctic, and Alpine Research.*

Mehringer, P.J. Jr., S.F. Arno and K.L. Petersen, 1977. Postglacial History of Lost Trail Pass Bog, Bitterroot Mountains, Montana. *Arctic and Alpine Research* **9,4:** 345-368.

Menounos, B., and M.A. Reasoner, 1997. Evidence for Cirque Glaciation in the Colorado Front Range during the Younger Dryas Chronozone. *Quaternary Research* **48:** 38-47.

Mikolajewicz, U., T.J. Crowley, A. Schiller and R. Voss, 1997. Modelling Teleconnections between the North Atlantic and North Pacific during the Younger Dryas. *Letters to Nature* **387:** 384-387.

Niessen, F., and K. Kelts, 1989. The Deglaciation and Holocene Sedimentary Evolution of Southern Perialpine Lake Lugano – Implications for Alpine Paleoclimate. *Eclogae Geologicae Helvetiae* **82, 1:** 235-263.

Nixon, D.J., and D.M. McClung, 1993. Snow Avalanche Runout from two Canadian Mountain Ranges. *Annals of Glaciology* **18:** 1-6.

Osborn, G., 1985. Holocene Tephrostratigraphy and Glacial Fluctuations in Waterton Lakes and Glacier National Parks, Alberta and Montana. *Canadian Journal of*

*Earth Sciences* **22:** 1093-1101.

Osborn, G., 1986. Lateral Moraine Stratigraphy and Neoglacial history of Bugaboo Glacier, British Columbia. *Quaternary Research* **26:** 171-178.

Osborn, G., C. Clapperton, P.T. Davis, M. Reasoner, D.T. Rodbell, G.O. Seltzer and G. Zielsinski, 1996. Potential Glacial Evidence for the Younger Dryas Event in the Cordillera of North and South America. *Quaternary Science Reviews* **14:** 823-832.

Osborn, G., and L. Gerloff, 1997. Latest Pleistocene and early Holocene Fluctuations of Glaciers in the Canadian and Northern American Rockies. *Quaternary International* **38/39:** 7-19.

Osborn, G., 2000. Personal Communication.

Prothero, D.R., and F. Schwab, 1996. Sedimentary Geology, an Introduction to Sedimentary Rocks and Stratigraphy. W.H. Freeman and Co., New York. 575 pp.

Reasoner, M.A., 1986. An Inexpensive, Lightweight Percussion Core Sampling System. *Géographie, Physique et Quaternaire* **40, 2:** 217-219.

Reasoner, M.A., G. Osborn and N.W. Rutter, 1994. Age of the Crowfoot Advance in the Canadian Rocky Mountains: A Glacial Event Coeval with the Younger Dryas Oscillation. *Geology* **22:** 439-442.

Ringius, G.S., and R.A. Sims, 1997. Indicator Plant Species in Canadian Forests. Canadian Forest Service, Ottawa, Ontario. 218 pp.

Rodbell, D.T., 2000. The Younger Dryas: Cold, Cold Everywhere? *Science* **290:** 285-286.

Rutter, N.W., A.J. Weaver, D. Rokosh, A.F. Fanning and D.G. Wright, 2000. Data-model Comparison of the Younger Dryas Event. *Canadian Journal of Earth Sciences* **37:** 811-830.

Ryder, J.M., and B. Thomson, 1986. Neoglaciation in the Southern Coast Mountains of British Columbia: Chronology Prior to the late-Neoglacial Maximum. *Canadian Journal of Earth Sciences* **23:** 237-238.

Scott, L., M. Steenkamp and B.P. Beaumont, 1995. Palaeoenvironmental Conditions in South Africa at the Pleistocene-Holocene Transition. *Quaternary Science Reviews* **14:** 937-947.

Shaw, J., 1977. Sedimentation in an Alpine lake during Deglaciation, Okanagan Valley,

British Columbia, Canada. *Geografiska Annaler* **59 A:** 221-240.

Shaw, R. J., and D. On, 1979. Plants of Waterton-Glacier National Parks. Mountain Press Publishing Co., Missoula, Montana. 160 pp.

Singer, C., J. Shulmeister and B. McLea, 1998. Evidence Against a Significant Younger Dryas Cooling Event in New Zealand. *Science* **281:** 812-814.

Smith, I.R., 2000. Diamictic Sediments within high Arctic Lake Sediment Cores: Evidence for Lake Ice Rafting along the Lateral Glacial Margin. *Sedimentology* **47:** 1157-1179.

Spooner, I.S., L.V. Hills and G.D. Osborn, 1997. Rconstruction of Holocene Changes in Alpine Vegetation and Climate, Susie Lake, British Columbia, Canada. *Arctic and Alpine Research* **29, 2:** 156-163.

Spooner, I.S., D. Mazzucchi, G. Osborn, R. Gilbert and I. Larocque, 2002. A Multi-Proxy Late Pleistocene and Holocene Record of Sediment of Skinny Lake, Iskut Region, Northern British Columbia, Canada. *Journal of Paleolimnology* **128:** 419-431.

Spurr, S.H., and B.V. Barnes, 1980. Forest Ecology, 3rd Ed. John Wiley and Sons Inc., Toronto. 687 pp.

Taylor, K.C., G.W Lamorey, G.A. Doyle, R.B. Alley, P.M. Grootes, P.A. Mayewski, J.W.C. White and L.K. Barlow, 1993. The 'Flickering Switch' of Late Pleistocene Climate Change. *Nature* **361:** 432-435.

Tomkins, J., 2000. Regional Holocene Climate of Alberta and Northwestern Montana through Lake Core Sediment Analysis. B.Sc Thesis, University of Calgary. 60 pp.

Waitt, R.B. Jr., and R.M. Thorson, 1983. The Cordilleran Ice Sheet in Washington, Idaho and Montana. *In:* Porter, S.C. (ed), *Late Quaternary Environments of the United States,* pp. 53-70. University of Minnesota Press, Minneapolis.

Weirich, F.H., 1984. Turbidity Currents: Monitoring their Occurrence and Movement with a Three-Dimensional Sensor Network. *Science* **224:** 384-386.

Westgate, J.A., and M.P. Gorton, 1981. Correlation Techniques in Tephra Studies. *In:* Self, S., and R.J. Sparks (eds), *Tephra Studies,* pp. 73-94. D. Reidel Publishing, Dordrecht, Netherlands.

White, J.M., and G. Osborn, 1992. Evidence for a Mazama-like Tephra Deposited ca. 10,000 B.P. at Copper Lake, Banff National Park, Alberta. *Canadian Journal of Earth Sciences* **29:** 52-62.

Wright, H.E. Jr., 1989. The Amphi-Atlantic Distribution of the Younger Dryas Paleoclimatic Oscillation. *Quaternary Science Reviews* **8:** 295-306.

Zhou, W., M.J. Head, Z. An, P.D. Deckker, Z. Liu, X. Liu, X. Lu, D. Donahue, A.J.T. Jull and J.W. Beck, 2001. Terrestrial Evidence for a Spatial Structure of Tropical-Polar Interconnections during the Younger Dryas Episode. *Earth and Planetary Science Letters* **191:** 231-239.

Zielinski, G.A., and P.T. Davis, 1987. Late Pleistocene age for the Type Temple Lake Moraine, Wind River Range Wyoming, U.S.A. *Géographie, Physique et Quaternaire* **41:** 397-401.

## Appendix A: Sonar Transects of Otokomi Lake

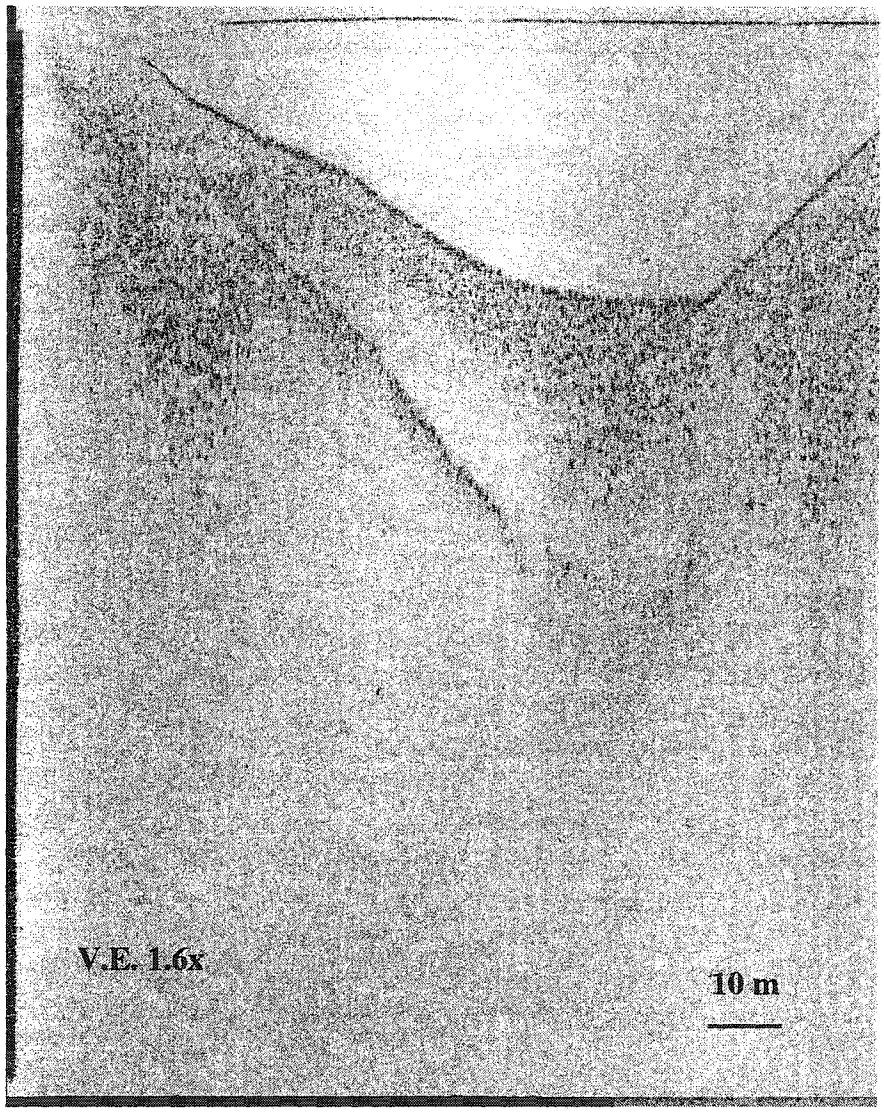


**Figure 35.** Sonar transect #1 for Otokomi Lake

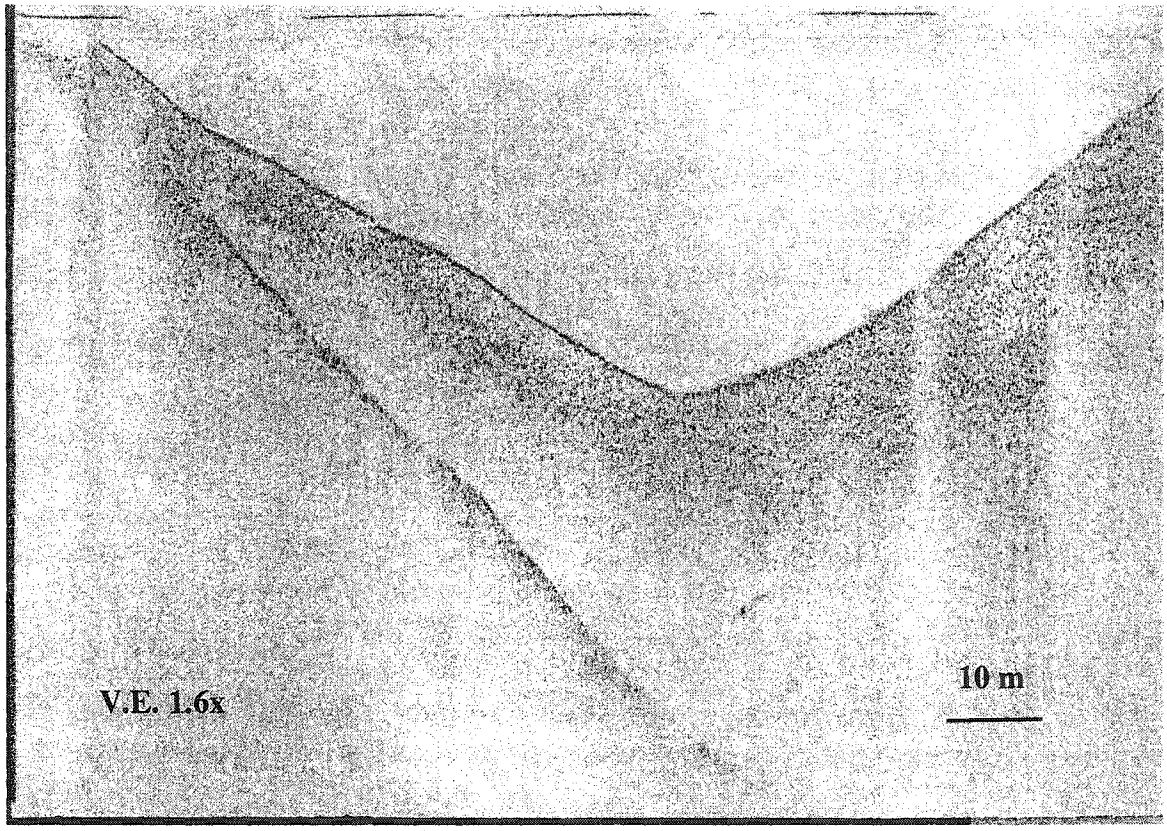


**Figure 36.** Sonar transect #2 for Otokomi Lake.

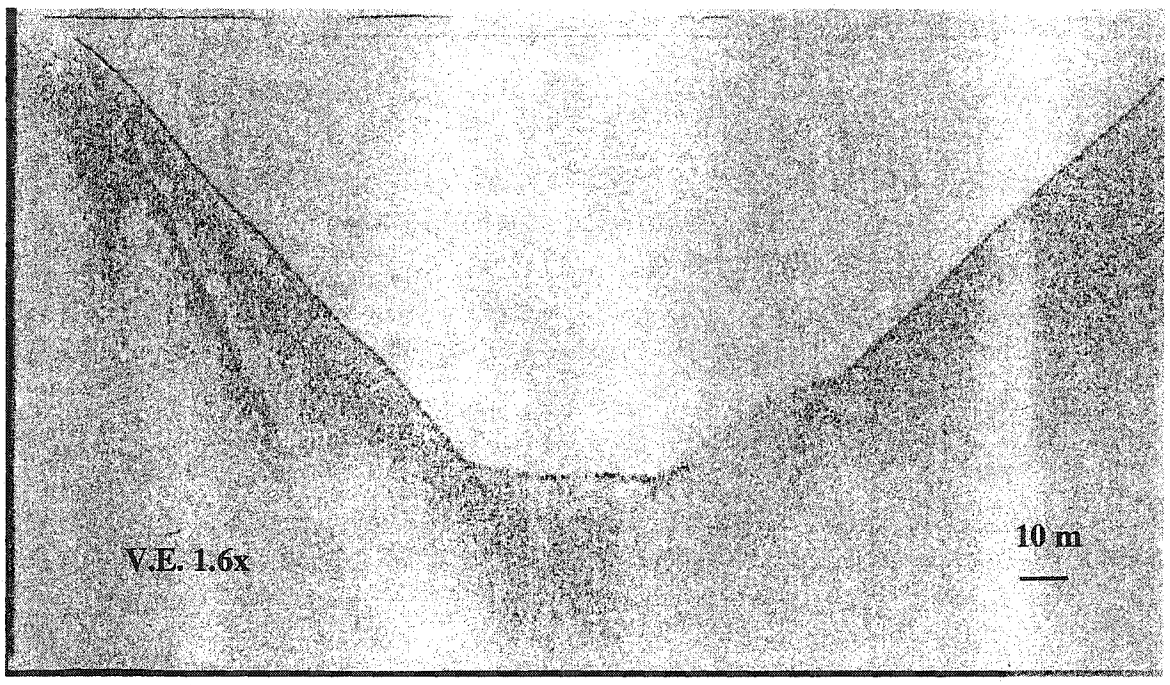


**Figure 37.** Sonar Transect #3 for Otokomi Lake.

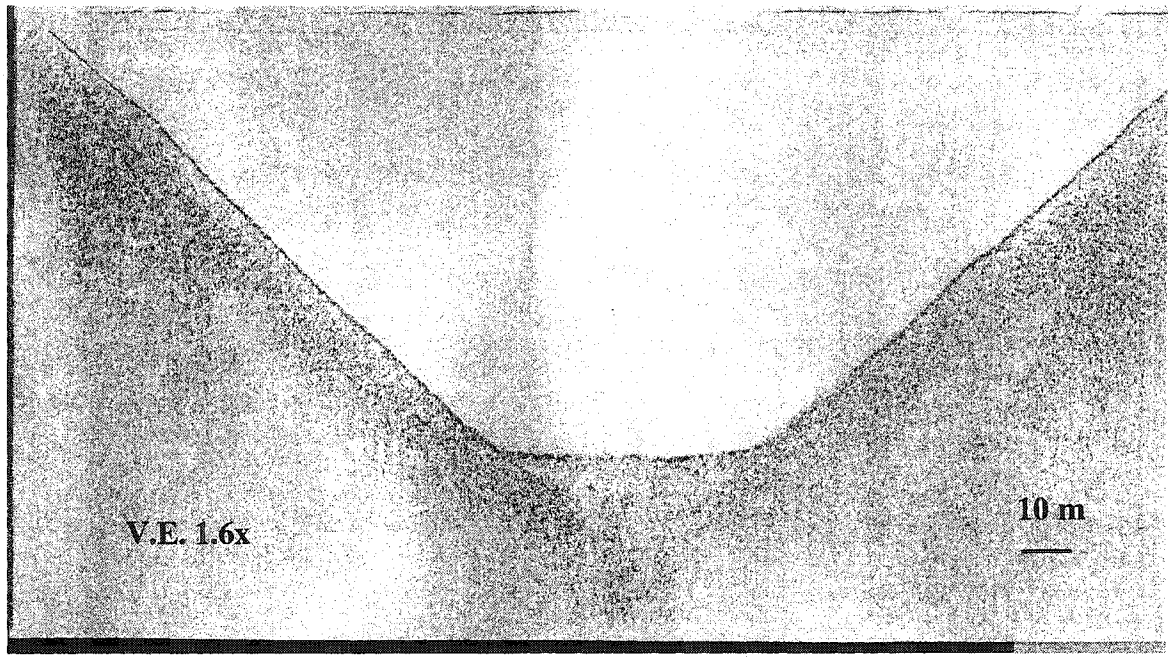


**Figure 38.** Sonar transect #4 for Otokomi Lake.

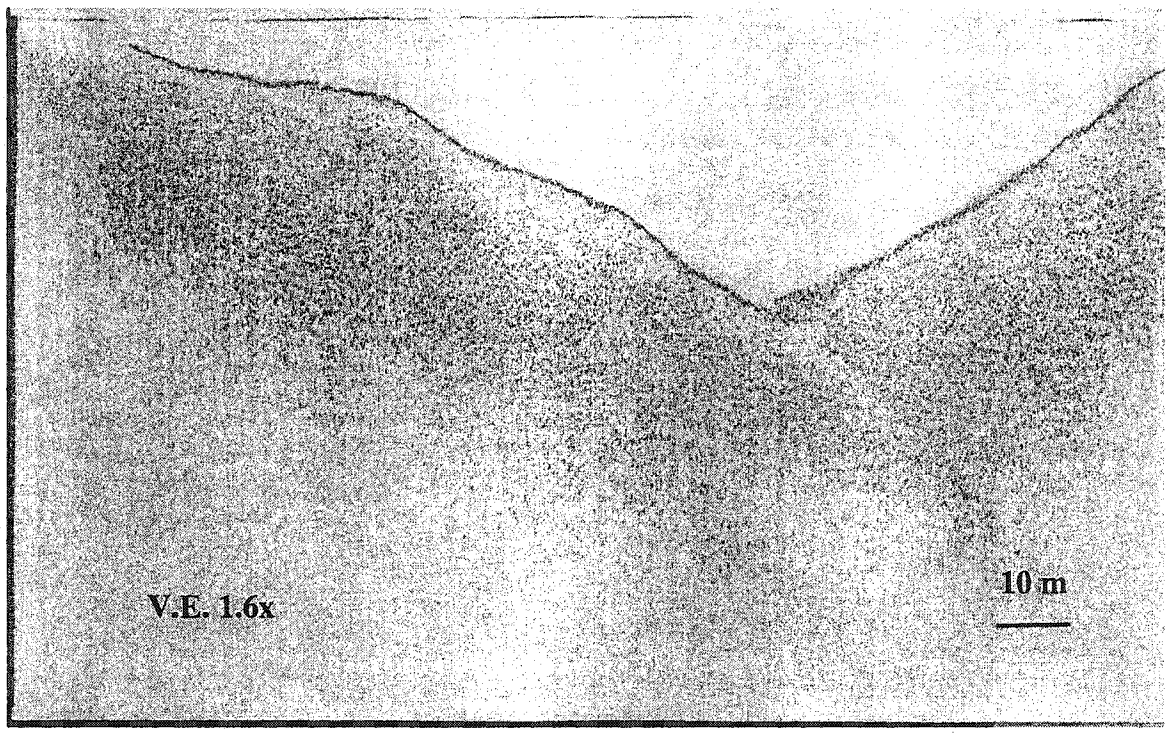


**Figure 39.** Sonar transect #5 for Otokomi Lake

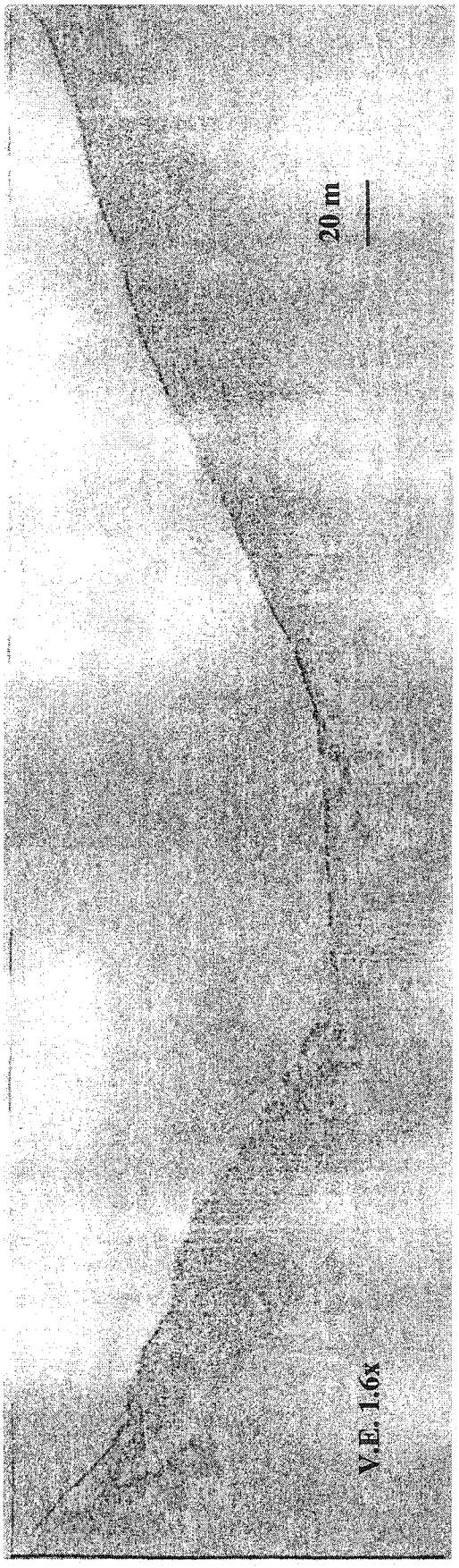


**Figure 40.** Sonar transect #6 for Otokomi Lake.

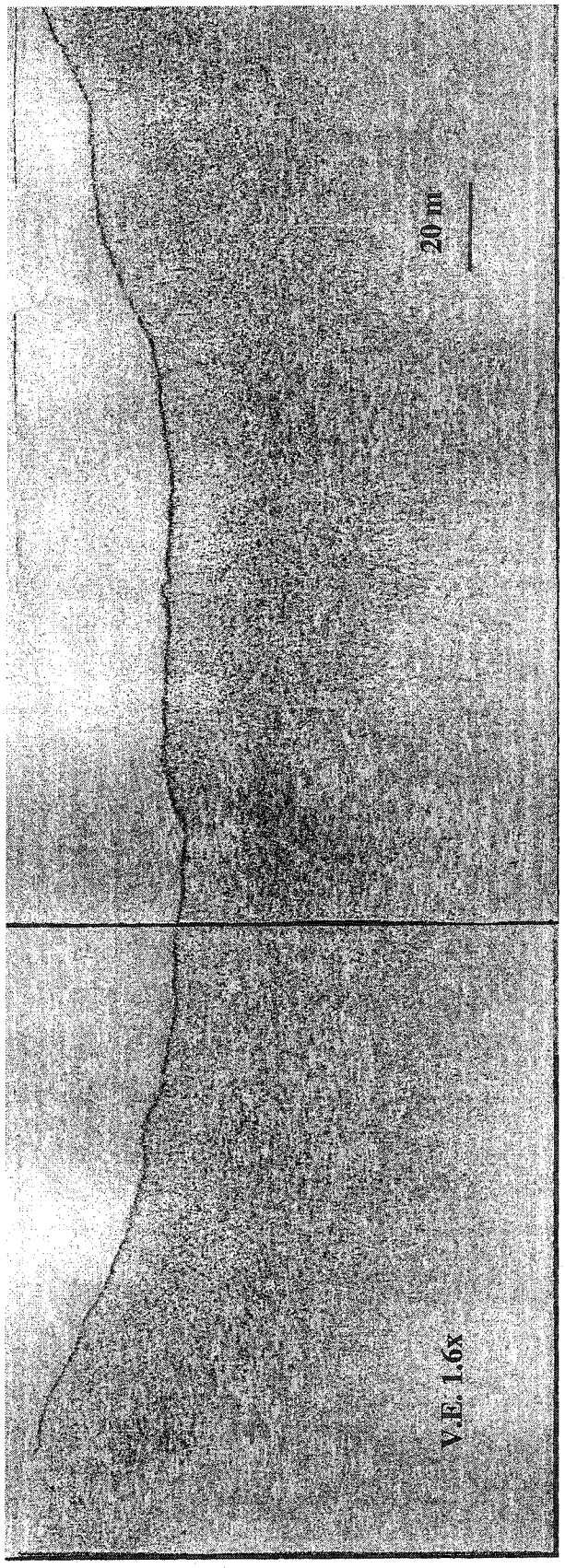


**Figure 41.** Sonar transect #7 for Otokomi Lake.